VOLUME 33 | SUPPLEMENT 2 | MARCH 2020

MODERN PATHOLOGY

ABSTRACTS

PANCREAS, GALLBLADDER, AMPULLA, AND EXTRA-HEPATIC BILIARY TREE

(1739-1801)

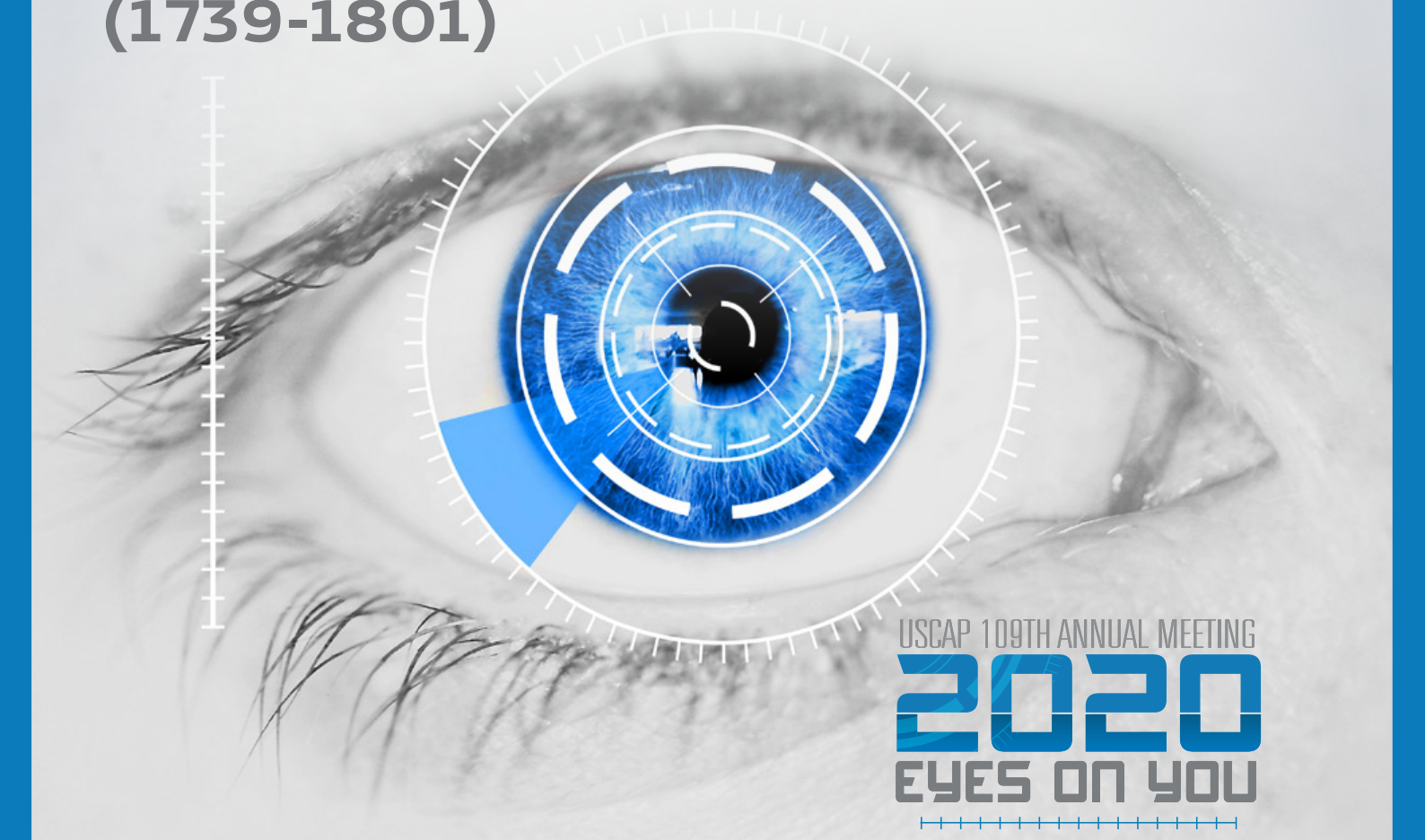

FEBRUARY 29-MARCH 5, 2020

LOS ANGELES CONVENTION CENTER
LOS ANGELES, CALIFORNIA

Published by
SPRINGER NATURE
www.ModernPathology.org

USCAP Creating a Better Pathologist
AN OFFICIAL JOURNAL OF THE UNITED STATES AND CANADIAN ACADEMY OF PATHOLOGY

EDUCATION COMMITTEE

Jason L. Hornick, Chair

Rhonda K. Yantiss, Chair, Abstract Review Board and Assignment Committee

Laura W. Lamps, Chair, CME Subcommittee

Steven D. Billings, Interactive Microscopy Subcommittee

Raja R. Seethala, Short Course Coordinator

Ilan Weinreb, Subcommittee for Unique Live Course Offerings

David B. Kaminsky (Ex-Officio)

Zubair Baloch
Daniel Brat
Ashley M. Cimino-Mathews
James R. Cook
Sarah Dry
William C. Faquin
Yuri Fedoriw
Karen Fritchie
Lakshmi Priya Kunju
Anna Marie Mulligan
Rish K. Pai
David Papke, Pathologist-in-Training
Vinita Parkash
Carlos Parra-Herran
Anil V. Parwani
Rajiv M. Patel
Deepa T. Patil
Lynette M. Sholl
Nicholas A. Zoumberos, Pathologist-in-Training

ABSTRACT REVIEW BOARD

Benjamin Adam
Narasimhan Agaram
Rouba Ali-Fehmi
Ghassan Allo
Isabel Alvarado-Cabrero
Catalina Amador
Roberto Barrios
Rohit Bhargava
Jennifer Boland
Alain Borczuk
Elena Brachtel
Marilyn Bui
Eric Burks
Shelley Caltharp
Barbara Centeno
Joanna Chan
Jennifer Chapman
Hui Chen
Beth Clark
James Conner
Alejandro Contreras
Claudiu Cotta
Jennifer Cotter
Sonika Dahiya
Farbod Darvishian
Jessica Davis
Heather Dawson
Elizabeth Demicco
Katie Dennis
Anand Dighe
Suzanne Dintzis
Michelle Downes
Andrew Evans
Michael Feely
Dennis Firchau
Gregory Fishbein
Andrew Folpe
Larissa Furtado
Billie Fyfe-Kirschner
Giovanna Giannico
Anthony Gill
Paula Ginter
Tamara Giorgadze
Purva Gopal
Anuradha Gopalan
Abha Goyal
Rondell Graham
Alejandro Gru
Nilesh Gupta
Mamta Gupta
Gillian Hale
Suntrea Hammer
Malini Harigopal
Douglas Hartman
John Higgins
Mai Hoang
Mojgan Hosseini
Aaron Huber
Peter Illei
Doina Ivan
Wei Jiang
Vickie Jo
Kirk Jones
Neerja Kambham
Chiah Sui Kao
Dipti Karamchandani
Darcy Kerr
Ashraf Khan
Francesca Khani
Rebecca King
Veronica Klepeis
Gregor Krings
Asangi Kumarapeli
Alvaro Laga
Steven Lagana
Keith Lai
Michael Lee
Cheng-Han Lee
Madelyn Lew
Zaibo Li
Faqian Li
Ying Li
Haiyan Liu
Xiuli Liu
Yen-Chun Liu
Lesley Lomo
Tamara Lotan
Anthony Magliocco
Kruti Maniar
Emily Mason
David McClintock
Bruce McManus
David Meredith
Anne Mills
Neda Moatamed
Sara Monaco
Atis Muehlenbachs
Bita Naini
Dianna Ng
Tony Ng
Michiya Nishino
Scott Owens
Jacqueline Parai
Yan Peng
Manju Prasad
Peter Pytel
Stephen Raab
Joseph Rabban
Stanley Radio
Emad Rakha
Preetha Ramalingam
Priya Rao
Robyn Reed
Michelle Reid
Natasha Rekhtman
Jordan Reynolds
Michael Rivera
Andres Roma
Avi Rosenberg
Esther Rossi
Peter Sadow
Steven Salvatore
Souzan Sanati
Anjali Saqi
Jeanne Shen
Jiaqi Shi
Gabriel Sica
Alexa Siddon
Deepika Sirohi
Kalliopi Siziopikou
Sara Szabo
Julie Teruya-Feldstein
Khin Thway
Rashmi Tondon
Jose Torrealba
Andrew Turk
Evi Vakiani
Christopher VandenBussche
Paul VanderLaan
Olga Weinberg
Sara Wobker
Shaofeng Yan
Anjana Yeldandi
Akihiko Yoshida
Gloria Young
Minghao Zhong
Yaolin Zhou
Hongfa Zhu
Debra Zynger

To cite abstracts in this publication, please use the following format: **Author A, Author B, Author C, et al. Abstract title (abs#). In "File Title."** ***Modern Pathology*** **2020; 33 (suppl 2): page#**

1739 Molecular Characteristics of Pancreatic Neuroendocrine Tumors, Do They Correlate with Metastases?

Beena Ahsan[1], Kannan Thanikachalam[1], Ariane Robison[2], Jia LI[1], Indrani Datta[1], Ifeoma Onwubiko[1], Gazala Khan[1], Mohammad Raoufi[1]
[1]Henry Ford Health System, Detroit, MI, [2]Henry Ford Hospital, Detroit, MI

Disclosures: Beena Ahsan: None; Kannan Thanikachalam: None; Ariane Robison: None; Jia LI: None; Indrani Datta: None; Ifeoma Onwubiko: None; Gazala Khan: None; Mohammad Raoufi: None

Background: Pancreatic neuroendocrine tumors (PNET) have an unpredictable biological behavior that cannot be reliably predicted by histological and clinical manifestations. We performed next generation sequencing (NGS) on PNET to understand the molecular pathogenesis and to identify potential biomarkers correlating with metastases and survival.

Design: Hybrid capture-based comprehensive genomic profiling was performed on both primary and metastatic PNET from 28 patients. Metastatic sites were grouped as lymph nodes and distant metastases (consisted of liver followed by bone). NGS was performed on genomic DNA & RNA isolated from formalin-fixed paraffin embedded tissue using the whole exome NGS assay covering 20,000 genes. Average number of DNA reads was 52 million at 3:1 somatic to germline. All variants were detected with >99% confidence based on allele frequency and amplicon coverage, with an average sequencing depth of coverage >500x and an analytical sensitivity of 5%. Tumor mutation burden and MSI status were compared using the two-sample t-test between tumor types. Frequency of mutations in each gene was compared between tumor types using the Fisher's exact test. To account for multiple comparisons, the False Discovery Rate was estimated using Benjamini-Hochberg procedure. R package "maftools" was used to summarize and visualize the findings.

Results: Mutation burden was higher in primary tumors with metastases versus primary tumors without metastases (p=0.034) while no significance was found in MSI status between these two groups.

Among the 20 mutated genes, MUC4 and MEN1 were the most frequently mutated genes in both primary and metastatic tumors (fig1&2). At a p-value threshold of 0.2, two distant metastatic tumors had mutation on PCNX3 gene, while none were found in lymph node metastases (p=0.057). In addition, more mutations on TGFBR1 in distant metastases compared to lymph node metastases (p=0.154). We also found that three primary tumors with metastases had mutations on E2F4, HRNR, LRP1B genes while none were found in primary tumors with no metastases (p=0.2).

Figure 1 - 1739

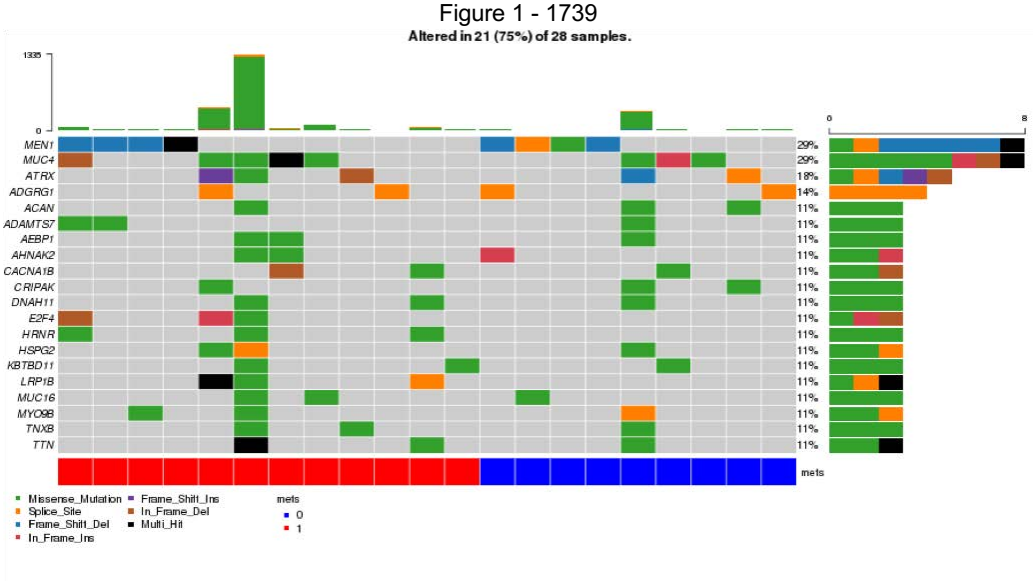

Figure 2 - 1739

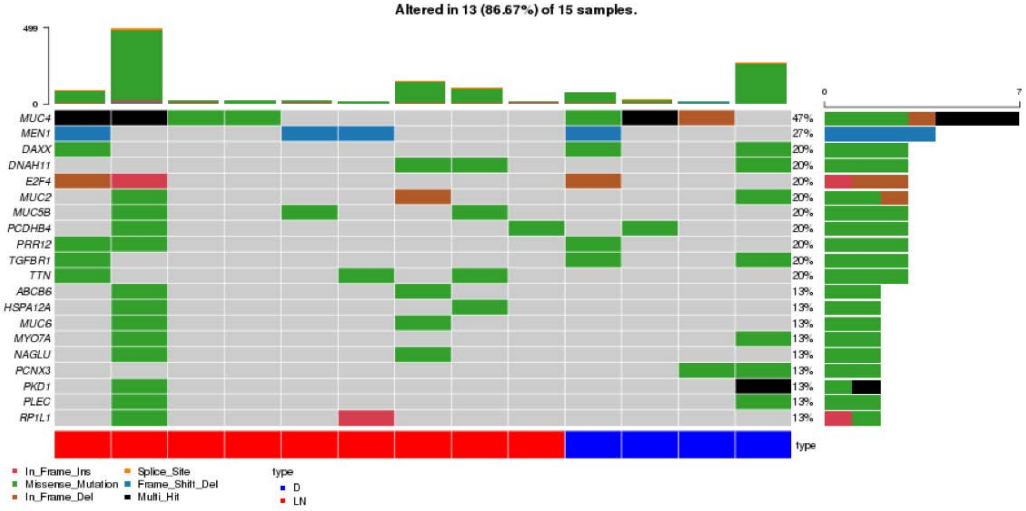

Conclusions: Decoding the complexity and unpredictable nature of PNET has been perplexing and the subject of many several research projects. The current project, the first ever done on the subject, with an attempt to distinguish the metastatic vs non-metastatic tumors try to underlie the difference of molecular signature between the two. Further studies are needed to consolidate the findings and bring them to clinical practice.

1740 Loss of Phosphomannose Isomerase Expression Associated with Worse Prognosis in Pancreatic Ductal Adenocarcinoma

Zahra Alipour[1], Diana Agostini-Vulaj[2], Jennifer Findeis-Hosey[2], Michael Drage[2], Lei Liu[3], Zhongren Zhou[4]
[1]Washington University in St. Louis, Clayton, MO, [2]University of Rochester Medical Center, Rochester, NY, [3]Washington University, St. Louis, MO, [4]Rutgers University, Ballwin, MO

Disclosures: Zahra Alipour: None; Diana Agostini-Vulaj: None; Jennifer Findeis-Hosey: None; Michael Drage: None; Lei Liu: None; Zhongren Zhou: None

Background: Pancreatic ductal adenocarcinoma (PDAC) is the fourth leading cause of cancer-related death in the United States. An unmet need exists to increase patient survival in PDAC. It is documented that adding mannose to conventional chemotherapy leads to accumulation of mannose metabolite in cancer cells, negates anti-apoptotic proteins of Bcl2 family and increases subsequent cell death. This susceptibility to mannose depends on the levels of phosphomannose isomerase (PMI); cancer cells with lower levels of PMI are more sensitive to mannose than cells with higher levels. Here, we aimed to investigate the association of PMI expression with clinical and pathological features of PDAC cases.

Design: PMI antibody immunohistochemistry was performed on tissue microarrays from 235 PDAC by a standard protocol on Ventana automated stainer. The PMI intensity was graded (0-3) and the proportion of positivity was scored. PMI expression were correlated with staging and survival at follow-up.

Results: Of the 235 cases, 51.5% (n=121) cases demonstrated grade 2 intensity with 90.1% of these (n=109) showing positivity in ≥70% of tumor cells. Ninety-eight (41.7%) cases exhibited grade 3 intensity with 94.9% (n=93) of these cases showing ≥70% reactivity. Sixteen cases (6.8%) were nonreactive (intensity grade 0-1). Intensity of PMI expression was significantly associated with better prognosis as assessed by median survival in months (M): Grade 0-1 intensity group: 11.2 M; grade 2 intensity group: 25.2 M; and grade 3 intensity group: 33.2 M (p=0.03).

Conclusions: A minority (6.8%) of PDACs show low PMI expression; mannose may be a particularly useful adjunct in this aggressive subgroup. PMI expression is also a potential biomarker to predict the prognosis.

1741 Pancreatic Neuroendocrine Neoplasms: A Comparison of the WHO 2010 and 2017 Classifications

Munita Bal[1], Aishwarya Sharma[1], Rajiv Kumar[2], Kedar Deodhar[3], Mukta Ramadwar[4]
[1]Tata Memorial Centre, Mumbai, India, [2]Mumbai, India, [3]Tata Memorial Hospital, Mumbai, Maharashtra, India, [4]Tata Hospital, Mumbai, MH, India

Disclosures: Munita Bal: None; Aishwarya Sharma: None; Rajiv Kumar: None; Kedar Deodhar: None; Mukta Ramadwar: None

Background: Pancreatic neuroendocrine neoplasms (PanNEN) encompass neoplasms ranging from well-differentiated neuroendocrine tumors (WDNET) to poorly-differentiated neuroendocrine carcinomas (PDNEC). Recently, the WHO 2010 classification was revised in 2017. We aimed to compare and correlate the WHO 2010 and 2017 classifications for grading of PanNENs with the outcome.

Design: A retrospective review of clinicopathologic features including the WHO 2010 and WHO 2017 classification of all PanNENs diagnosed from 2011-2017 and correlation with outcome was undertaken

Results: The study comprised 97 PanNENs. The median age was 52 years with M:F ratio of 1.3. Majority tumors were non-functional (88%). 40% patients had distant metastasis at presentation. With the use of WHO 2017, there was downgrading from G2 to G1 in 8 WDNET cases and reclassification from PDNEC to G3 WDNET in 8 cases. Grade change at the metastatic site was observed in 43% cases. Two-year overall survival was 96.4%; the event-free survival (EFS) at 12 months, 24 months was 92.5% and 90.7%, respectively Advanced T stage (p=0.017), distant metastasis (p=0.001), perineural invasion (p=0.019), nodal metastasis (p=0.001), R1 resection (p=0.017), mitotic rate (p=0.037), Ki-67 labeling (0.020), WHO 2010 grading (p=0.009) and WHO 2017 grading (p=0.014) significantly correlated with the EFS. Both grading systems (2010 and 2017) correlated with prognosis.

WHO 2010	n	WHO 2017	n
Well-differentiated grade 1, (WDNET G1)	29	Well-differentiated grade 1, (WDNET G1)	37
Well-differentiated grade 2, (WDNET G2)	53	Well-differentiated grade 2, (WDNET G2)	45
		Well-differentiated neuroendocrine carcinoma, grade 3, (WDNET G3)	8
Poorly-differentiated neuroendocrine carcinoma, grade 3, (PDNEC G3)	14	Poorly-differentiated neuroendocrine carcinoma, grade 3, (PDNEC G3)	6
Small cell carcinoma	*6*	*Small cell carcinoma*	*6*
Large cell neuroendocrine carcinoma	*0*	*Large cell neuroendocrine carcinoma*	*0*
Mixed adenoneuroendocrine carcinoma (MANEC)	1	Mixed neuroendocrine non-neuroendocrine neoplasm (MINEN)	1

Conclusions: PanNENs are rare albeit a heterogeneous group of neoplasms. Both classifications (2010 and 2017) were significantly associated with survival. However, grade migration and classification change occurred in a proportion of PanNENs with the use of WHO 2017 that has implications for treatment.

1742 Whipple-Ables: Clinicopathologic Comparison of 1032 Cancers Removed by Pancreatoduodenectomy Based on Pathologic Re-Review Using Refined Site-Specific Criteria

Serdar Balci[1], Michelle Reid[2], Ipek Erbarut Seven[3], Burcu Saka[4], Burcin Pehlivanoglu[5], Bahar Memis[6], Pelin Bagci[3], Olca Basturk[7], N. Volkan Adsay[8]
[1]Ankara, Turkey, [2]Emory University Hospital, Atlanta, GA, [3]Marmara University, Istanbul, Turkey, [4]Istanbul Medipol University, Istanbul, Turkey, [5]Adiyaman University Training and Research Hospital, Adiyaman, Turkey, [6]SBU Sisli Hamidiye Etfal Training and Research Hospital, Istanbul, Turkey, [7]Memorial Sloan Kettering Cancer Center, New York, NY, [8]Koç University Hospital, Istanbul, Turkey

Disclosures: Serdar Balci: None; Michelle Reid: None; Ipek Erbarut Seven: None; Burcu Saka: None; Burcin Pehlivanoglu: None; Bahar Memis: None; Pelin Bagci: None; Olca Basturk: None; N. Volkan Adsay: None

Background: The literature is highly conflicted on the differential clinicopathologic characteristics of cancers arising from different compartments of the ampulla-pancreato-biliary tract and duodenum that are removed by pancreatoduodenectomy (Whipple) operation, largely due to differences in the criteria employed (or lack thereof) in the site-specific classification of these cancers until recently. Lack of standardized grossing approaches and careful evaluation appear to be significant contributors to the controversy.

Design: Pathologic re-review of archival slides as well as reports (pathology reports and radiologic information) was performed in 1032 consecutive pancreatoduodenectomies (2004-2016) that had invasive carcinoma and adequate material. Grossing/sampling methods, surgical approaches and post-resection therapies were not-standardized in this retrospective review of archival material.

Results: In this Western cohort, using the more refined criteria, 71.4% of invasive carcinoma in Whipple resections were deemed pancreatic (PDAC), 21% ampullary (AC), 4.6% distal CBD (DBC) and 3% non-ampullary duodenal (NADC). There were significant differences in clinicopathologic characteristics (Table). NADC appeared to be slightly more common in men, the others did not show sex predilection. ACs were the smallest at diagnosis, followed by DBCs; and NADCs and PDACs were large. Lymph node metastases rate was the highest in NADCs (76.7%) and the lowest in ACs (50.7%). Perineurial invasion was common in PDACs & DBCs (84.8% & 91.5%) and much less in ACs & NADCs. LVI was most common in NADCs (80%) but relatively low on DBCs. There were also significant differences in survival (Figure), with PDACs and DBCs having highly similar outcome that is significantly more aggressive than NADCs and ACs.

	Ampulla	NADC	DBC	PDAC	Total	p-value
Gender (N)						0.006
Female	88	9	21	383	501	
Male	123	22	26	354	525	
Age, year	64.8	62.5	60.2	64.9	64.6	0.026
T Stage (N)						<0.001
T1	26	3	2	62	93	
T2	81	3	2	71	157	
T3	75	7	24	578	684	
T4	34	12	3	19	68	
T Group (N)						<0.001
Low (T1+T2)	107	6	4	133	250	
High (T3+T4)	109	19	27	597	752	
LN Metastasis (N)						0.003
Present	102	23	27	466	618	
Absent	99	7	18	266	390	
Invasion Size, mm	19.8	30.1	28.9	32.2	29.4	<0.001
PNI (N)						<0.001
Present	85	12	43	616	756	
Absent	132	18	4	110	264	
LVI (N)						0.004
Present	136	24	19	415	594	
Absent	81	6	28	252	367	
Margin (N)						<0.001
Negative	202	21	34	555	812	
Positive	10	0	10	179	199	

Figure 1 - 1742

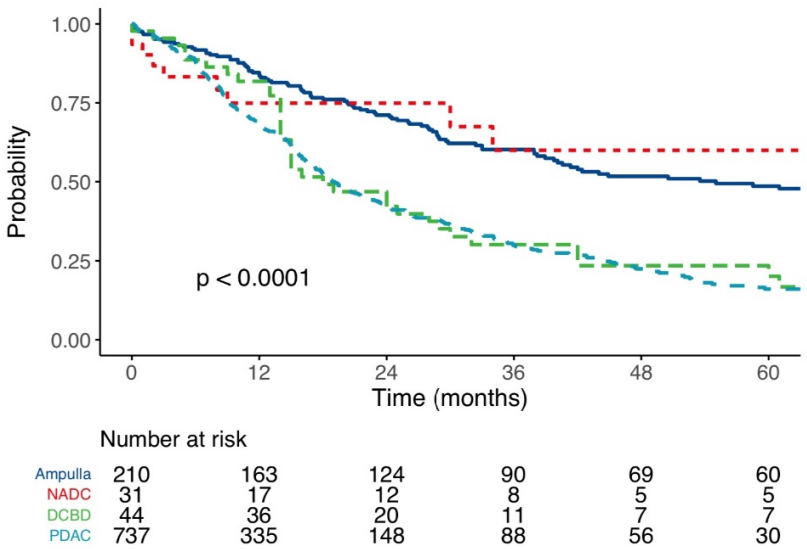

Conclusions: Although certain crucial parameters such as grossing/sampling were not standardized, this review of archival material nonetheless provides important clues to the different clinicopathologic characteristics of cancers of the “peri-ampullary region” (Whipple-ables). In contrast to the current impression in the literature, DBCs are as aggressive as PDACs. NADCs are large tumors with very high propensity for LVI, and are fairly aggressive cancers, far more so than colorectal cancers, but less than PDACs/DBCs. ACs are incomparably better than any other “Whipple-ables” partly due to their R0 resectability and early detection.

1743 A Proposal for Improved T-Staging of Pancreatic Ductal Adenocarcinoma by Using Microscopic Examination as the Basis for Determining the Size and T-Stage

Olca Basturk[1], Michelle Reid[2], Serdar Balci[3], Ipek Erbarut Seven[4], Burcu Saka[5], Burcin Pehlivanoglu[6], Bahar Memis[7], Pelin Bagci[4], N. Volkan Adsay[8]
[1]Memorial Sloan Kettering Cancer Center, New York, NY, [2]Emory University Hospital, Atlanta, GA, [3]Ankara, Turkey, [4]Marmara University, Istanbul, Turkey, [5]Istanbul Medipol University, Istanbul, Turkey, [6]Adiyaman University Training and Research Hospital, Adiyaman, Turkey, [7]SBU Sisli Hamidiye Etfal Training and Research Hospital, Istanbul, Turkey, [8]Koç University Hospital, Istanbul, Turkey

Disclosures: Olca Basturk: None; Michelle Reid: None; Serdar Balci: None; Ipek Erbarut Seven: None; Burcu Saka: None; Burcin Pehlivanoglu: None; Bahar Memis: None; Pelin Bagci: None; N. Volkan Adsay: None

Background: Stage remains as the most helpful prognosticator in pancreatic ductal adenocarcinoma (PDAC). However, accurate gross measurement of PDAC tumor size, the main stage parameter, is a well-known challenge due to its notoriously ill-defined nature. It has been well documented that there are often satellite microtumor foci beyond the grossly appreciated tumor (PMID: 26832882), which in fact may represent intraparenchymal metastases. This becomes a bigger challenge if the gross room personnel are not experienced enough for the subtleties of PDAC.

Design: 354 pancreatoduodenctomies performed with ordinary therapy-naive PDAC processed with the orange-peeling/axial-sectioning (PMID: 18820663 and 24451278) methods were re-evaluated by the authors microscopically for the spread of the tumor to anterior and posterior orange peeled soft tissues dissected during the processing of the specimen. The cases that had had been classified as T1/T2 but had carcinoma foci by microscopic examination involving *both* the anterior and posterior soft tissues were concluded to be > 4 cm in and thus moved to the T3 category based on the microscopic findings.

Results: There were 37 cases that had been recorded as < 4 cm in the gross room (and thus officially staged as T1/T2) but revealed microfoci of carcinoma documented in *both* the posterior and anterior orange-peeled soft tissues. This group had a survival rates significantly worse than the rest of the T2 group (p<0.0001) and was very comparable to the T3 group (Figure). Along those lines, the node positivity rate for this group was 89% as opposed to 70% of the rest of the T2 group (p=0.015, significant after Bonferroni correction). Moreover, this rate was comparable (even higher) than the 86% of the T3 category (p=0.7771).

Figure 1 - 1743

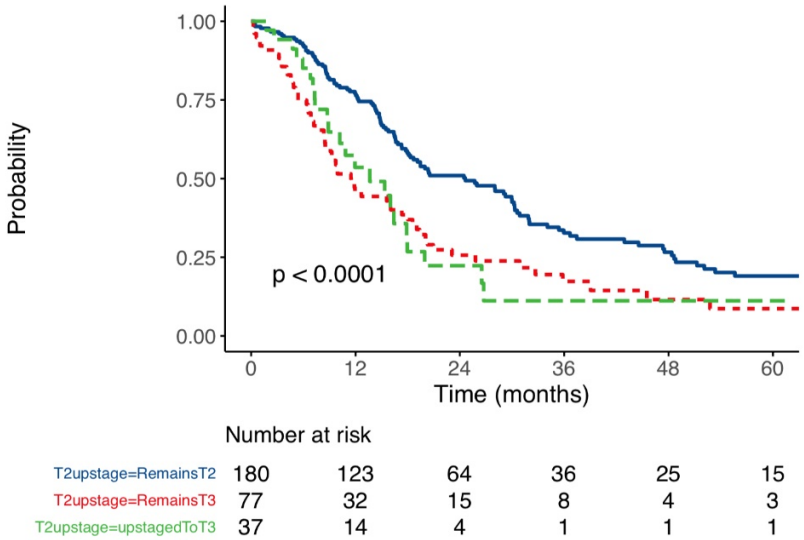

Conclusions: Microscopic correction is warranted in determining the true extent/size of carcinoma in PDACs. In cases with microcarcinoma foci identified in *both* the anterior and posterior soft tissues close to the surfaces, the real size of the tumor can be presumed to be > 4 cm and thus staged as T3 even if the macroscopic examination gave the impression of a smaller tumor. Such cases behave indeed like T3 category therefore, they warrant reporting as “estimated size (by gross-micro) correlation is > 4 cm (pT3)”.

1744 Comparison of the Axial and Bivalve Approach for Staging of Pancreatic Ductal Adenocarcinoma Pancreatoduodenectomy Specimens, a Single-Institution Experience

Phoenix Bell[1], Diana Agostini-Vulaj[1], Mark Ettel[2], Michael Drage[1]
[1]University of Rochester Medical Center, Rochester, NY, [2]University of Rochester, Rochester, NY

Disclosures: Phoenix Bell: None; Diana Agostini-Vulaj: None; Mark Ettel: None; Michael Drage: None

Background: Accurate orientation and gross examination of pancreatoduodenectomy specimens (PDEs) is critical for tumor staging, margin assessment, and prognostication for patients with pancreatic ductal adenocarcinoma (PDAC). There is currently no standardized approach to PDE dissection. In the United States, the bivalve (BV) method (in which the specimen is cut along the plane of the common bile duct (CBD) and main pancreatic duct) predominates. Some European institutions have recently adopted the axial (AX) approach in which the specimen is sectioned in the axial plane, reporting enhanced sensitivity for detection of positive margins. In 2017, our institution converted from the BV to the AX approach for PDEs with solid lesions. We report our experience applying the AX method and the differences in resultant stage classification between the two approaches.

Design: We retrospectively reviewed 336 cases of PDAC removed by PDE (1998-2019) and compared gross tumor size, lymph node number and status, margin status, T stage, N stage, and number of tissue blocks between the two groups. Statistical analyses were performed using Fisher's exact test, Kruskal-Wallace H test, and t-test. *P* values < 0.05 were considered significant.

Results: The 336 cases included 54 (16%) and 282 (84%) grossed via the AX and BV methods, respectively. 29% of cases received neoadjuvant therapy in the AX group compared to only 10% in the BV group (p<0.001). Positive margin status was more likely in AX than BV method (p<0.001), whereby the PV margin was more often positive in the AX method (p<0.001). There was no difference in status of other margins, including pancreatic neck, CBD, uncinate, and posterior surfaces (p=0.216, p=1, p=0.135, p=0.807, respectively). Total lymph nodes harvested and number of positive lymph nodes were higher in the AX than BV method (p<0.001 and p=0.01), corresponding to a higher N stage (p=0.006). The number of tissue blocks processed was higher in the AX than BV method (p<0.001). There was no significant difference in tumor size (p=0.458) or T stage (p=0.707) (Table 1).

	Axial	Bivalve	p-value
Tumor gross size (cm), *mean ± sd*	3.41 ± 1.00	3.29 ± 1.55	0.458
Positive lymph nodes, *mean ± sd*	4.5 ± 4.6	2.7 ± 3.3	0.010
Total lymph nodes, *mean ± sd*	25.0 ± 8.7	16.4 ± 10.1	<0.001
Margin status (all margins), *n (%)*			<0.001
R0	10 (18.5)	146 (51.8)	
R1	44 (81.5)	136 (48.2)	
Neck margin status, *n (%)*			0.216
Negative	43 (79.6)	242 (86.1)	
Positive	11 (20.4)	39 (13.9)	
Bile duct margin status, *n (%)*			1
Negative	53 (98.1)	271 (97.5)	
Positive	1 (1.9)	7 (2.5)	
Portal vein margin status, *n (%)*			<0.001
Negative	20 (40)	66 (70.2)	
Positive	30 (60)	28 (29.8)	
SMA margin status, *n (%)*			0.135
Negative	36 (67.9)	124 (79.0)	
Positive	17 (32.1)	33 (21.0)	
Posterior margin status, *n (%)*			0.807
Negative	33 (75)	29 (70.7)	
Positive	11 (25)	12 (29.3)	
pT stage (TNM 8), *n (%)*			0.707
1a	0 (0)	2 (0.7)	
1b	0 (0)	0 (0)	
1c	2 (3.7)	33 (11.8)	
2	43 (79.6)	185 (66.1)	
3	9 (16.7)	58 (20.7)	
4	0 (0)	2 (0.7)	
pN stage (TNM 8), *n (%)*			0.006
0	11 (20.8)	82 (29.1)	
1	16 (30.2)	126 (44.7)	
2	26 (49.1)	74 (26.2)	
Tissue blocks sampled, *mean ± sd*	32.1 ± 9.6	22.9 ± 8.6	<0.001

Conclusions: The AX method provides a consistent approach to PDE dissection that is not altered by variable anatomy, facilitates correlation with imaging studies performed in the axial plane, and in our experience reveals more positive margins and provides a greater lymph node yield. We recommend widespread adoption of the AX approach for gross examination of PDE specimens removed for solid primary pancreatic lesions.

1745 Pancreatoblastomas and Acinar Cell Carcinomas Share Epigenetic Signatures Distinct from Other Neoplasms of the Pancreas

Jamal Benhamida[1], Monika Vyas[2], Olca Basturk[3], Lu Wang[4], Armita Bahrami[5], Liliana Villafania[3], Justyna Sadowska[6], Pier Selenica[3], Nitya Raj[3], Britta Weigelt[3], Jorge Reis-Filho[3], Maurizio Scaltriti[3], David Klimstra[3]
[1]Memorial Sloan Kettering Cancer Center, New York City, NY, [2]Beth Israel Deaconess Medical Center, Harvard Medical School, Newton MA, MA, [3]Memorial Sloan Kettering Cancer Center, New York, NY, [4]St Jude Children's Research Hospital, Memphis, TN, [5]St. Jude Children's Research Hospital, Memphis, TN, [6]New York, NY

Disclosures: Jamal Benhamida: None; Monika Vyas: None; Olca Basturk: None; Lu Wang: None; Armita Bahrami: None; Liliana Villafania: None; Justyna Sadowska: None; Pier Selenica: None; Nitya Raj: None; Britta Weigelt: None; Jorge Reis-Filho: None; Maurizio Scaltriti: *Grant or Research Support*, Puma Biotechnology; *Grant or Research Support*, Daiichi-Sankio; *Consultant*, Menarini Ricerche; *Grant or Research Support*, Targimmune; *Grant or Research Support*, Immunomedics; David Klimstra: None

Background: Pancreatic neoplasms are a heterogeneous group with differentiation along ductal, neuroendocrine, acinar, and undefined lines. Some pancreatic neoplasms with divergent differentiation share key genomic drivers, whereas others with similar differentiation patterns are genomically quite distinct. Genome-wide methylation profiling has been successfully utilized for distinguishing cellular differentiation as well as providing a classification system for certain classes of tumors. In this study we explore the relationship between histopathologic diagnostic classes and genome-wide DNA methylation patterns with an emphasis on defining the methylation signature of pancreatoblastomas and acinar cell carcinomas vis-à-vis other solid tumors of the pancreas.

Design: We obtained 38 primary neuroendocrine tumors (PanNETs; 21 grade 1, 15 grade 2, 2 grade 3), 13 acinar cell carcinomas (ACCs) including both pure and mixed (neuroendocrine and ductal) variants, 13 solid pseudopapillary neoplasms (SPNs), and 16 pancreatoblastomas (PBs) from our institutions' archives. The H&E slides were reviewed and DNA was processed on the Infinium methylation EPIC (850k) platform. Additionally, methylation profiles of 10 ductal adenocarcinomas (DAs) were obtained from the TCGA. Data were analyzed with R using the minfi package and dimensionality reduction (t-SNE) was performed using the Rtsne package on the 10,000 most variably methylated CpG sites (by variance). Cross-reactive probes, probes targeting the sex chromosomes, and failed probes were excluded from analysis.

Results: Three pancreatoblastoma samples were removed from the analysis due to poor sample quality metrics. Clustering on the remaining tumors' methylation profiles demonstrated 4 distinct clusters (figure 1). Cluster #1 was comprised of all the PanNETs and 1 DA; Cluster #2 contained all of the ACCs and PBs; Cluster #3 contained the remaining 9 DAs and 1 SPN; and cluster #4 contained the remaining 12 SPNs.

Figure 1 - 1745

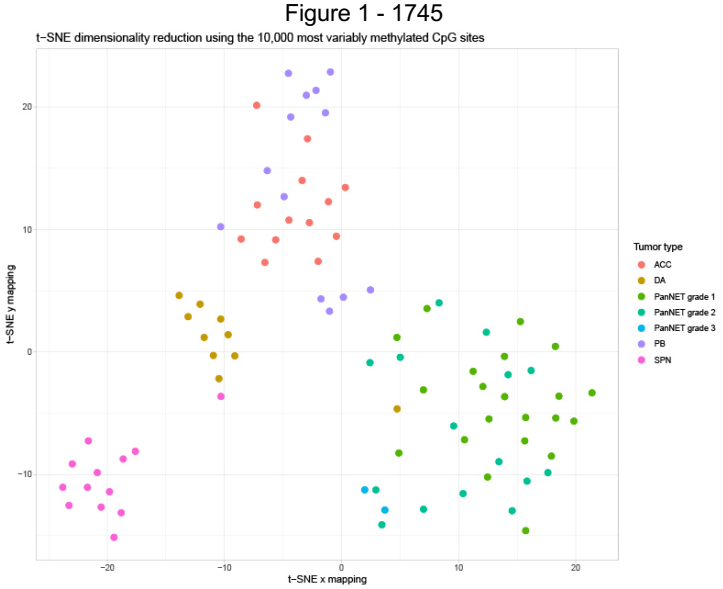

Conclusions: DAs, PanNETs (irrespective of grade) and SPNs each cluster largely independently based on methylation profiling. PBs and ACCs share epigenetic signatures, suggesting similar differentiation and origins. Mixed acinar carcinomas with ductal or neuroendocrine elements possess a methylation pattern similar to pure ACCs. This study sheds light on the origin and differentiation of these neoplasms and demonstrates the utility of high-throughput epigenetic platforms in refining tumor classification.

1746 Pancreatic Frozen Section Guides Operative Management with Rare Deferrals and Errors; Five Year Experience at a Large Academic Institution

Jesus Chavez[1], Wei Chen[2], Wendy Frankel[2]
[1]The Ohio State University, Marble Cliff, OH, [2]The Ohio State University Wexner Medical Center, Columbus, OH

Disclosures: Jesus Chavez: None; Wei Chen: None; Wendy Frankel: None

Background: Pancreatic adenocarcinoma (Adc) is the 4th cause of cancer death in the US, with an overall poor survival. Surgery remains the only possible curative treatment, and frozen section (FS) analysis is useful to confirm diagnosis and help surgeons determine resectability and margin status. Our goal was to evaluate the current status of FS and how diagnoses impact the surgical procedure.

Design: We reviewed patients with planned pancreatic resections between 1/2014 and 3/2019 where at least 1 FS was performed. Pathology reports including FSs, cytology, and operative notes were reviewed. FSs were categorized as margin, primary diagnosis, metastasis or vascular resectability. We noted deferrals, errors and surgeons' response to FSs. Surgeons' response was considered expected if they aborted resection for metastasis or additional tissue was taken with a positive margin.

Results: We identified 898 planned pancreatic resections and reviewed the 155 (17%) with FS. A total of 222 FSs (1-5/case, 1.4 mean) were performed for 102 margin assessments (59 pancreatic, 37 bile duct, 6 uncinate), 21 primary diagnoses, 95 metastatic lesions (70 liver, 7 lymph node, 18 other) and 4 to confirm vascular resectability (Table 1). Final diagnoses in cases with FSs included: 93 pancreatic Adc, 21 cystic tumors or pseudocysts, 17 bile duct Adc, 9 chronic pancreatitis, 4 ampullary Adc, 2 neuroendocrine tumors, and 9 others. Preoperative cytology was performed in 73 (47%) cases and was diagnostic of Adc in 53. The diagnosis was deferred to permanent sections (PS) in 10 FS (5%): 4 were for metastasis evaluation (the surgeon aborted 2 cases due to intraoperative findings and resected the other 2), 4 were for margin evaluation (additional tissue was taken in 3/4 cases), while both cases for primary diagnosis were resected based on clinical concern for Adc. Discrepancy/errors between FS and PS were identified in 2 (0.9%); FS Adc with PS bile duct hamartoma, and FS negative uncinate margin with PS Adc. Surgeons' response was different than expected in 8 (4%) FS, but their actions were explained by other intraoperative findings in 7/8.

Table 1. Frozen Section Category, Deferrals, Errors and Surgical Response

FS Category (n=222)	Definitive diagnosis	Deferral	*FS diagnostic error	*Surgical response not consistent with FS
Primary diagnosis	19	2	0	1
Resectability	4	0	0	1
Metastasis	91	4	1	3
Margin status	98	4	1	3
Total	212 (95%)	10 (5%)	2 (1%)	8 (4%)

*Only for cases with definitive diagnosis.

Conclusions: During pancreatectomy, FS is an important diagnostic tool used primarily for liver metastasis and margins. In most cases, a definitive diagnosis is rendered with only occasional deferrals and very rare errors. Surgeons act on our diagnosis almost all the time, and other intraoperative findings explain most cases where they act differently than expected based on FS diagnosis.

1747 Prevalence of Histological Features Resembling Autoimmune Pancreatitis in Pancreas Resection Specimens

Lina Chen[1], Christine Orr[2], Tao Wang[2]
[1]Queen's University, Kingston, ON, [2]Queen's University/Kingston Health Sciences Centre, Kingston, ON

Disclosures: Lina Chen: None; Christine Orr: None; Tao Wang: None

Background: Autoimmune pancreatitis (AIP) is a mimicker of pancreatic neoplasia. There are two types of AIP. Type 1 is an IgG4-related disease; type 2 is associated with neutrophilic duct-centric inflammatory lesions known as granulocytic epithelial lesions. Diagnosis on biopsy can be critical to management, but the quantity of tissue in pancreas biopsies is often scant. Occasionally, inflammatory features are seen in mass-targeted biopsies that raise the differential of AIP. However, the frequency of AIP-like histology in pancreas with other

pathologies, including neoplasia, is poorly characterized. The specificity of inflammatory lesions on biopsy with respect to the diagnosis of AIP is uncertain.

Design: Pancreas resections performed at our institution between 2014 to 2019 are reviewed. Features of AIP, including dense lymphoplasmacytic infiltrates, obliterative venulitis, storiform fibrosis, and granulocytic epithelial lesions are assessed in non-neoplastic areas. Inflammation in malignant glands or dysplasia is not considered an AIP mimicking feature. Chronic pancreatitis without any neutrophilic or dense lymphoplasmacytic infiltrates is also not considered a mimicker of AIP. If features of IgG4 associated AIP are seen, IgG4 and IgG immunohistochemistry is performed.

Results: Of the 100 pancreas resections, one was diagnosed as AIP type 1; none were diagnosed as AIP type 2. There were 45 pancreatic adenocarcinoma, 10 ampullary/duodenal adenocarcinoma, 13 neuroendocrine tumors, 6 distal bile duct carcinoma, 5 intraductal papillary mucinous neoplasms, 4 metastatic carcinoma, 3 mucinous cystic neoplasms, 11 other neoplasms, and 3 nonneoplastic cases. In the neoplastic cases, seventeen were found to have one or more types of inflammatory lesions in non-neoplastic pancreatic tissue. Dense lymphoplasmacytic inflammation mimicking type 1 AIP was found in 3 cases (IHC pending). Neutrophilic infiltrates in lobulated small ductules were found in 9 cases. Mild neutrophilic ductitis or microabscess was found in 7 cases. Marked neutrophilic duct destruction that resembled granulocytic epithelial lesions was found in 6 cases.

Conclusions: Approximately 18% of the pancreas resections showed foci that could raise the differential of autoimmune pancreatitis if sampled on a biopsy, and some showed areas that closely resembled granulocytic epithelial lesions. Pathologists should be cautious about making a diagnosis of AIP on biopsies based on histological findings alone.

1748 Expression of PD-L1, PD1 and Her2 neu in Gall Bladder Carcinomas: Experience from a Tertiary Care Centre in India

Prasenjit Das[1], Sudha Battu[2], Vandana Baloda[3], Ranjit Sahoo[4], Atul Sharma[4], Siddhartha Datta Gupta[2]
[1]New Delhi, India, [2]All India Institute of Medical Sciences, New Delhi, India, [3]AIIMS New Delhi, New Delhi, Delhi, India, [4]All India Institute of Medical Sciences, New Delhi, Delhi, India

Disclosures: Prasenjit Das: None; Vandana Baloda: None

Background: India has a high incidence of gall bladder carcinomas (GBCas) with poor overall survival. In the era of targeted therapy and available biologicals, it is important to study the expression of actionable immune-check point inhibitors and tumor markers for personalizing treatment.

Design: FFPE blocks of 132 cases of GBCa, who underwent surgical resection were included and immunohistochemical stains for PD-L1, PD1, CD8+ T cells and Her2 neu were performed. The PD-L1 and PD1 stain positivity were scored (P-score) in tumor cells, intra-tumoral, peritumoral stromal and immune cells at infiltrative margin as follows: score 0, no stained cells; score 1, ≤5% of cells showing membranous positivity; score 2, >5% to ≤50%; and score 3, >50% cell positivity. For the correlation analysis, P-scores of 2 and 3 were regarded as positive. The abundance of TILs was evaluated by examining five representative high-power fields under 400x magnifications and the cell counts were averaged. Her2neu positivity was also scored as 1+: incomplete basolateral membrane positivity, 2+: incomplete membranous positivity noted in >10% tumor cells and 3+: complete membranous positivity in >10% tumor cells. The immune expressions were compared with clinical parameters of aggressiveness and survival data.

Results: In our cohort the following pattern of positivity were seen in tumor: PD-L1- 96/132 (72.7%), PD1- 87/111 (78.3%), Her2 neu- 15/130 (11.5%), CD8+ tumor infiltrating lymphocytes (TILs)- 59/91 (64.8%). In PD-L1+ GBCa, PD-L1+ stromal TILs and TILs at infiltrative tumor margin were significantly more (0.01 & 0.001 P values respectively). More number of lymph node metastasis was also noted in PD-L1+ GBCas (P 0.06). There was no definite correlation of PD-L1 expression in tumors with overall TIL density, PD1 expression in tumor or immune cells, tumor grade, type, T-stage, stage groups, lymphovascular and perineural invasion, positive tumor margin status, tumor necrosis, or progression free survival. Presence of PD1+ intra-tumoral TILs was associated with low median survival in GBCa (P 0.06). Tumor grade, T-stage, nodal status and stage groups were found to be independent marker of median survival. Her2 neu+ tumors did not show any survival benefit over Her2neu negative GBCas.

Figure 1 - 1748

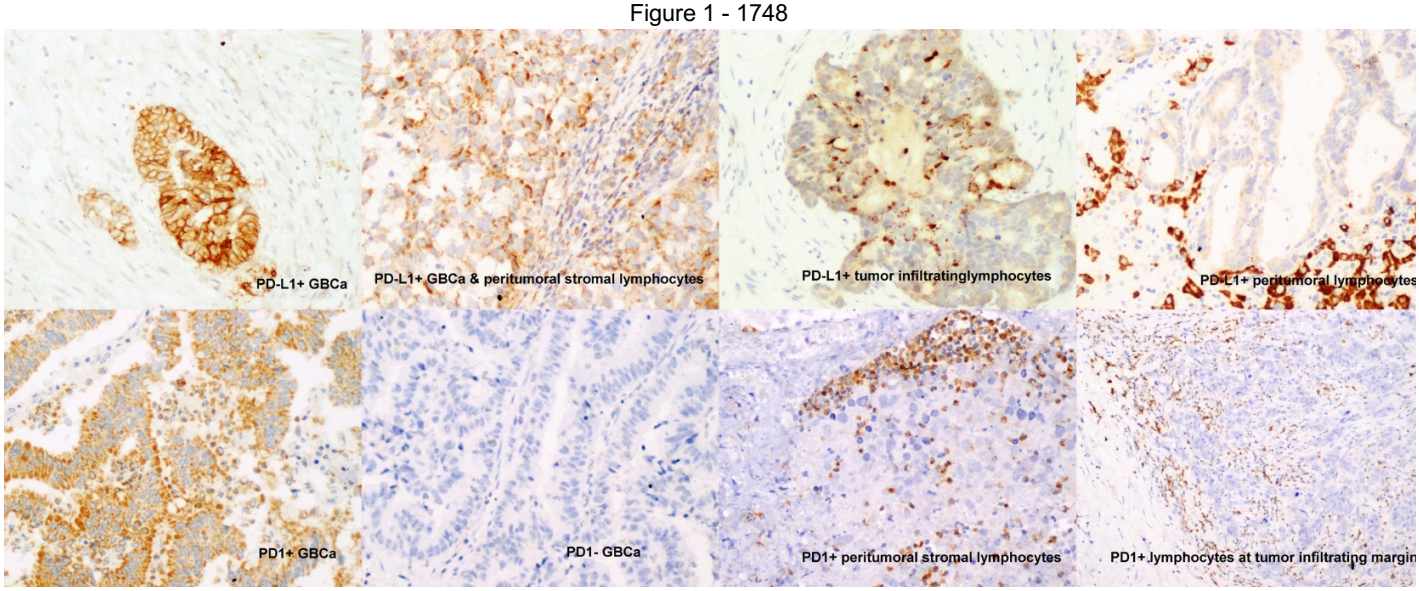

Figure 2 - 1748

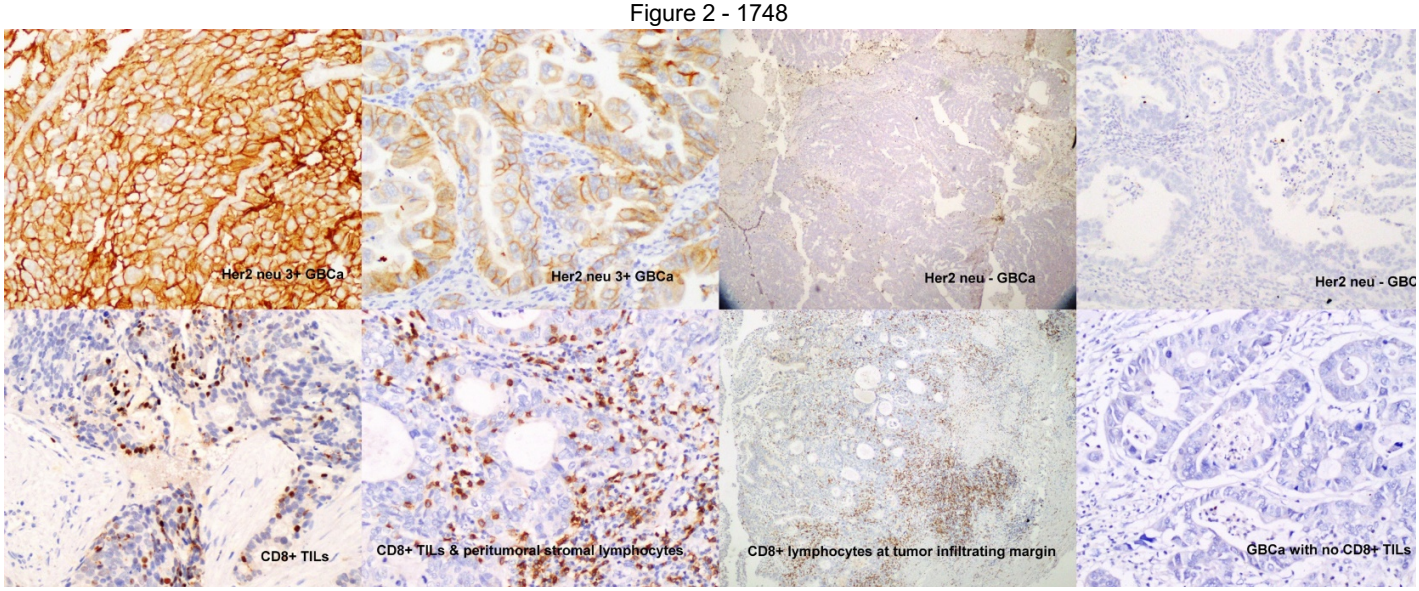

Conclusions: High expression of PD-L1 and PD1 in GBCa raise a possibility that check-point inhibitors may be beneficial in these patients. Though, PDL1+ TILs was associated with low median survival, no distinct correlation of Her2 neu+ and median survival.<

1749 Immunohistochemical and mRNA Analysis of SATB2 Expression in Neuroendocrine Neoplasms of Pancreas and Midgut

Simona De Michele[1], Igor Katsyv[2], Sonya Purushothaman[3], Helen Remotti[4]
[1]Columbia University Medical Center/New York Presbyterian Hospital, New York, NY, [2]Columbia University/New York Presbyterian Hospital, New York, NY, [3]New York, NY, [4]Columbia University Medical Center, New York, NY

Disclosures: Simona De Michele: None; Igor Katsyv: None; Sonya Purushothaman: None; Helen Remotti: None

Background: Neuroendocrine neoplasms include both well differentiated neuroendocrine tumors (NET) and poorly differentiated neuroendocrine carcinomas (NEC). Special AT-rich sequence-binding protein 2 (SATB2) is a transcriptional regulator highly expressed in the lower gastrointestinal mucosa, adenocarcinomas and neuroendocrine tumors of the same site. Discordant SATB2 immunohistochemical (IHC) staining has been reported in midgut NET/mNET (0 to 48%) and pancreatic NET/pNET (0 to 15%). Very limited data is available for pancreatic NEC/pNEC. In this study, we assessed SATB2 IHC expression in a cohort of pancreatic neuroendocrine neoplasms of different levels of differentiation, in addition to mNET. RNA expression data was not available for this cohort; SATB2 mRNA expression was evaluated in a separate cohort of pNET and mNET.

Design: IHC for SATB2 (clone EP281) was performed on tissue microarrays (Fig.1) of 54 pNET and 8 pNEC, in addition to 30 cases of mNET. A minimum of 4 separate 2mm tumor cores were sampled on each case. SATB2 IHC was scored for extent (%) and intensity (0-3+) with an H-score calculated. RNA-sequencing data (GSE98894) was downloaded from the NCBI Gene Expression OmniBus. Expression data was normalized for library size, lowly-expressed transcripts were removed, and the data was transformed to log2 counts per million (log2CPM). Differentially-expressed genes were called using the edgeR (v 3.24.3) and limma (v 3.38.3) R packages.

Results: Positive SATB2 staining (defined as >2% nuclear staining) was identified in 2% (1 of 54 cases) of pNET (H-score 50) and 25% (2 of 8 cases, mean H-score 125) of pNEC. SATB2 staining was positive in 53% (16 of 30) of mNET (mean H-score of 78). SATB2 mRNA was expressed 3.43-fold higher in mNET (Fig.2) compared to pNET (FDR < 0.01).

Table 1. Number and Percentage of Midgut and Pancreatic Neuroendocrine Neoplasms Showing Positivity for SATB2

Location	Number of cases	Total SATB2+ cases (%)	Mean H-score
mNET	30	16 (53)	78
pNET	54	1 (2)	50
pNEC	8	2 (25)	125

Figure 1 - 1749

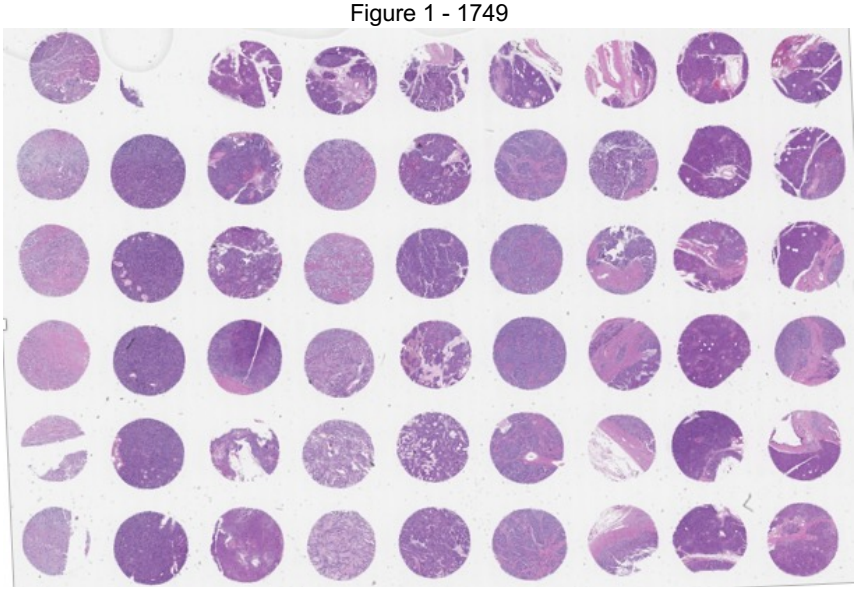

Figure 2 - 1749

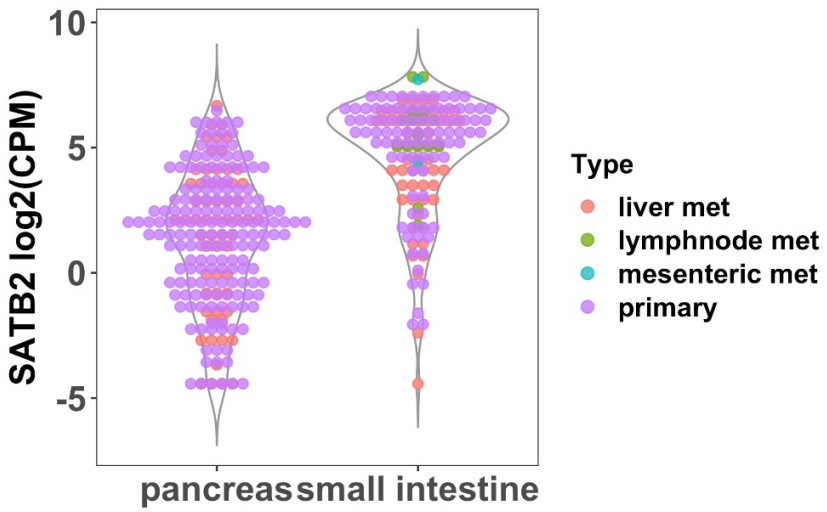

Conclusions: Higher SATB2 mRNA expression was identified in mNET compared to pNET, which correlates with IHC results. Furthermore, based on IHC, SATB2 was more commonly expressed in pNEC vs pNET. More studies and a larger cohort of cases are needed to establish SATB2 expression in pNEC. Ultimately, SATB2+ pNET are rare (<2%); while mNET commonly show SATB2 IHC staining, and should therefore be included in the differential of SATB2+ NET metastasis.

1750 Inter-Observer Variability and Challenges in Intraoperative Assessment of Pancreatic Resection Margins

Sadhna Dhingra[1], Maria Machado Heredia[1], Melissa Taggart[2], Wai Chin Foo[2], Asif Rashid[2], Sarah May[1], Huamin Wang[2]
[1]Baylor College of Medicine, Houston, TX, [2]The University of Texas MD Anderson Cancer Center, Houston, TX

Disclosures: Sadhna Dhingra: None; Maria Machado Heredia: None; Asif Rashid: None; Sarah May: None

Background: Pancreas resection with negative margins (R0 resection) is the optimal treatment for patients with resectable pancreatic ductal adenocarcinoma (PDAC). Multiple studies have shown that extending the resection to convert a positive pancreatic neck margin (R1 resection) to R0 resection does not improve overall survival. However, the practice continues as R0 resection is a quality metric for surgeons. Frozen section evaluation of this margin is challenging because of the difficulty in differentiating infiltrating tumor from chronic pancreatitis, which often accompanies PDAC. In addition, the frozen section artifact and neoadjuvant therapy further compounds the difficulty in assessment. There are limited studies in literature determining the accuracy of frozen section analysis. This study is to determine the inter-observer variability among gastrointestinal (GI) pathologists for assessment of frozen section of pancreatic neck margin.

Design: Forty-five patients who underwent pancreas resection for PDAC, and had marked chronic pancreatitis changes at pancreas resection margin were selected for study. There were 27 males and 18 females with a mean age of 66 years (range 47-73). Twenty-seven patients received neoadjuvant chemotherapy. Decoded frozen section slides of pancreatic neck margin from each case were reviewed by 5 GI pathologists who have practiced at academic institutions for 5 years to 25 years. Each pathologist independently assessed for “presence” or “absence” of carcinoma, and for “presence” and “absence” of high grade dysplasia (HGD). The results were collated and inter-observer agreement amongst pathologists was calculated as kappa co-efficient. All pathologists jointly reviewed the discordant cases and consensus was used as the final diagnosis. The permanent section of the frozen tissue was considered as the gold standard for final diagnosis.

Results: Of 45 cases, 34 were negative for carcinoma and 11 positive for carcinoma on permanent sections of margin . On frozen section review, carcinoma missed in 5 cases, overcalled in 1, and HGD missed in 2 cases by at least one pathologist. Overall, sensitivity was 83% and the specificity was 100%.

	% agreement	Fleiss’ kappa	Brennan-Prediger kappa coefficient
Carcinoma	87	0.78	0.86
HGD	96	0.37	0.96

Conclusions: Excellent interobserver agreement is noted amongst GI pathologists for reading of both carcinoma as well as HGD in frozen pancreas margin. Missed carcinoma was due to overlooking a tiny focus of cancer in the background of marked chronic pancreatitis. Evaluation of levels and permanent sections led to perfect agreement.

1751 Quantitative, Multiplexed Analysis of the Pancreatic Cancer Microenvironment Reveals Prognostic Significance for T cell Subset Densities and Spatial Distribution

Andressa Dias Costa[1], Chen Yuan[1], Sara Väyrynen[1], Juha Väyrynen[1], Hannah Williams[1], Vicente Morales-Oyarvide[1], Mai Chan Lau[2], Douglas Rubinson[1], Richard Dunne[3], Margaret Kozak[4], Wenjia Wang[5], Diana Agostini-Vulaj[5], Daniel Chang[6], Shuji Ogino[2], Brian Wolpin[1], Jonathan Nowak[2]
[1]Dana-Farber Cancer Institute, Boston, MA, [2]Brigham and Women's Hospital, Boston, MA, [3]University of Rochester, Rochester, NY, [4]Stanford Cancer Institute, Palo Alto, CA, [5]University of Rochester Medical Center, Rochester, NY, [6]Stanford Cancer Institute, Stanford, CA

Disclosures: Andressa Dias Costa: None; Chen Yuan: None; Sara Väyrynen: None; Juha Väyrynen: None; Hannah Williams: None; Vicente Morales-Oyarvide: None; Mai Chan Lau: None; Douglas Rubinson: None; Richard Dunne: None; Margaret Kozak: None; Wenjia Wang: None; Diana Agostini-Vulaj: None; Daniel Chang: None; Shuji Ogino: None; Brian Wolpin: *Consultant*, Grail; *Consultant*, Celgene, Inc; *Consultant*, BioLineRx; Jonathan Nowak: None

Background: T lymphocytes are a prominent component of the tumor microenvironment and play a key role in driving the anti-tumor immune response in many tumor types. Pancreatic adenocarcinoma (PDAC) is a tumor type that has been notably resistant to treatment with immunotherapy and harbors incompletely characterized T lymphocyte populations. To better define the significance and composition of T lymphocytes in PDAC, we developed a novel multiplex assay to enable deep T cell phenotyping in a multi-institutional cohort of primary, resected PDAC specimens with extensive clinicopathologic and genomic characterization.

Design: Tumors (n=299) were analyzed using a panel of antibodies directed against CD3, CD4, CD8, FOXP3, CD45RO, and cytokeratin. Multispectral immunofluorescent images of tissue microarrays were computationally processed to calculate T cell subpopulation densities in tumor and stroma. Multivariable Cox proportional hazard regression models were used to assess prognostic

associations of quartile categories of T cell subset densities, adjusting for potential confounders, including age, sex, tumor characteristics, perioperative treatment, and institution.

Results: T lymphocytes were more abundant in peritumoral stromal regions (median 393 $CD3^+$ cells/mm^2) than in tumor intraepithelial regions (median 66 $CD3^+$ cells/mm^2). Higher overall T cell density was associated with longer overall survival (OS) (Q4 vs. Q1: Hazard Ratio (HR) 0.69, 95% CI 0.48-1.00, P_{trend}=0.02) and disease-free survival (DFS) (Q4 vs. Q1: HR 0.64, 95% CI 0.44-0.94, P_{trend}=0.02). This association was driven predominantly by $CD3^+CD4^+$ T helper cells present within tumor stroma (OS Q4 vs. Q1: HR 0.69, 95% CI 0.48-1.00, P_{trend}=0.02; DFS Q4 vs. Q1: HR 0.69, 95% CI 0.47-1.01, P_{trend}=0.04). Notably, $CD3^+CD8^+$ cytotoxic T cell density was not significantly associated with survival. Higher overall T cell density was associated with R0 resection status (P=0.03) and N1 nodal status (P=0.04). No statistically significant associations were identified with *KRAS*, *TP53*, *SMAD4*, *CDKN2A*, or *ARID1A* driver gene status or tumor mutational burden.

Conclusions: T lymphocytes are abundant in the PDAC microenvironment. Higher overall T lymphocyte density is associated with better survival, and this effect may be mediated by stromal T helper cells rather than cytotoxic T cells. PDAC driver gene status is not associated with T cell density, suggesting that non-genomic factors may instead govern this aspect of the PDAC immune microenvironment.

1752 Demographic, Pre-Operative, and Grossing Parameters Can Efficiently Triage Gallbladder Resected for Non-Neoplastic Disease for Pathological Analysis

Philippe Echelard[1], Yves Collin[2], Sameh Geha[3]
[1]Université de Sherbrooke, Sherbrooke, QC, [2]Sherbrooke University, Sherbrooke, QC, [3]University of Sherbrooke, Sherbrooke, QC

Disclosures: Philippe Echelard: None; Yves Collin: None; Sameh Geha: None

Background: The finding of incidental gallbladder cancer (GC) in a gallbladder resected for non-neoplastic disease is both rare and the main cause for routine histological examination. In this study, we explored whether known and suspected clinical and demographic parameters between patients with and without GC allow for a selective approach to microscopic examination without compromising patient safety.

Design: We reviewed the files of all cholecystectomies (CCK) performed at our institution from 01/01/2006 to 01/01/2018. Cases with missing pathology reports, patients <18 years old, or patients in which a GC or other neoplastic disease was suspected pre-operatively were excluded. The cancer cases and a ratio of 30 controls per cancer case were selected for further analysis. Clinical, pathological, and radiological characteristics of the 2 groups were extracted by a systematic review of the patient files and compared. The statistically significant data were used for the creation of a decision-making algorithm. Statistics were performed using SPSS v23.0. The algorithm was created using “ctree” from the “party” package on Rx64 3.6.1. A second algorithm was also inferred from the results.

Results: 5663 CCKs were initially reviewed; 551 met one or more exclusion criteria. 12 cases of incidental GC and 1 case of moderate dysplasia were identified. 390 control were randomly selected from the remaining CCKs. Demographic, clinical, and pathological parameters were analysed in both groups. The finding of incidental GC was associated with older age (P<0.0001) an open surgical approach (P<0.0001), a longer operating time (P<0.0001), dilatation of the biliary tract at imaging (P=0.01), gallbladder wall thickening at gross examination (p=0.006) and a greater gallbladder wall thickness in mm (p=0.001). The final algorithm (Figure 1) included the operating time, the surgical approach, and the patient age. Those elements alone were sufficient to isolate the 13 GC cases from 267 of the 390 controls (66.3% of the 403 CCK). We also suggest a checklist (Figure 2) that could be more appropriate for use in a clinical setting.

TABLE 1. Clinical, Imaging, Gross and Laboratory Parameters of Cases and Controls Groups.

Parameter (n/13*)	Controls (n=390)	Cases (n=13)	P**
Clinical parameters			
Female sex (%)	63.6	61.5	1.000
Mean age (+/- standard deviation) (13/13)	51.3 (18)	71.6 (10.4)	**0.0000078**
Smoking history (%) (10/13)	28.4	40.0	0.481
Emergency surgery (%) (13/13)	48.3	53.8	0.695
Open surgical approach (%) (13/13)	1.3	30.8	**0.0000767**
Median operating time in minutes (25-75%) (13/13)	62 (49.8-80)	125 (106-172.5)	**0.0000012**
Imaging parameters			
Gallstones (%) (12/13)	93.1	91.7	0.586
Thickened gallbladder wall (%) (12/13)	48.6	58.3	0.567
Median gallbladder thickness mm (25-75%) (5/13)	5 (4-6)	6 (3.5-8.5)	0.723
Dilated biliary tract (%) (13/13)	17.8	46.2	**0.010**
Acute/Subacute cholecystitis (%) (12/13)	38.8	58.3	0.230
Gross evaluation			
Thickened gallbladder wall (%) (9/13)	55.1	100	**0.006**
Median gallbladder wall thickness in mm (25-75%) (7/13)	3 (2-4)	8 (3-12)	**0.001**
Gallstones (%) (13/13)	91.5	84.6	0.314
Laboratory results			
Median total bilirubin (µmol/L) (25-75%) (12/13)	11.4 (6.5-24.1)	10.7 (7.55-28.7)	0.961
Median ALP (IU/L) (25-75%) (12/13)	85 (67-127)	137 (105.3-212)	**0.001**
Median GGT (IU/L) (25-75%) (11/13)	49 (23.5-182)	91 (52-644)	0.144
Median ALT (IU/L) (25-75%) (13/13)	34 (19-124)	69 (25.5-148)	0.326
Median AST (IU/L) (25-75%) (13/13)	29 (19-137.5)	66 (23-94)	0.359
Gross and Imaging parameters combined			
Thickened gallbladder wall if 3 mm is considered thickened (%) (13/13)	54.4	84.6	**0.044**
Thickened gallbladder wall if 4 mm is considered thickened (%) (13/13)	32.4	61.2	**0.037**
Median gallbladder thickness (mm) (25-75%) (10/13)	3 (2-4)	6.5 (3-9.75)	**0.001**

*Corresponds to the number of cancer cases in which the information was available

** Pearson, Chi-Square, and Anova tests

Figure 1 - 1752

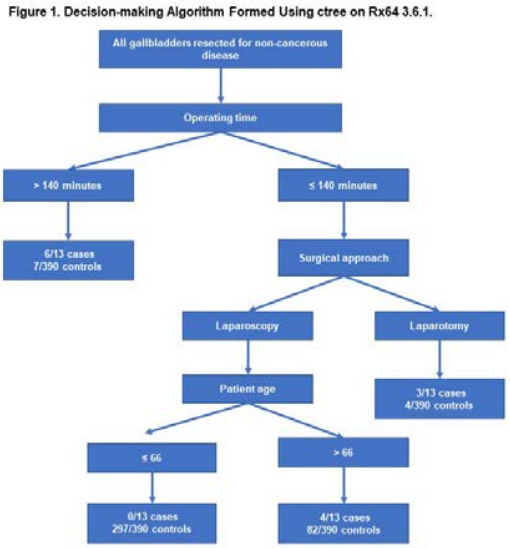

Figure 2 - 1752

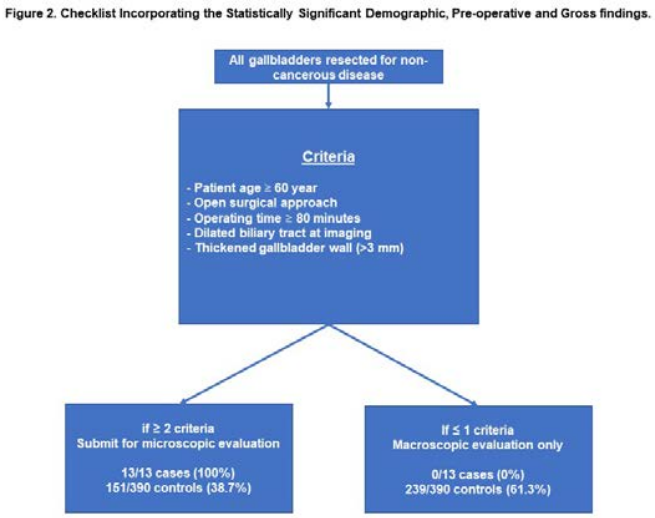

Conclusions: Our results seem to indicate that the association of clinical parameters with a quality gross examination can detect most, if not all incidental GC. The algorithms we created could allow for a more reasoned and economically responsible approach to gallbladder examination. Additional validation is needed before application of the algorithm in clinical practice.

1753 Impact of Whipple Grossing Method on Tumor Size, Lymph Node Yield, Margin, and Staging

Jiayun Fang[1], Chelsea Styles[2], Lili Zhao[3], Jiaqi Shi[3]
[1]University of Michigan Hospitals, Ann Arbor, MI, [2]Ann Arbor, MI, [3]University of Michigan, Ann Arbor, MI

Disclosures: Jiayun Fang: None; Chelsea Styles: None; Lili Zhao: None; Jiaqi Shi: None

Background: Whipple procedure is the most common surgery to remove tumors of the head of the pancreas. There is currently no standard grossing protocol for Whipple specimens. The most commonly used are axial and bivalve methods. The axial method slices the specimen perpendicular to the duodenal longitudinal axis. The bivalve method requires probing of the main pancreatic and common bile ducts. The specimen is sectioned along the plane defined by the probes. Studies have shown that grossing method can affect margin assessment and lymph node yield, and thus clinical stage. The 8th edition of the American Joint Committee on Cancer (AJCC) Cancer Staging Manual recently recommended a size-based tumor staging system. The effect of Whipple grossing method on tumor size and thus staging is not clear. This study will investigate the impact of grossing method on tumor size, lymph node yield, margin, staging, and survival.

Design: We collected 96 Whipple resections for pancreatic ductal adenocarcinoma from 2015-18. Pathology report and chart review were performed to collect patient demographics, tumor size (gross, reported [based on gross or microscopic], and imaging measurements), lymph node yield, margin status, stage, and patient outcomes. To compare these grossing methods, two-sample t tests were used for continuous data and χ^2 or Fisher's exact tests were used for categorical data. Standard survival analysis (i.e., Kaplan-Meier method and proportional hazards regression models) was used to analyze overall survival and recurrence-free survival. Pearson correlation coefficients were computed to assess correlations between continuous variables. All survival analyses were performed in SAS 9.4 software, and $p < 0.05$ was considered significant.

Results: There were 49 males and 47 females with a mean age of 67 years (range 37-84). 36 specimens were grossed axially and 60 by bivalve method. We observed no difference in tumor size, lymph node yield, margin status, or survival between the 2 grossing methods. Gross tumor size from both grossing methods significantly correlated with reported/imaging tumor size. However, the bivalve method yielded a stronger correlation (r=0.91 vs 0.74). Grossing method did not affect correlations between gross tumor size, stage, lymph node yield, or margin and survival [Figure 1].

Figure 1 - 1753

Figure 1 Comparison of the correlation of gross tumor size with reported tumor size between axial (blue) and bivalve (red) grossing methods (Pearson Correlation coefficients)

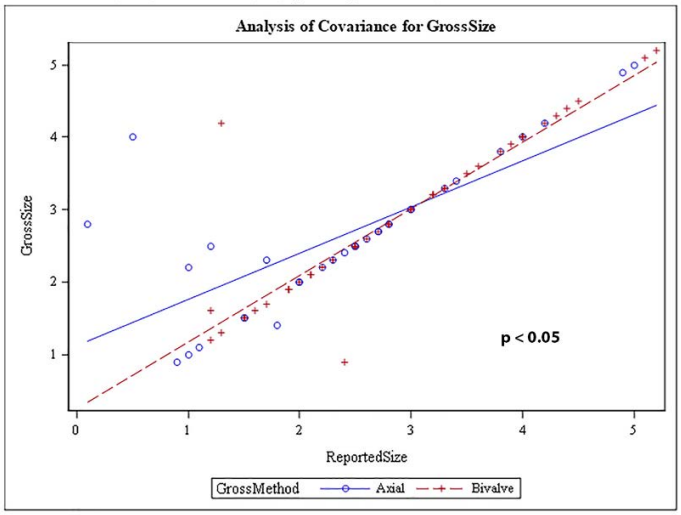

Conclusions: Whipple grossing method does not seem to impact lymph node yield, margin status, stage, or survival. However, the bivalve method appears to be superior for accurate determination of tumor size.

1754 The Response of Intraductal Pancreatic Cancer to Neoadjuvant Chemotherapy

Kohei Fujikura[1], Elizabeth D Thompson[2], Laura Wood[2]
[1]Johns Hopkins University School of Medicine, Baltimore, MD, [2]Johns Hopkins Hospital, Baltimore, MD

Disclosures: Kohei Fujikura: None; Elizabeth D Thompson: None; Laura Wood: None

Background: Pancreatic ductal adenocarcinoma (PDAC) is the third leading cause of cancer-related death in the United States. Neoadjuvant chemotherapy (NAC) is the standard treatment for borderline resectable and locally advanced invasive PDAC; however, residual tumor patterns in resected specimens after NAC remain unknown. In this study, we hypothesized that the responsiveness to chemotherapy is different between invasive PDAC cells and intraductal spread of PDAC (also called cancerization of ducts [COD]). To evaluate this, we performed quantitative analysis of residual PDAC cells after NAC.

Design: Pancreatic resections from a total of 174 PDAC patients (NAC group, n=97 and immediate surgery group, n=77) were analyzed in this study. All hematoxylin and eosin (H&E)-stained slides were jointly reviewed by three pathologists, and duct lesions were classified as CODs (Figure 1A,B) according to our strict criteria. Pathologic treatment response, estimated by the extent of residual tumor, was graded according to the College of American Pathologists (CAP) criteria. Quantitative CK19 immunohistochemistry (IHC) assays were performed to calculate the proportion of cancer cells that were intraductal (ratio of COD cells to the total number of PDAC cells).

Results: COD was identified on H&E-stained sections at the same frequency between NAC group (50/97 cases, 52%) and immediate surgery group (39/77 cases, 51%) (P=0.879). In contrast, the proportion of cancer cells that were intraductal was significantly different between the NAC and immediate surgery groups (median; 12.7% versus 1.99%, P < 0.0001) (Figure 2A). This proportion was highest in patients with marked therapy responses (CAP Score 1, median; 36.2%) compared with patients with moderate (CAP Score 2, 7.2%) or poor responses (CAP Score 3, 7.9%) (Figure 2B). In addition, cytologic changes associated with chemotherapy were more prominent in invasive PDAC than in COD in the NAC group (Figure 1C,D). No significant difference in overall survival was observed between cases with versus those without COD (hazard ratio, 0.847; P=0.778).

Figure 1 - 1754

Figure 1: Representative H&E sections of cancerization

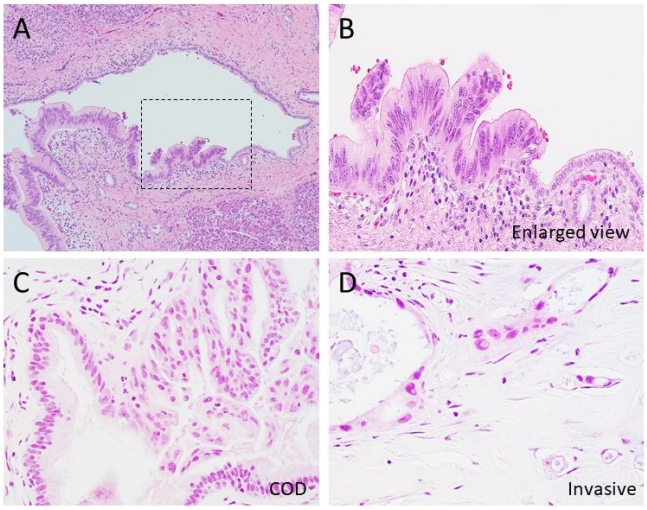

Figure 2 - 1754

Figure 2: Quantification of CK19-positive cells

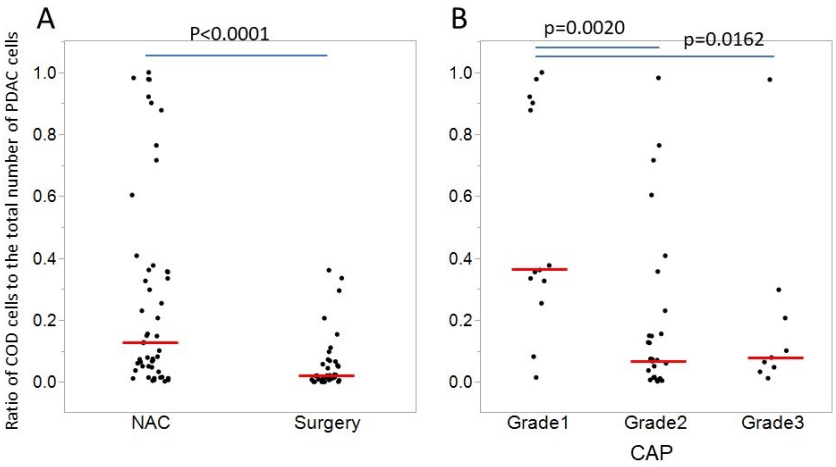

Conclusions: Intraductal components in PDAC are less responsive to neoadjuvant chemotherapy than the remainder of the tumor. This study could have the important implications for therapy resistance and recurrence as well as for how response to therapy is graded pathologically.

1755 Comparison of FNA and FNB for Pathologic Diagnosis of Pancreatic Lesions: A Single Institution Study

Ayaz Ghani[1], Mehran Taherian[2], Kazunori Kanehira[3]
[1]Roswell Park Comprehensive Cancer Center, Buffalo, NY, [2]University at Buffalo, Buffalo, NY, [3]Roswell Park Cancer Institute, Buffalo, NY

Disclosures: Ayaz Ghani: None; Mehran Taherian: None

Background: Currently, endoscopic ultrasound (EUS) guided fine needle aspiration (FNA) is the standard method for tissue diagnosis of pancreatic masses. To overcome limitations of EUS-FNA, EUS guided fine needle biopsy (FNB) was introduced with better tissue adequacy and preservation. The aim of this in house study is to compare the efficacy of EUS-FNA with rapid onsite evaluation (ROSE) and EUS-FNB without ROSE in the diagnosis of pancreatic lesions.

Design: A retrospective review of the electronic health record (EHR) was performed from 2016 to 2018 to look for patients who underwent concurrent EUS-FNA and EUS-FNB of the same pancreatic lesion. FNA samples were assessed for adequacy with ROSE and a final interpretation was provided by cytopathologist. FNB samples were analyzed by surgical pathologists.

Results: Fifty patients underwent a total of 207 needle passes (FNA: 130 and FNB: 77) of pancreatic lesions varying in size from 10-80 mm (median 41 mm). The size of the needle most commonly utilized for FNA and FNB sampling was 25 gauge. ROSE was performed in 46 (92%) of patients with adequate sampling in 28 (56%) cases and inadequate in 18 (36%) cases. 18 (36%) patients had a benign histologic diagnosis and 27 (54%) were called positive for malignancy on both FNA and FNB. Diagnosis of atypical cells was rendered in 3 (6%) patients on both FNA and FNB. 12 out of 50 (24%) patients underwent subsequent resection. The overall concordance in pathologic diagnosis between FNA with ROSE versus FNB without ROSE was 98%.

Conclusions: Based on the results of this small cohort study there is a possibility that FNB without ROSE can replace EUS-FNA with ROSE without loss of diagnostic accuracy. Although no cost effective analysis is performed in our study, but we presume that eliminating ROSE can make the procedure more economical and can possibly provide better specimens for histologic evaluation.

1756 Histologic Features Helpful for Diagnosing Adenocarcinoma on Pancreas Fine Needle Biopsy

Raul Gonzalez, Beth Israel Deaconess Medical Center, Boston, MA

Disclosures: Raul Gonzalez: None

Background: Pancreatic ductal adenocarcinoma (PDAC) is an aggressive neoplasm often requiring aggressive surgery. Though clinical suspicion for PDAC is typically high in most patients with suggestive presentation, findings can overlap with other mass-forming processes, including pancreatitis. Historically, the pancreas has been difficult to sample, and cytologic techniques were commonly used. With the advent of new biopsy devices, such as SharkCore, some pathology departments now routinely evaluate pancreas fine needle tissue biopsies. This study aims to report the histologic spectrum of PDAC on SharkCore and the device's accuracy.

Design: We searched our departmental archive for SharkCore biopsies taken from patients with a high clinical concern for PDAC versus pancreatitis. After excluding cases of serous cystadenoma, neuroendocrine tumor, and metastasis, a cohort of 100 consecutive cases was formed. For each, we recorded patient age and sex, percentage of diagnostic tissue in each sample (as opposed to blood/fibrin), and tumor site, size, and histology, focusing on features proven to help diagnose PDAC.

Results: The 100 cases came from 93 patients (42 men, 51 women; mean age 70 years). Median tumor size was 2.9 cm, and most (70%) arose in the head. Median diagnostic tissue amount in the samples was 40%. Final clinical diagnoses for the 93 patients were adenocarcinoma (n=77), pancreatitis (n=10), intraductal neoplasm (n=3), and unknown (n=3, generally from short follow-up). Of the adenocarcinoma patients (82 total biopsies), the diagnosis was established by the evaluated SharkCore sample in 62, by cytology in 6, and by subsequent biopsy or resection in 11. Common histologic findings in the 100 cases included desmoplasia (52%), single cells (42%; Fig. 1), haphazard glandular growth pattern (51%), nuclear pleomorphism $\geq$4:1 (35%), and incomplete gland lumens (16%; Fig. 2). Of the 82 cases ultimately representing adenocarcinoma, 17 (87%) showed at least one of those five features. One case each showed glands adjacent to a blood vessel or invading fat; none showed perineural invasion. Levels were ordered on 31 cases.

Figure 1 - 1756

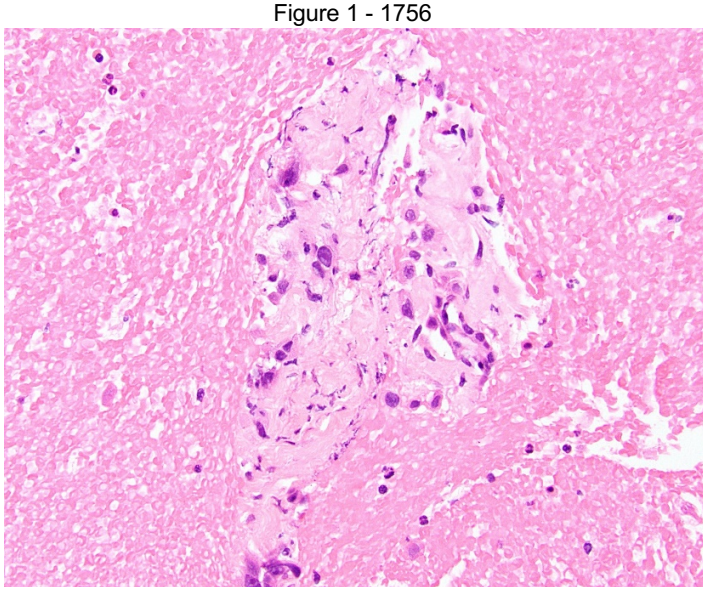

Figure 2 - 1756

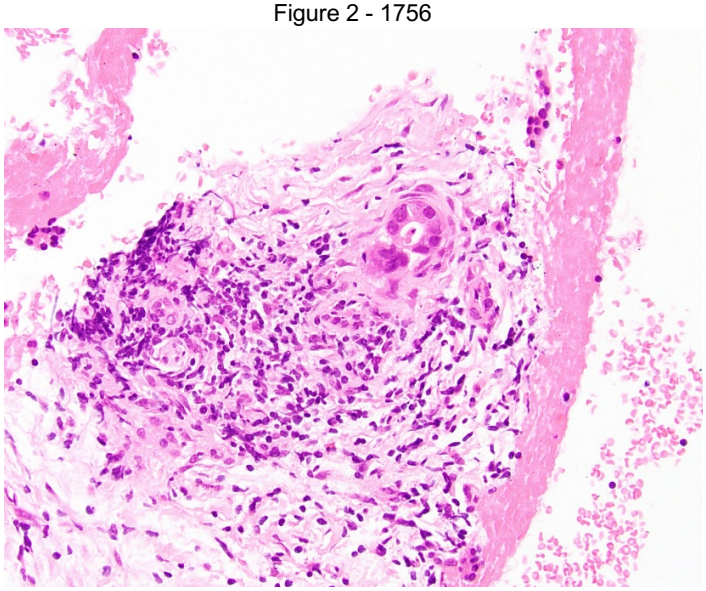

Conclusions: The diagnosis of PDAC can be challenging on resection, let alone biopsy. The SharkCore device showed an accuracy of 76% for diagnosing PDAC in our series. In challenging cases, pathologists should hunt for single cells, desmoplasia, haphazard gland growth, and nuclear pleomorphism. Additional levels and possibly cytokeratin immunohistochemistry can aid evaluation.

1757 INSM1 is a Robust Nuclear Immunostain to Distinguish Pancreatic Neuroendocrine Tumor from Solid Pseudopapillary Neoplasm of the Pancreas

Wenchang Guo[1], Geoffrey Sempa[1], Di Lu[1], Vishal Chandan[1], Xiaodong Li[2]
[1]University of California Irvine, Orange, CA, [2]UCI Medical Center, South Pasadena, CA

Disclosures: Wenchang Guo: None; Geoffrey Sempa: None; Di Lu: None; Vishal Chandan: None; Xiaodong Li: None

Background: Solid pseudopapillary neoplasm (SPN) of the pancreas is a low-grade malignant tumor which can show morphologic and immunohistochemical overlap with well differentiated pancreatic neuroendocrine tumor (WDPNET). Definitive distinction between both these tumors can sometimes be challenging, specially on small biopsies. Insulinoma-associated Protein 1 (INSM1) is a recently described sensitive and specific nuclear marker of neuroendocrine differentiation. In this study, we investigated the usefulness of INSM1 in differentiating SPN from PNET.

Design: Whole tumor sections of 21 well differentiated WDPNETs and 19 SPNs were stained for INSM1, chromogranin and synaptophysin. Any nuclear staining for INSM1 with moderate or strong intensity or cytoplasmic staining for synaptophysin and chromogranin was considered positive and the percentage of positive tumor cells were also recorded.

Results: INSM1 was positive in all WDPNETs (21/21) while it was negative in all SPNs (0/19) (Table 1). Synaptophysin was also positive in all pancreatic WDPNETs (21/21) but showed patchy positivity in 84% (16/19) of SPNs. Chromogranin was also positive in all WDPNETs (21/21) and in a small subset of SPNs (2/19, 11%). For the INSM1 positive WDPNETs, 20 of 21 (95%) showed diffuse (>50%) positivity, while 1 case showed patchy staining (about 30% of tumor positivity).

Table 1. Positivity of INSM1, synaptophysin, chromogranin in WDPNETs and SPNs

Tumor	INSM1	Synaptophysin	Chromogranin	Total
WDPNET	21/21 (100%)	21/21 (100%)	21/21 (100%)	21
SPN	0/19 (0%)	16/19 (84%)	2/19 (11%)	19

WDNET – well differentiated pancreatic neuroendocrine tumor, SPN – solid pseudopapillary neoplasm, INSMI – Insulinoma associated protein 1

Conclusions: INSM1 is a very useful nuclear marker for distinguishing SPN from WDPNET. All 19 cases of SPN in our study were negative for INSM1 while all 21 cases of WDNET were positive for INSM1.

1758 Effects of Neoadjuvant Therapy on Pancreatic Tumor Staging, Regression Scoring, and Patient Outcome: A Multi-Institutional Study

Suntrea Hammer[1], Raul Gonzalez[2], Megan Wachsmann[3], Zaid Mahdi[4]
[1]University of Texas Southwestern Medical Center, Dallas, TX, [2]Beth Israel Deaconess Medical Center, Boston, MA, [3]Dallas, TX, [4]Emory University Hospital, Atlanta, GA

Disclosures: Suntrea Hammer: None; Raul Gonzalez: None

Background: Current College of American Pathology and American Joint Committee on Cancer staging criteria for pancreatic adenocarcinoma (PanCa) are based on size criteria. Neoadjuvant therapy for PanCa prior to surgery is becoming more commonplace and affects the histologic and gross appearance. Treatment-associated fibrosis is difficult to separate from tumor grossly. Microscopically, tumor nests may become discontinuous and difficult to measure. In this study, we investigate whether current measurement-based guidelines hold predictive value in neoadjuvant cases.

Design: Neoadjuvantly treated cases of PanCa were identified from the pathology archives of two academic institutions. Clinical data was collected on demographics, preoperative therapy, pre- and post-therapy imaging, recurrence, and mortality data. Pathologic data was collected on tumor location, margin status, lymphovascular and perineural invasion, gross and microscopic size, nodal and distant metastases, and tumor regression. Tumor measurements were defined as largest single focus, additive dimension, inclusive dimension, and percent tumor bed involvement. Secondary PanCa arising from pre-existing lesions were excluded.

Results: The cohort included 113 cases, with an average follow-up time of 17.1 months. Significant differences in pathologic tumor (pT) staging existed between the various measurement methods (additive vs largest single focus P<0.0001; additive vs inclusive focus P <0.001). The recommended additive size was generally larger than the largest single tumor focus and smaller than the largest inclusive and gross measurements. Current staging criteria do not stratify risk of recurrence or death for any measurement method. On the other hand, percent tumor bed involvement did predict mortality risk (*P*=0.0218) when a 30% cutoff value was used. Lymphovascular invasion correlated with risk of recurrence (*P*=0.01762). Mortality risk correlated with nodal stage (*P*=0.04837), while tumor site also approached significance (*P*=0.0678).

Correlation of Pathologic Features in Neoadjuvant Pancreas with Recurrence and Mortality

Dependent Variable	Recurrence P-Value	Mortality P-value
Gross Percentage of Tumor bed <30%	0.423148714	0.038659761
Lymphovascular Invasion	0.017618747	0.977690546
Location of Tumor	0.178251	0.067772
Pathologic Nodal Stage	0.346461	0.048373
Additive Measurement	0.9088311	0.689979
Largest Single Focus Measurement	0.53189	0.143707
Inclusive Focus Measurement	0.736156	0.899559

Figure 1 - 1758

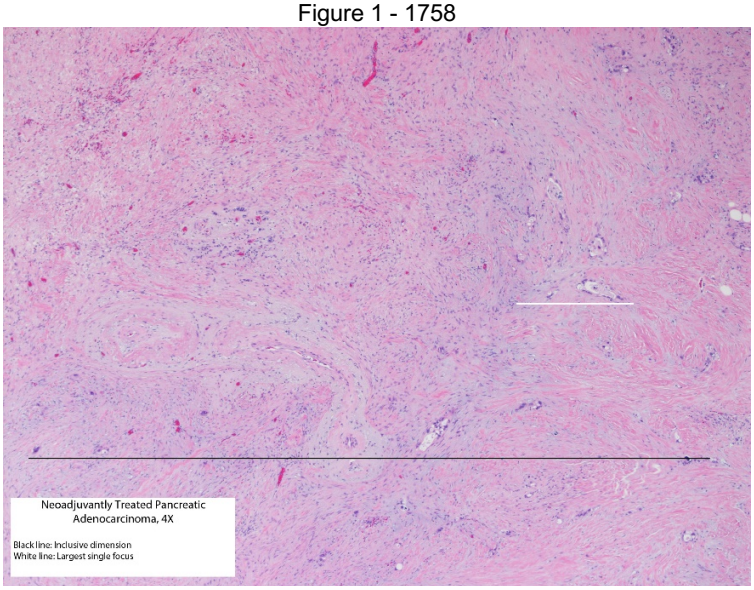

Conclusions: The increasing use of neoadjuvant therapy in the treatment of PanCa creates challenges in applying current staging criteria, with small variances in measurement technique leading to changes in stage. pT staging in this setting did not predict recurrence or mortality. Percent gross tumor bed involvement showed some value in predicting mortality, which likely represents the overall tumor response to therapy.

1759 CD47, a Prognostic Predictor, is Strongly Associated with Lymph Node Metastasis in Pancreatic Neuroendocrine Tumor

Rami Imam[1], Margaret Black[2], Wenqing Cao[3]
[1]Memorial Sloan Kettering Cancer Center, New York, NY, [2]NYU, Long Island City, NY, [3]New York University Langone Health, New York, NY

Disclosures: Rami Imam: None; Margaret Black: None; Wenqing Cao: None

Background: Pancreatic neuroendocrine tumors (pNETs), originating from diffuse neuroendocrine cells, are a clinically rare and heterogeneous disease of the pancreas which have increased significantly in incidence over the past few decades. As the therapeutic options continue to expand, it is necessary to define robust prognostic markers to guide clinical decision making and improve patient outcome. Although several biomarkers for NETs exist, sensitive and specific markers that diagnose tissue-specific NETs and predict tumor growth and behavior are generally lacking. CD47 is a transmembrane ligand which inhibits phagocytosis. Overexpression of CD47 has

been associated with increased tumor growth and metastasis in a variety of malignancies. In this study, we examine the prognostic implications of CD47 expression in pNETs.

Design: 44 well differentiated pNET resection specimens (17 G1, 23 G2, and 4 G3) were selected and analyzed using CD47 immunohistochemistry. Staining intensity and percentage of positive tumor cells was quantified using the H-score method. Statistical analysis was utilized to correlate H-score with various clinicopathologic parameters.

Results: Membranous and cytoplasmic staining of CD47 was seen in pNETs and normal endocrine cells. High expression of CD47 was seen in all samples of pNETs compared to the surrounding noncancerous pancreatic tissues. H-score of CD47 in pNETs with lymph node metastasis was significantly lower than in pNETs without lymph node metastasis (128.2±9.0 and 161.7±11.0, P=0.038). CD47 expression inversely correlate with perineural invasion (127.4±7.7 vs 170.0±11.6, P=0.004), and lymphovascular invasion (128.8±7.6 vs 178.8±13.6, P=0.002). Further analysis revealed that CD47 expression in pNETs was also inversely related to mitotic count (P=0.045). CD47 expression did not correlate with patient's age, gender, tumor size, stage, grade, or Ki-67 proliferation index.

Conclusions: CD47 was overexpressed in all pNETs. CD47 expression significantly correlated with lymph node metastasis, perineural invasion, lymphovascular invasion, and mitosis. The data indicated that CD47 may be a promising marker for predicting pNET prognosis.

1760 A Multicenter Interobserver Study Identifies ITBCC-Scoring as a Reliable and Reproducible Method for the Assessment of Tumor Budding in Pancreatic Cancer

Eva Karamitopoulou-Diamantis[1], Irene Esposito[2], Inti Zlobec[3], Andrea Insilla[4], Martin Wartenberg[3], David Schaeffer[5], Steve Kalloger[6], Stefano La Rosa[7], Christine Sempoux[8], Philipp Lohneis[9]
[1]Institute of Pathology, University of Bern, Zurich, Switzerland, [2]Heinrich-Heine University and University Hospital of Dusseldorf, Duesseldorf, Germany, [3]Bern, Switzerland, [4]Heinrich-Heine University and University Hospital of Dusseldorf, Düsseldorf, Germany, [5]Vancouver General Hospital, Vancouver, BC, [6]University of British Columbia, Vancouver, BC, [7]CHUV, Lausanne, VD, Switzerland, [8]Lausanne University Hospital, Lausanne, Switzerland, [9]University Hospital Cologne Institute of Pathology, Cologne, NRW, Germany

Disclosures: Eva Karamitopoulou-Diamantis: None; Inti Zlobec: None; David Schaeffer: None; Stefano La Rosa: None; Philipp Lohneis: None

Background: Pancreatic ductal adenocarcinoma (PDAC) has dismal prognosis and rising incidence. Tumor budding (TB) is a strong and independent prognostic factor in PDAC and its implication into daily diagnostics would improve the prognostic stratification of patients. However, its inclusion in pathology reports is hampered by the lack of a unified and practical scoring system. We performed a multicenter interobserver study to identify the optimal method of TB assessment in PDAC.

Design: TB was scored by independent pathologists at five participating centers in Switzerland, Germany and Canada. Two serial sections of 50 resected PDACs TNM-stage I-III, were stained for H&E and pan-cytokeratin. Pathologists assessed TB on a digital pathology platform comparing hematoxylin and eosin (H&E) with pancytokeratin staining in 10 high power fields (10HPF) and one HPF hotspot (1HPF), as well as in one H&E hotspot at 20x magnification as suggested by the International Tumor Budding Consensus Conference (ITBCC) 2016.

Results: Correlation coefficients for TB-counts between centers ranged from r=0.58648 to r=0.78641 for H&E and from r=0.69288 to r=0.81764 for pancytokeratin stained slides. Interobserver agreement across all centers was excellent for pancytokeratin 10HPF: ICC=0.81764 followed by ITBCC: ICC=0.78641. Assessment of TB on 1HPF reached only moderate agreement both for H&E (ICC=0.59526) and for pancytokeratin (ICC=0.69288).

Figure 1 - 1760

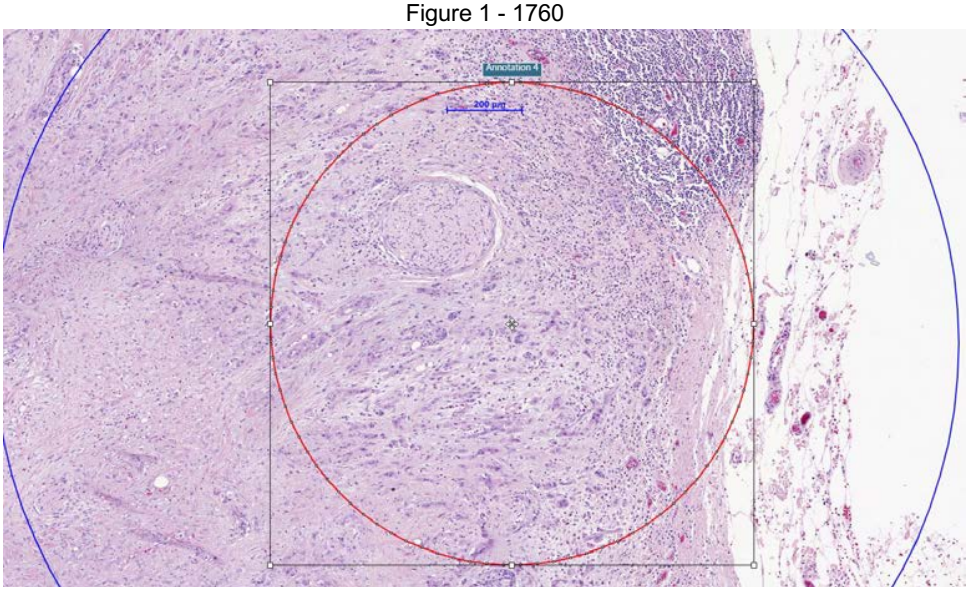

Figure 2 - 1760

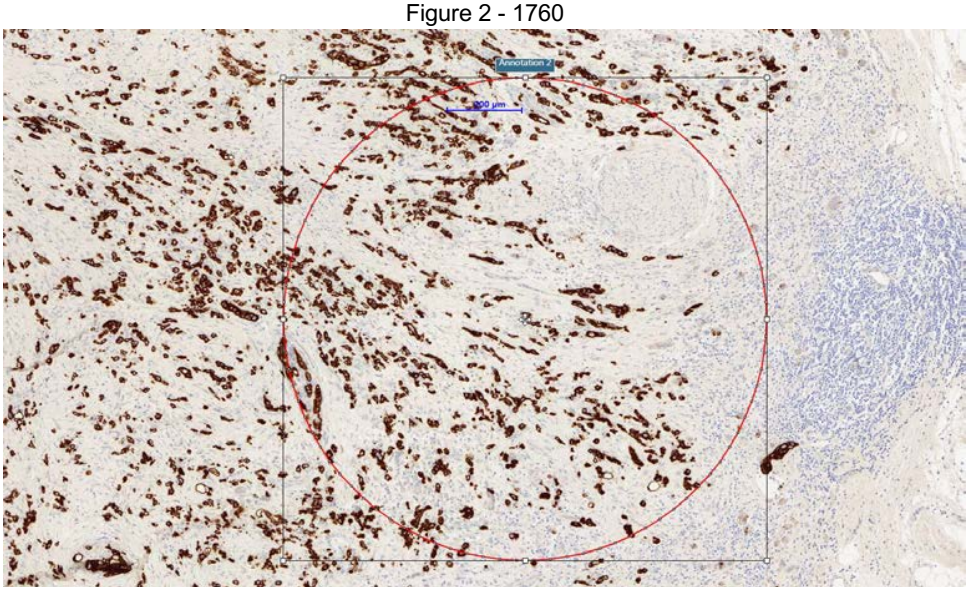

Conclusions: Based on the rates of interobserver agreement as well as the practicability and the feasibility of the method, we recommend the ITBCC score as a simple, reliable and reproducible method for assessing TB in PDAC in everyday practice.

1761 Predictive Biomarkers for Immunotherapy are Associated with Increased Survival in Pancreatic Cancer

Eva Karamitopoulou-Diamantis[1], Martin Wartenberg[2], Erik Vassella[3], Aurel Perren[4], Beat Gloor[5]
[1]Institute of Pathology, University of Bern, Zurich, Switzerland, [2]Bern, Switzerland, [3]Institut of Pathology, University of Bern, Bern, Switzerland, [4]University of Bern, Bern, Switzerland, [5]Insel University Hospital, University of Bern, Bern, Switzerland

Disclosures: Eva Karamitopoulou-Diamantis: None; Aurel Perren: None

Background: Immunotherapy can be used alone or in combination with chemotherapy to improve treatment responses in pancreatic ductal adenocarcinoma (PDAC). The success of immunotherapy in cancer has been associated to an inflamed tumor microenvironment (TME) and linked to the presence of microsatellite instability (MSI-H), high tumor mutational burden (TMB-H) and PD-L1 expression. We evaluated the immune cell density in the TME and assessed the MSI status, the PD-L1 expression as well as the TMB in our PDAC cohort to identify patient collectives with higher probability of response to immunotherapy.

Design: A well characterized cohort of 150 resected PDACs, TNM stage I-III, enriched for long-term survivors (LTS, overall survival (OS)>60 months, n=25) was used for this study. We evaluated the expression of PD-L1, the MSI-status and the immune cell counts by immunohistochemistry for PD-L1, MLH1, PMS2, MSH2, MSH6, CD3, CD4, CD8, FOXP3 and CD68 on tissue microarrays (n=150). TMB of the tumor DNA (n=70) was assessed by using the oncomine tumor mutation load assay. The results were correlated with the immune cell density in the TME and the clinicopathologic characteristics of the patients.

Results: MSI-H was found in 2.6% of all patients (50% were LTS, corresponding to 8% of the LTS-cohort, 75% were also TMB-H, none expressed PD-L1); TMB-H (i.e.>10) in 15% of patients (10% were also MSI-H and 60% expressed PD-L1); and PD-L1 expression in 37% of patients (4% were also MSI-H; 20% were also TMB-H). MSI-H and significant PD-L1 expression (i.e. score >4) were associated with an inflamed TME. TMB-H cases had slightly better median OS (22.5 months) and significantly better progression-free survival (PFS, 17 months) compared to that of the whole cohort (17.5 months and 7 months respectively).

Figure 1 - 1761

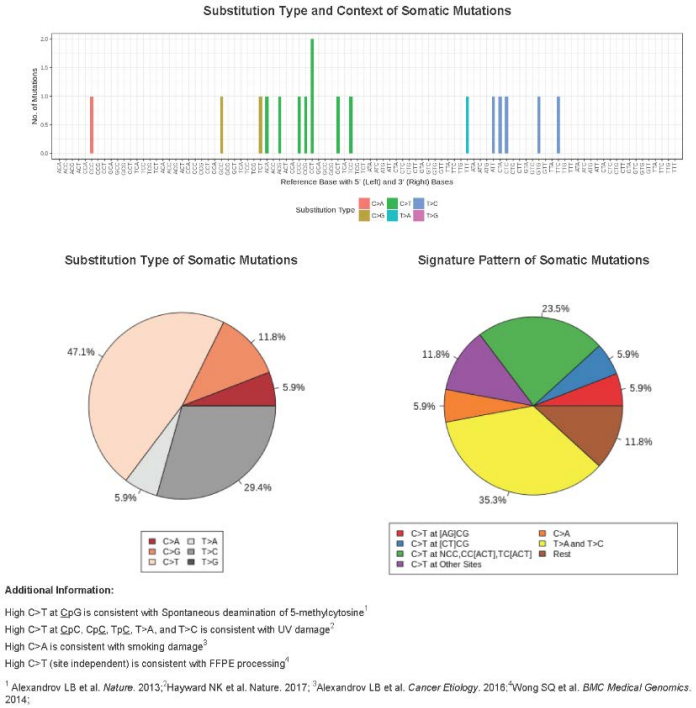

Figure 2 - 1761

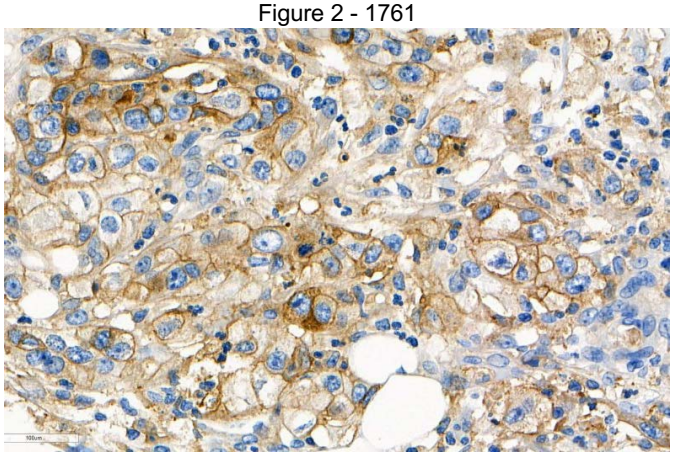

Conclusions: Based on concurrent biomarker expression, MSI-H and TMB-H patients have frequently prolonged OS and PFS, indicating a better anti-tumor immune response. The TMB-H patient collective might further profit from checkpoint inhibition, while other strategies inducing immune response should be searched for in the remaining majority of the patients. Markers of potential immunotherapy response along with TMB can help support rational combinations as part of an individualized, precision oncology approach.

1762 Tumoral and Immunological Features Associated with Long-Term Survival in Pancreatic Cancer

Eva Karamitopoulou-Diamantis[1], Hassan Sadozai[2], Martin Wartenberg[2], Thomas Gruber[3], Mirjam Schenk[3], Inti Zlobec[2], Beat Gloor[4], Erik Vassella[3], Aurel Perren[5]
[1]Institute of Pathology, University of Bern, Zurich, Switzerland, [2]Bern, Switzerland, [3]Institut of Pathology, University of Bern, Bern, Switzerland, [4]Insel University Hospital, University of Bern, Bern, Switzerland, [5]University of Bern, Bern, Switzerland

Disclosures: Eva Karamitopoulou-Diamantis: None; Hassan Sadozai: None; Thomas Gruber: None; Mirjam Schenk: None; Inti Zlobec: None; Aurel Perren: None

Background: Pancreatic ductal adenocarcinoma (PDAC) is a highly lethal disease with limited treatment options and few long-term survivors. The success of chemotherapy and/or immunotherapy in PDAC may rely on precise patient selection. We compare the stromal, immune and histomorphological characteristics of the tumor microenvironment (TME) as well as tumor mutational profiles in three survival stratified patient cohorts to identify biological features associated with improved clinical outcomes.

Design: Immune cell counts were assessed immunohistochemically on tissue microarrays of PDAC-tissue from patients with long-term- (LTS, overall survival (OS)>60 months, n=30); mid-term- (MTS, OS:13-60 months, n=41) and short-term survival (STS, OS:≤12 months,

n=44). Stromal subtyping was performed via combined evaluation of aSMA and Collagen stains. Mutational analysis was performed by targeted next generation sequencing. Clinicopathologic and histomorphological features such as tumor budding and gland-forming component were evaluated.

Results: LTS-cases exhibited a TME rich in T lymphocytes, including an expanded $CD4^{+}$T cell population with reduced numbers of tumor associated macrophages (TAMs), dormant ($aSMA^{low}$/$collagen^{low}$) stromal profiles, favorable histomorphology (low tumor budding and high gland-forming component) and low mutational frequency in the key PDAC genetic drivers CDKN2A and SMAD4. Inversely, a TME poor in effector T cells and rich in immunosuppressive leukocytes such as $FOXP3^{+}$ Tregs and TAMs, an activated stroma ($aSMA^{high}$/$collagen^{high}$), aggressive histomorphology (high tumor budding and low gland-forming component) and high mutational frequency in all known PDAC genetic drivers (KRAS, TP53, CDKN2A and SMAD4) were the primary features associated with the STS-cohort. Finally, MTS-cases exhibited a TME rich in T cells but with increased numbers of TAMs, a mostly activated stroma, histomorphologic variation and high mutational frequency in non-main drivers.

LTS-cases in PDAC are associated with unique stromal and immune landscapes resulting in a strongly immunogenic TME, in conjunction with distinct mutational profiles and histomorphological features. Our findings highlight the necessity of integrating tumor-specific TME-signatures to better stratify PDAC-patients for combinatorial treatment selection.

Figure 1 - 1762

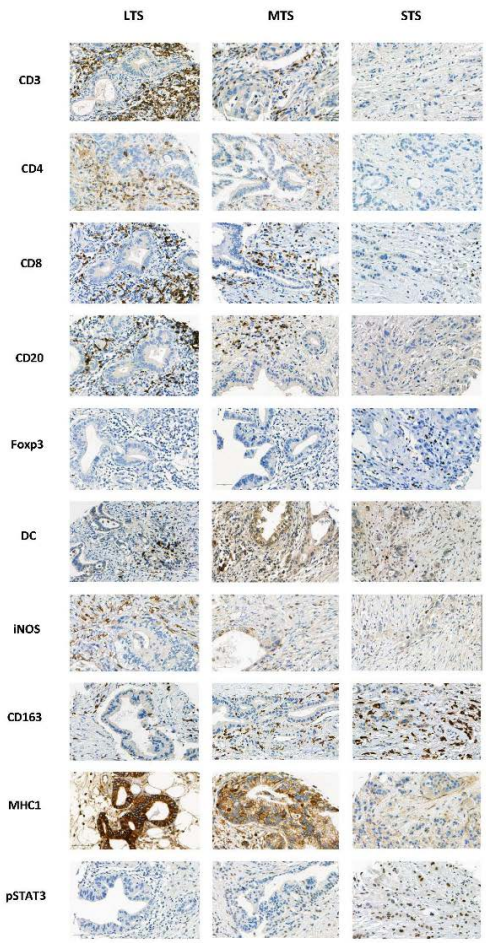

Conclusions: LTS-cases in PDAC are associated with unique stromal and immune landscapes resulting in a strongly immunogenic TME, in conjunction with distinct mutational profiles and histomorphological features. Our findings highlight the necessity of integrating tumor-specific TME-signatures to better stratify PDAC-patients for combinatorial treatment selection.

1763 Histone Modification of H3K9me3, H4K20me3, H3K4me3 and H3K36me3 in Distal Bile Duct Cancer Correlate with Worse Prognosis

Hangyeol Kim[1], Kiyong Na[2], Ji-Youn Sung[2]
[1]Seoul, Korea, Republic of South Korea, [2]Kyung Hee University, Seoul, Korea, Republic of South Korea

Disclosures: Hangyeol Kim: None; Ji-Youn Sung: None

Background: Histone modification is associated with tumoriogenesis and cancer progression. Recent studies have revealed prognostic value of histone modification. However, its prognostic role in distal bile duct cancer is unclear.

Design: Tissue samples from 88 patients with distal bile duct cancer were examined by immunohistochemical staining for H3K9me3, H4K20me3, H3K4me3 and H3K36me3.

Results: Most of cases (H3K9me3: 71.6%, H4K20me3: 80.7% and H3K36me3:84.1%) showed at least focal nuclear histone marker positivity in tumor cells except H3K4me3. High H3K4me3 expression was associated with N status (p=0.024) and advanced stage (p=0.047). Other histone markers were not related to clinicopathological parameters. In survival analysis, high expression of H3K9me3 (p=0.003), H4K20me3 (p=0.008) and H3K36me3 (p=0.047) showed significantly better survival outcomes than those with low expression. Multivariate Cox regression analysis revealed that H3K9me3 (p=0.001), H3K36me3 (p=0.033) expression were independently predicted shorter overall survival.

Conclusions: High expression of H3K4me3 was associated with adverse parameters. High expression of H3K9me3, H4K20me3 and H3K36me3 was significantly associated with better survival, and H3K9me3, H3K36me3 were found to be independent predictors of the overall survival. Our result suggest that histone markers can be a prognostic marker for patients with distal bile duct cancer.

1764 Predicting Metastasis Risk in Pancreatic Neuroendocrine Tumor (PanNET) using a Multi-Label Deep Learning Approach

Sergey Klimov[1], Yue Xue[2], Rondell Graham[3], Arkadiusz Gertych[4], Yi Jiang[5], Shristi Bhattarai[5], Emad Rakha[6], Michelle Reid[7], Ritu Aneja[5]
[1]Roswell, GA, [2]Northwestern University Feinberg School of Medicine, Chicago, IL, [3]Mayo Clinic, Rochester, MN, [4]Cedars-Sinai Medical Center, West Hollywood, CA, [5]Georgia State University, Atlanta, GA, [6]University of Nottingham, Nottingham, Nottinghamshire, United Kingdom, [7]Emory University Hospital, Atlanta, GA

Disclosures: Sergey Klimov: None; Yue Xue: None; Rondell Graham: None; Arkadiusz Gertych: None; Yi Jiang: None; Shristi Bhattarai: None; Emad Rakha: None; Michelle Reid: None; Ritu Aneja: None

Background: Pancreatic neuroendocrine tumors (PanNET) are the second most common type of pancreatic cancer, and its incidence is steadily rising. Unlike pancreatic neuroendocrine carcinomas (PanNECs), PanNET patients have a wide range of progression free survival intervals. Unfortunately, clinical prognostic markers are inadequate in identifying patient metastasis risk. There is an unmet clinical need for more accurate prognostication. Deep learning pipelines provide novel approaches to annotate whole slide images and identify features that may predict the risk of metastasis.

Design: H&E stained, full-face, surgical resections of 90 well differentiated PanNETs (Fig 1A) were used for training and testing sequential deep learning models. First, a Convolutional Neural Network (CNN) was trained (through pathologist annotation) to identify regions of PanNET, including stromal poor/clearly delineated and stromal rich, stroma without PanNET, normal pancreas parenchyma, and fat (Fig 1B) in high-resolution digital slides. A separate CNN was trained, using patient metastasis outcome as the label, to score cancer and stromal annotated tiles for metastasis risk (Fig 1C). Finally, the metastasis probability scores from all tiles in the slide were aggregated into a distribution. Distribution statistics were extracted and fit into 18 machine learning models, with feature selection, to identify a model that assesses the overall patient risk with the highest accuracy.

Results: The cross-validated accuracy for classification of tile annotation reached 92.8%, with a sensitivity and specificity of over 90% for each label. Tiles with very high risk scores probabilities (>99.9%) from the metastasis CNN produced a sensitivity/specificity of 62%/89% for stromal tiles and 76%/69% for cancer tiles. Finally, utilizing a subset of the full slide distribution statistic features provided a cross-validated high-risk group with an 11% metastasis-free survival (p<0.005) (Fig 2) and a hazard ratio of 8.06 (2.7-24.3) regardless of cofounding variables (sex, age, and tumor size).

Figure 1 - 1764

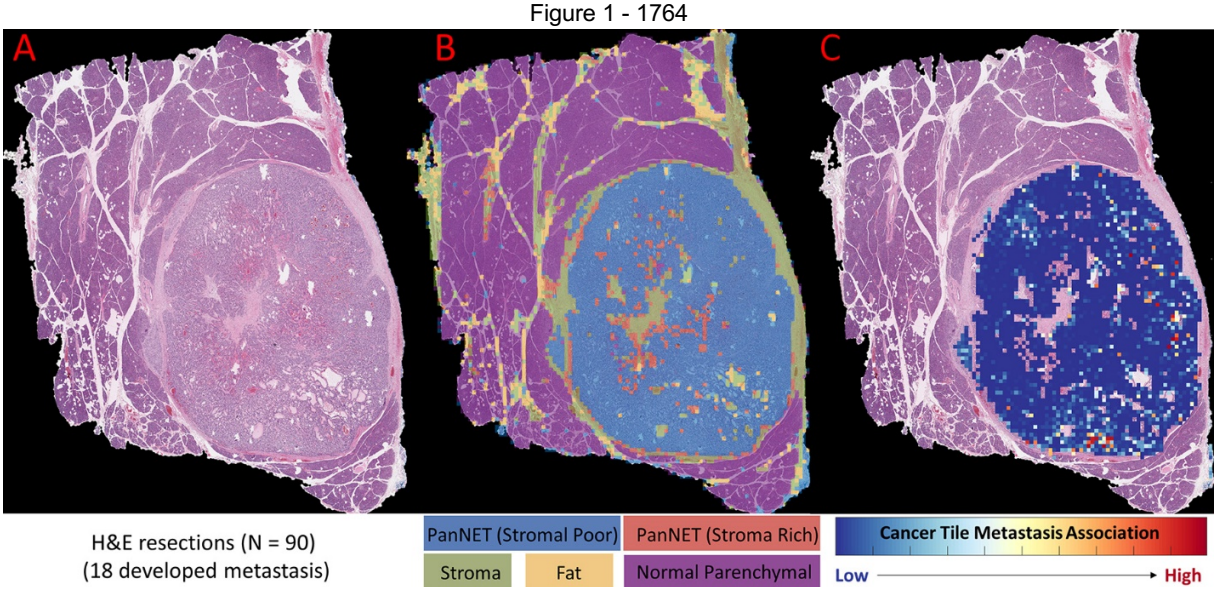

Figure 2 - 1764

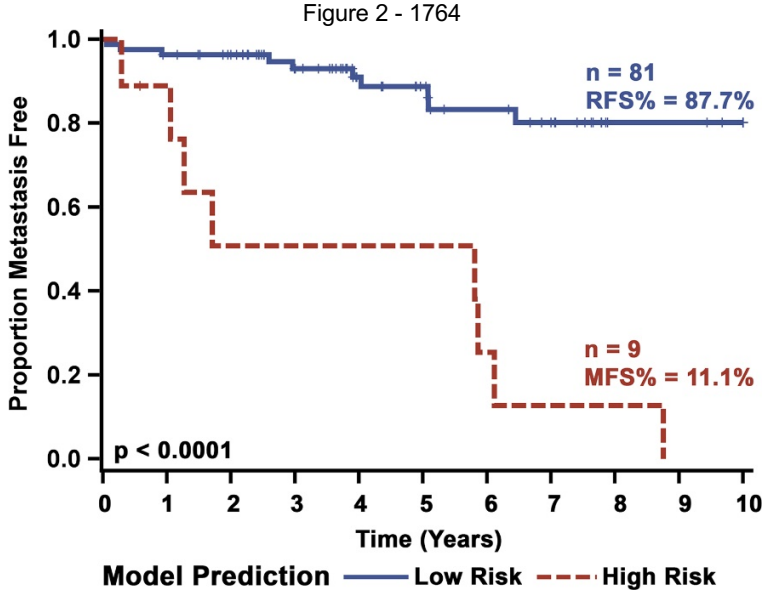

Conclusions: Our 3 layered AI-based model accurately predicts future metastasis risk for well differentiated PanNETs.

1765 Mutational Profile of Site-Specific Ampullary Carcinoma: Is There Any Difference?

Narendra Krishnani[1], Niraj Kumari[2], Raghvendra L[3]
[1]Department of Pathology, Sanjay Gandhi Postgraduate Institute of Medical Sciences, Lucknow, Uttar Pradesh, India, [2]Sanjay Gandhi Postgraduate Institute of Medical Sciences, Lucknow, Uttar Pradesh, India, [3]Department of Pathology, Sanjay Gandhi Postgraduate Institute of Medical Sciences, Lucknow, UP, India

Disclosures: Narendra Krishnani: None; Niraj Kumari: None; Raghvendra L: None

Background: Ampullary cancers (AC) are classified as intraampullary (IA), intraampullary-ductal (IA-D), periampullary-duodenal (PA) & ampullary-NOS (A-NOS). ACs are morphologically & genetically heterogeneous. We studied genetic profile of the 4 site-specific ACs by whole exome sequencing (WES).

Design: Grossly 37 ACs were classified as IA, IA-D, PA & A-NOS and clinicopathological features were compared. Sure Select XT (V5+UTR) was used for library preparation in fresh tissues of 37 ACs & matched blood. WES was done on HiSeq 2500 Ilumina platform.

Results: There were 16 cases of IA, 8 of IA-D, 5 of PA & 8 of A-NOS. Histological features in 4 groups showed significant correlation with tumor size, T-stage & differentiation (table 1). Intestinal differentiation was predominant in IA and PA while pancreatobiliary differentiation was predominant in IA-D & A-NOS groups. WES revealed overall read alignment of 99.97% with passed alignment of 97% & on-target coverage of 85.67% in 37 cases of AC. Germline variants from blood (mean coverage 100X, 10-560 reads/variant) were excluded from tissue (mean coverage 200X, 1-378 reads/variant). Deleterious somatic variants in coding regions with >5% mutant allele frequency & >50 reads were found in 32 cases comprising of 172 SNVs, 6 duplications, 4 deletions & 1 insertion. IA and IA-D group showed higher somatic variants comprising of 100 (68 genes) & 46 variants (43 genes) respectively compared to PA and A-NOS tumors comprising of 23 (20 genes) & 27 variants (19 genes) respectively. Somatic mutation in genes of 5 major targetable cancer pathways showed. TP53 was largely mutated in PA while TGF-beta in A-NOS & chromosomal remodeling genes in IA-D groups. PI3/AKT/RAF/MAPK was mutated in all groups. Gene ontology showed mutations in genes coding transcription factors to be most prevalent in A-NOS whereas mutation in nucleic acid binding genes was prevalent in other 3 groups. Amongst the genes responsible for different biological processes, those coding for metabolic & cellular processes, biological regulation & localization were mutated most in all types. Genes coding for different molecular functions had similar mutation frequency in all groups of AC (Fig 2).

Table 1. Histological characteristics in site-specific subgroups of ampullary carcinoma

Features		Intra-ampullary (n=16, 42%)	Intra-mpullary Ductal (n=9, 23.7%)	Peri-ampullary (n=5, 13%)	Ampullary NOS (n=8, 21%)	P Value
Gender	Male	12 (75%)	6 (66.7%)	4 (80%)	5 (62.5%)	0.8
	Female	4 (25%)	3 (33.3%)	1 (20%)	3 (37.5%)	
Tumor Grade	Well	12 (75%)	5 (55.6%)	4 (80%)	5 (62.5%)	0.4
	Moderate	4 (25%)	2 (22.2%)	0	2 (25%)	
	Poor	0	2 (22.2%)	1 (20%)	1 (12.5%)	
Tumor size	<1 cm	4 (25%)	5 (55.6%)	0	0	**0.001**
	1.1-3 cm	12 (75%)	3 (33.3%)	4 (80%)	3 (37.5%)	
	>3 cm	0	0	1 (20%)	5 (62.5%)	
Differentiation	Intestinal	12 (75%)	2 (22.2%)	5 (100%)	3 (37.5%)	**0.009**
	Pancreatobiliary	3 (18.8%)	7 (77.8%)	0	4 (50%)	
T-stage	T1	8 (50%)	1 (11.1%)	0	0	**0.002**
	T2	1 (6.3%)	2 (22.2%)	4 (80%)	1 (12.5%)	
	T3	7 (43.8%)	6 (66.7%)	1 (20%)	7 (87.5%)	
Perinural invasion		3 (18.8%)	4 (44.4%)	1 (20%)	4 (50%)	0.2
Lymphovascular invasion		3 (18.8%)	2 (22.2%)	0	3 (37.5%)	0.4
Nodal metastasis		3 (18.8%)	1 (11.1%)	2 (40%)	3 (37.5%)	0.5
TNM Stage	Stage I	7 (43.8%)	3 (33.3%)	1 (20%)	1 (12.5%)	0.6
	Stage II	6 (37.5%)	5 (55.6%)	2 (40%)	4 (50%)	
	Stage III	3 (18.8%)	1 (11.1%)	2 (40%)	3 (37.5%)	

Figure 1 - 1765

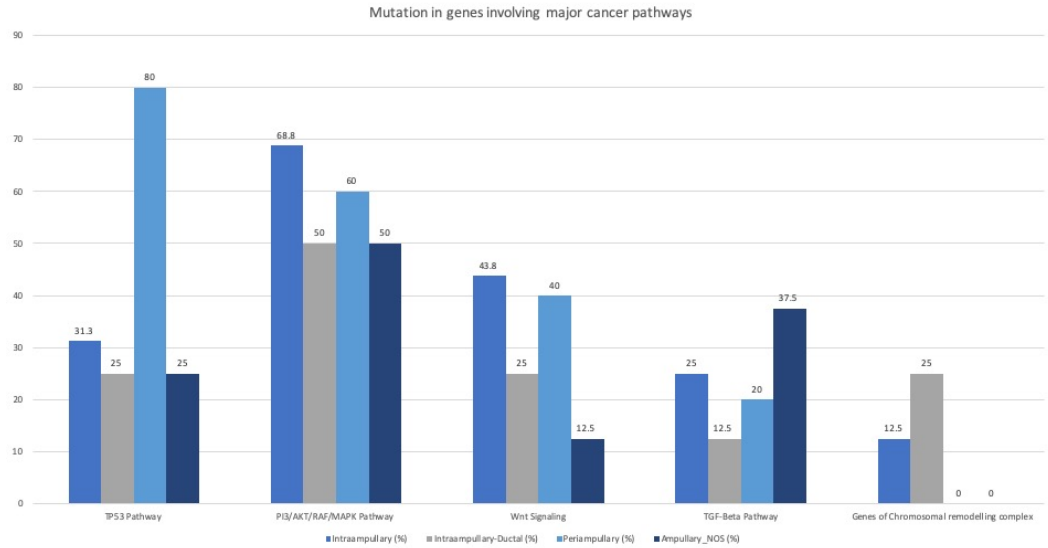

Figure 2 - 1765

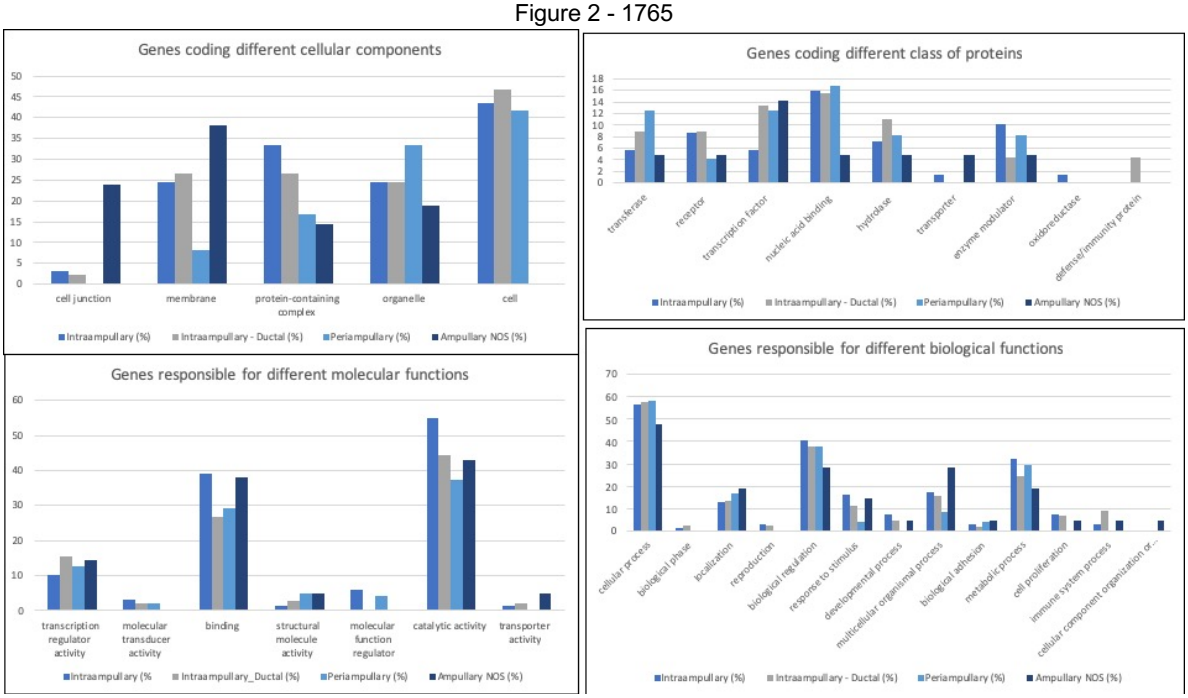

Conclusions: Genetic profile of site-specific ACs shows a distinct pattern. Histologically IA & PA are similar while molecularly IA resembles IA-D. A-NOS morphologically with overlaps with all the othe 3 groups but shows distinct molecular pattern.

1766 Whole Exome Sequencing Reveals a Distinct Spectrum of Somatic Mutations in Ampullary Carcinomas with Intestinal and Pancreatobiliary Differentiation

Niraj Kumari[1], Rajneesh Kumar Singh[1], Shravan Kumar Mishra[1], Raghvendra L[2], Saumya Sarkar[3], Narendra Krishnani[4]
[1]Sanjay Gandhi Postgraduate Institute of Medical Sciences, Lucknow, Uttar Pradesh, India, [2]Department of Pathology, Sanjay Gandhi Postgraduate Institute of Medical Sciences, Lucknow, UP, India, [3]Common Research Facility, Sanjay Gandhi Postgraduate Institute of Medical Sciences, Lucknow, UP, India, [4]Department of Pathology, Sanjay Gandhi Postgraduate Institute of Medical Sciences, Lucknow, Uttar Pradesh, India

Disclosures: Niraj Kumari: None; Rajneesh Kumar Singh: None; Shravan Kumar Mishra: None; Raghvendra L: None; Saumya Sarkar: None; Narendra Krishnani: None

Background: Ampullary carcinomas (AC) are histologically classified as having intestinal (INT) or pancreatobiliary (PB) differentiation. Little is known about genetic landscape of these two subtypes. We studied genetic profile of AC to identify mutational profile of INT & PB tumors.

Design: Fresh tissues from 37 ACs & matched blood was subjected to whole exome sequencing. Histologic differentiation was categorized as INT, PB or mixed. Library was prepared using Agilent Sure Select XT Kit. Sequencing was done on HiSeq 2500 Illumina platform with 100X coverage for blood & 200X for tissue. Deleterious variants with >50 reads & >5% mutant allele frequency were analyzed. Germline variants were excluded.

Results: ACs (n=37, M:F=2.4:1, age range 24-76 years) showed 22 cases of INT, 13 of PB & 2 of mixed differentiation. Total 1263 somatic variants were identified in coding regions, with 2-257 variants/patient. 183 deleterious variants [missense - 149 (81.4%), nonsense - 24 (13.1%), frameshift indels - 10 (5.5%)] included 172 SNVs, 6 duplications, 4 deletions & 1 insertion across 112 genes. INT tumors showed higher number of variants across 78 genes (1-31/case) compared to 51 genes in PB type (1-29/case). Targetable mutations in genes involving one or more major pathways in cancer were found in 86.5% of all cases involving both INT and PB types. Five genes with hotspot mutations were validated by deep sequencing (APC, CTNNB1, TP53, KRAS, SMAD4). Mutations in APC, CTNNB1, ERBB family, SMAD4, NOTCH, KMT2 & EPHA were more prevalent in INT (table 1). Nuclei acid binding genes were mutant in both types while transcription factor mutations were more prevalent in PB type (Fig. 1). Mutations involved angiogenesis, Wnt, TP53, EGF and FGF signaling pathways in both INT & PB tumors (Fig. 2). INT type showed higher mutations in apoptosis, glutamate receptor, JAK/STAT, Toll like, hedgehog & notch pathways while PB showed higher mutations in DNA replication & FAS signaling pathways. Significantly signaling pathways (p>0.002) showed PI3/AKT/RAS/MAPK to be mutated in 59% of AC with PI3/AKT related mutations being more prevalent in INT & RAS/RAF in PB types.

Table. Most commonly mutated targetable genes in patients with intestinal and pancreatobiliary differentiation

Genes	Intestinal Differentiation (n=22)	Pancreatobiliary Differentiation (n=13)
TP53	8 (36.4%)	4 (30.7%)
KRAS	5 (22.7%)	3 (23%)
ERBB Family	6 (27.3%)	2 (15.4%)
SMAD4	5 (22.7%)	2 (15.4%)
APC	6 (27.3%)	1 (7.8%)
CTNNB1	3 (13.6%)	1 (7.8%)
KMT2 (Family)	9 (41%)	2 (15.4%)
NOTCH Family	4 (18.2%)	1 (7.8%)
EPHA Familiy	5 (22.7%)	0
ARID2	2 (9%)	1 (7.8%)
PIK3CA	2 (9%)	0
TAP1	1 (4.5%)	2 (15.4%)
ROS1	1 (4.5%)	2 (15.4%)

Figure 1 - 1766

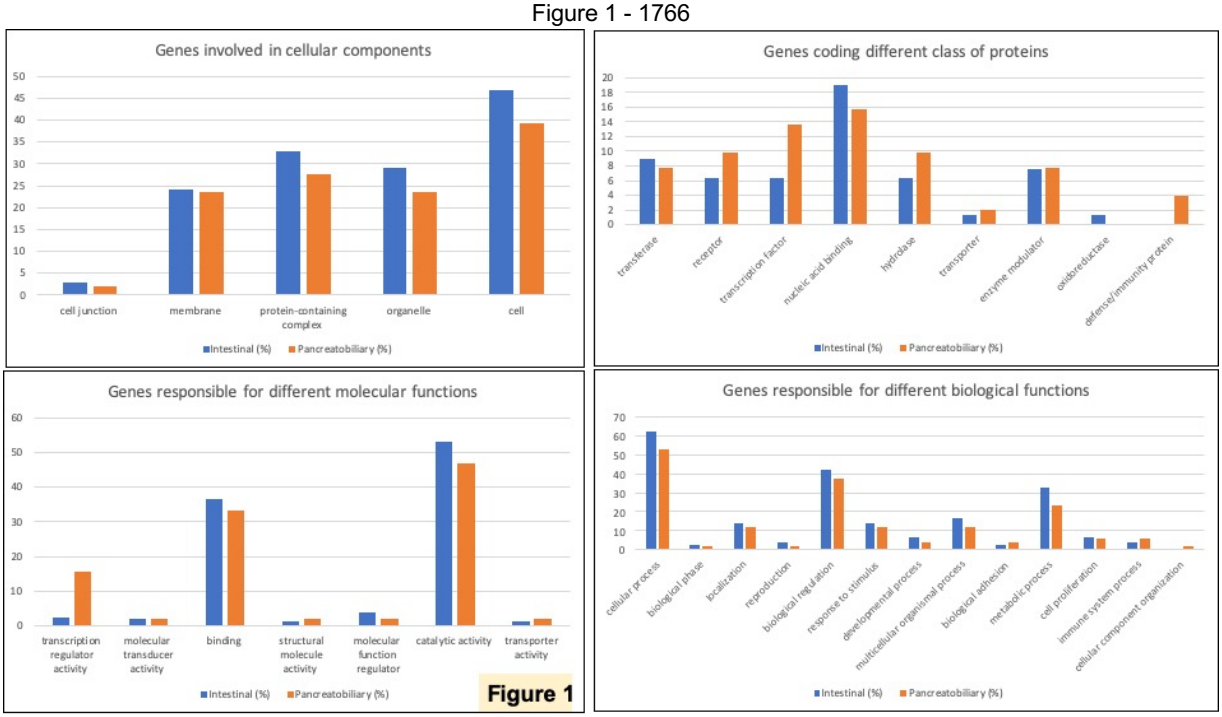

Figure 2 - 1766

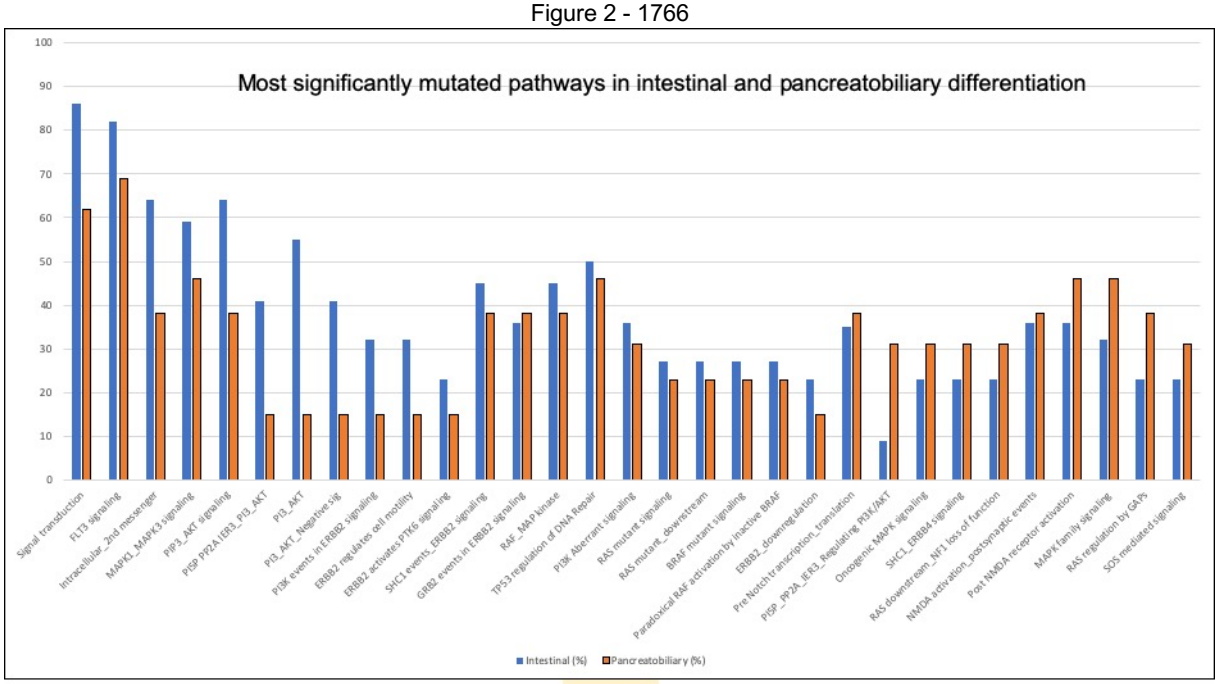

Figure 2

Conclusions: WES data suggests that INT type AC are genetically more unstable than PB & both involve mutations in tumor suppressor, oncogenes, transcription factors & chromatin remodeling complex genes. Our data suggests distinct genetic profile of INT & PB type ACs & supports targeting of PI3/AKT pathway in INT & RAS/RAF pathways in PB carcinomas.

1767 DNA Flow Cytometric Analysis of Paraffin-Embedded Tissue for the Diagnosis of Malignancy in Bile Duct Biopsies

Hannah Lee[1], Peter Rabinovitch[2], Aras Mattis[1], Sanjay Kakar[1], Won-Tak Choi[1]
[1]University of California San Francisco, San Francisco, CA, [2]University of Washington, Seattle, WA

Disclosures: Hannah Lee: None; Peter Rabinovitch: None; Aras Mattis: None; Sanjay Kakar: None; Won-Tak Choi: None

Background: Differentiation of reactive versus neoplastic epithelial changes can be challenging in bile duct biopsies. The samples are often scant, distorted, and mixed with significant inflammation and/or ulceration. Histological confirmation of malignancy is often required before the initiation of surgical therapy, while an erroneous diagnosis of malignancy can lead to unnecessary clinical management. This study examines if aneuploidy detected by DNA flow cytometry can serve as a diagnostic marker of malignancy using formalin-fixed paraffin-embedded (FFPE) tissue from bile duct biopsies.

Design: DNA flow cytometry was performed on 10 biopsies with adenocarcinoma (n = 7) or at least high-grade dysplasia (HGD; n = 3); 3 "atypical" biopsies with rare atypical glands/cells, concerning but not definite for malignancy; 28 likely "reactive" biopsies with acute/chronic inflammation, ulceration, and/or mild nuclear atypia; and 22 additional benign biopsies without significant inflammation, ulceration, or nuclear atypia.

Results: Aneuploidy was detected in 7 (70%) of the 10 adenocarcinoma (5 of 7) or at least HGD (2 of 3) biopsies, 3 (100%) of the 3 "atypical" biopsies, and none of the 50 likely "reactive" or benign biopsies. All 3 "atypical" cases with aneuploidy were subsequently found to have adenocarcinoma (n = 2) or HGD (n = 1). Among the 2 at least HGD cases with aneuploidy, 1 case developed adenocarcinoma, but no follow-up information was available in the other case. The remaining 1 at least HGD case, despite having normal DNA content, was found to have adenocarcinoma on follow-up. None of the likely "reactive" or benign cases (further supported by normal DNA content) developed adenocarcinoma within a mean follow-up time of 37 months (range: 0–282 months). The estimated sensitivity of aneuploidy as a diagnostic marker of malignancy or HGD was 70% with the specificity of 100%, 100% positive predictive value, and 94% negative predictive value.

	Benign (n = 50)	Atypical (n = 3)	Malignant (n = 10)
Aneuploidy	0 (0%)	3 (100%)	7 (70%)

Conclusions: Aneuploidy detected by DNA flow cytometry using FFPE tissue from bile duct biopsies can potentially serve as a diagnostic marker of malignancy (HGD and adenocarcinoma). A high rate of aneuploidy (77%) was observed in malignant cases, whereas all likely "reactive" or benign biopsies showed normal DNA content. This assay can be especially useful in establishing the diagnosis of malignancy in challenging "atypical" cases, where morphologic evaluation is limited by scarcity of atypical glands/cells, inflammation, and/or ulceration.

1768 Mutations in KMT2C are Associated with Increased Tumor Infiltration by CD8+ T cells in Intrahepatic Cholangiocarcinoma

Jae Lee[1], Amy Ziober[2], Rashmi Tondon[2]
[1]University of Pennsylvania, Philadelphia, PA, [2]Hospital of the University of Pennsylvania, Philadelphia, PA

Disclosures: Jae Lee: None; Amy Ziober: None; Rashmi Tondon: None

Background: Despite recent advances in chemo- and immunotherapies, the overall survival of patients with pancreaticobiliary tumors remains low. These tumors harbor a wide range of genetic alterations, yet the impact of distinct mutations on the presence of intratumoral immune cells is poorly understood. We studied associations between tumor infiltration by $CD8^+$ T cells and genetic mutations in two types of pancreaticobiliary tumors, intrahepatic cholangiocarcinoma (ICC) and pancreatic ductal adenocarcinoma (PDAC).

Design: A total of 26 cases (14 cases of ICC and 12 cases of PDAC) were used for our study. DNA isolated from paraffin-embedded tumor sections was examined using a targeted next-generation sequencing to detect genetic abnormalities among 152 most commonly mutated genes in cancer (Fig. 1). Representative tumor sections were also analyzed using immunohistochemistry to determine the number of intratumoral $CD8^+$ T cells.

Results: ICC and PDAC displayed distinct mutations in 39 and 16 genes, respectively, and 20 genes were mutated in both tumor types (Fig. 2a). Consistent with literature, missense mutations in *TP53* and *KRAS* were the most common genetic alterations in PDAC (6 and 9 out of 12, 50% and 75%, respectively). In contrast, genes involved in chromatin remodeling and epigenetic regulation, including *KMT2C* and *ARID1A*, were most frequently affected in ICC (5 out of 14, 36%). Mutations in *KMT2C* and *ARID1A* were detected in only 2 out of 12 cases of PDAC (17%). In addition, both ICC and PDAC displayed varying degrees of tumor infiltration by $CD8^+$ T cells, but tumors that harbored missense mutations in *KMT2C* were associated with an increased number of intratumoral $CD8^+$ T cells (Fig. 2b-d). In ICC, tumors with mutations in *KMT2C* showed an approximately 5-fold increase in the number of intratumoral $CD8^+$ T cells (34 versus 7 cells per high-power field, $P = 0.0035$).

Figure 1 - 1768

ABL1	AKT1	AKT2	AKT3	ALK
APC	AR	ARAF	ARID1A	ARID2
ATM	ATRX	AURKA	BAP1	BRAF
BRCA1	BRCA2	BRIP	BTK	CBP
CCND1	CCND2	CCND3	CCNE1	CDH1
CDK4	CDK6	CDKN2A	CHEK2	CIC
CRKL	CSF1R	CTNNB1	DAXX	DDR2
DNMT3A	EGFR	EIF1Ax	EPHA3	ERBB2
ERBB3	ERBB4	ERCC2	ERG	ESR1
ESR2	EZH2	FBXW7	FGF3	FGFR1
FGFR2	FGFR3	FGFR4	FLT3	FUBP1
GATA3	GNA11	GNAQ	GNAS	HRAS
H3F3A	IDH1	IDH2	IGF1R	JAK1
JAK2	JAK3	KDM5A	KDM5C	KDM6A
KDR	KIT	KMT2C	KRAS	MAP2K1
MAP2K2	MAP2K4	MAPK1	MAPK3	MAX
MCL1	MDM2	MDM4	MED12	MEN1
MET	MITF	MLH1	MRE11A	MSH2
MSH6	MTOR	MYC	MYCN	NBN
NF1	NF2	NTRK1	NTRK2	NTRK3
NKX2-1	NOTCH1	NOTCH2	NOTCH3	NRAS
EP300	PAK1	PALB2	PBRM1	PDGFRA
PIK3CA	PIK3CB	PIK3R1	PTCH1	PTEN
PTPN11	RAB35	RAC1	RAD50	RAD51
RAD51B	RAD51C	RAD51D	RAF1	RB1
RET	RHOA	RNF43	SETD2	SF3B1
SLIT2	SMAD4	SMARCA4	SMO	SPOP
SRC	STAG2	STK11	SUFU	SUZ12
SYK	TET2	TGFBR2	TP53	TRAF7
TSC1	TSC2	TSHR	U2AF1	VHL
WT1	XRCC2			

Figure 1 | List of genes analyzed for mutations. DNA isolated from paraffin-embedded tumor sections was examined using a targeted next-generation sequencing to identify genetic mutations.

Figure 2 - 1768

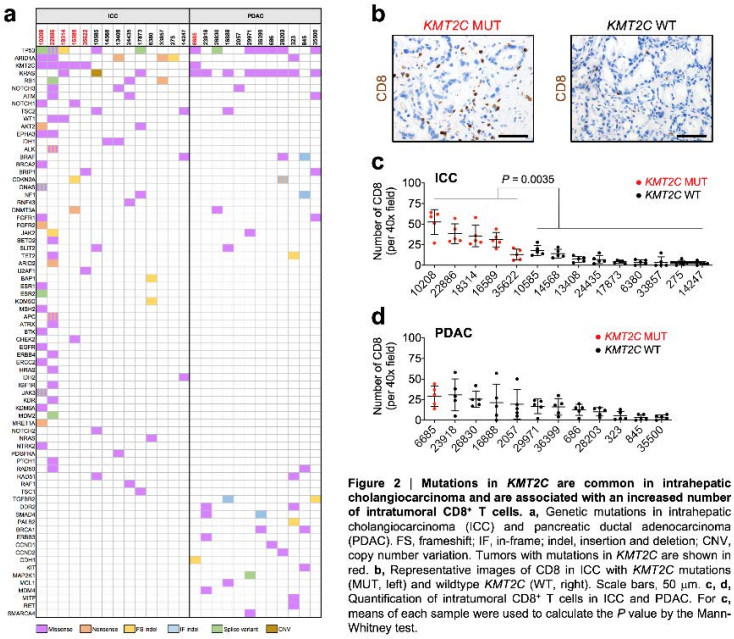

Figure 2 | Mutations in *KMT2C* are common in intrahepatic cholangiocarcinoma and are associated with an increased number of intratumoral CD8⁺ T cells. a, Genetic mutations in intrahepatic cholangiocarcinoma (ICC) and pancreatic ductal adenocarcinoma (PDAC). FS, frameshift; IF, in-frame; indel, insertion and deletion; CNV, copy number variation. Tumors with mutations in *KMT2C* are shown in red. **b,** Representative images of CD8 in ICC with *KMT2C* mutations (MUT, left) and wildtype *KMT2C* (WT, right). Scale bars, 50 μm. **c, d,** Quantification of intratumoral CD8⁺ T cells in ICC and PDAC. For **c,** means of each sample were used to calculate the *P* value by the Mann-Whitney test.

Conclusions: ICC and PDAC are heterogeneous diseases marked by a range of genetic mutations. In our small cohort of patients with ICC and PDAC, we found that alterations in genes involved in chromatin remodeling and epigenetic regulation are associated with significant increase in tumor infiltration by CD8⁺ T cells. Understanding mechanisms that underlie this association may improve immune-based strategies to treat pancreaticobiliary cancers. In our future studies, we will further validate our results by examining a larger number of tumor specimens.

1769 Characterization of Tumor Heterogeneity in Pancreatic Cancer Desmoplastic Stroma by Multiplex Immunohistochemistry-Based Image Analysis

Yohei Masugi[1], Tokiya Abe[2], Ogawa Yurina[3], Michiie Sakamoto[4]
[1]Shinjuku-Ku, Tokyo, Japan, [2]Keio University School of Medicine, Shinjuku-Ku, Tokyo, Japan, [3]Keio University School of Medicine, Tokyo, Japan, [4]Keio University School of Medicine, Tokyo, Kanto, Japan

Disclosures: Yohei Masugi: None; Tokiya Abe: None; Ogawa Yurina: None; Michiie Sakamoto: None

Background: Emerging evidence suggests that pancreatic cancer stroma comprises distinct subpopulations of cancer-associated fibroblasts which may contribute to multifaced roles of desmoplastic stroma in cancer progression. This study aimed to characterize inter- and intratumoral heterogeneity in pancreatic cancer desmoplasia utilizing multiplex immunohistochemistry-based image analysis.

Design: To define fibroblast phenotypes in human pancreatic ductal adenocarcinomas (PDAs), fibroblastic markers including ACTA2 (alpha smooth muscle actin), FAP (fibroblast activation protein alpha), PDPN (podplanin) and CD74 (a marker for antigen presenting fibroblasts) were examined by multiplex immunohistochemistry. Using multilayered whole-tissue slide data on fluorescent immunohistochemistry superimposed by van Gieson stain, we analyzed 104 surgically resected PDAs to compute area ratios of fibroblast subpopulations and collagen fibers for each tumor region.

Results: ACTA2-dominant fibroblasts and FAP-dominant fibroblasts represented as major fibroblastic components of PDA stroma. Thickened collagen bundles were spatially located in the vicinity of ACTA2-dominant fibroblastic areas. Computational tissue sorting revealed considerable differences between tumors in the amounts of collagen fibers (range of area ratio, 10.7-54.9%; mean, 29.1%; median, 27.8%), ACTA2-dominant fibroblasts (range, 2.8-22.4%; mean, 10.0%; median, 9.0%), and FAP-dominant fibroblasts (range, 0.06-12.7%; mean, 2.4%; median, 1.6%). Collagen area ratio showed a weak inverse correlation with area ratio of FAP-dominant fibroblasts (Spearman correlation coefficient, r = -0.27; P = 0.005) and no significant correlation with that of ACTA2-dominant fibroblasts (r = 0.04). Tumor grade was negatively associated with collagen area ratio, but positively with area ratio of FAP-dominant fibroblasts.

Conclusions: Multiplex immunohistochemistry-based image analyses found heterogeneous inter-relationships between tumor cells, fibroblastic subpopulations, and collagen fibers in pancreatic cancer tissues, suggesting the importance of tumor-stroma interactions in shaping the tumor microenvironment of pancreatic cancer.

1770 Appropriate Handling of Resected Pancreatic Specimens for the Assessment of Residual Pancreatic Cancer after Neoadjuvant Therapy

Yoko Matsuda[1], Masanao Yokohira[2], Keiko Yamakawa[2], Yuko Nakano-Narusawa[2], Minoru Oshima[2], Keiichi Okano[2], Yasuyuki Suzuki[2]
[1]Kagawa University, Faculty of Medicine, Kagawa, Japan, [2]Kagawa University, Faculty of Medicine, Kita-gun, Kagawa-ken, Japan

Disclosures: Yoko Matsuda: None; Yasuyuki Suzuki: None

Background: Pathology assessments on treatment effects are considered important to predict patient outcomes after neoadjuvant resections for pancreatic cancers. Several grading systems to assess tumor regression are often used. Evans and the Japanese Pancreas Society (JPS) grading systems are commonly used in Japan, while the College of American Pathologists (CAP) grading system is typically used in the USA. Evans and JPS grading systems specify a percentage of tumor regression for each grade, but the CAP system does not. Additionally, treatment-related fibrosis is considered secondary to tumor cell death and is taken into consideration in the CAP and JPS grading systems, but not in Evans grading system. Furthermore, appropriate technique for tissue preparation has not been well demonstrated. In this study, we compared tumor regression grade in all sections of the pancreas and the largest tumor area.

Design: The study cohort consisted of 77 patients with pancreatic cancer who had undergone pancreatectomy after neoadjuvant therapy. Most patients received gemcitabine and S-1-based chemotherapies with radiation at Kagawa University Hospital. We reviewed post-neoadjuvant resections to assess tumor regression using CAP, Evans, and JPS grading systems. The evaluation was performed using all sections from the pancreas, and the largest residual tumor sections were determined by macroscopy and microscopy.

Results: The largest residual tumor sections determined by macroscopy and microscopy were similar in 64 patients and different in 13 patients. One patient had complete remission (no residual tumor). Using the 3 grading systems, the results of tumor regression from the whole section and largest tumor section were statistically different in 13 patients showing different largest tumor sections by macroscopy and microscopy, whereas the other 64 patients showed similar results from the whole section and largest tumor section. The largest tumor section tended to overestimate the treatment effect determined by the 3 grading systems.

Conclusions: The largest tumor section, which is easily identified macroscopically, is sufficient to evaluate tumor regression of pancreatic cancer. However, when pancreatic cancer is difficult to be identified macroscopically owing to fibrosis and sclerosis, we need to prepare all sections from the pancreas to obtain an accurate evaluation of tumor regression.

1771 Computerized Nuclear Morphology Features Aid in Diagnosis of Cell Clusters on Digitized Bile Duct Brushing Slides

Shayan Monabbati[1], Cheng Lu[1], Patrick Leo[2], Kaustav Bera[1], Anant Madabhushi[1], Aparna Harbhajanka[3], Claire Michael[4], Behtash Nezami[5]
[1]Case Western Reserve University, Cleveland, OH, [2]Pittsburgh, PA, [3]Cleveland, OH, [4]University Hospitals Cleveland Medical Center, Cleveland, OH, [5]University Hospitals-Cleveland Medical Center, Beachwood, OH

Disclosures: Shayan Monabbati: None; Cheng Lu: None; Patrick Leo: None; Kaustav Bera: None; Anant Madabhushi: *Consultant*, Inspirata Inc.; *Stock Ownership*, Inspirata Inc; Aparna Harbhajanka: None; Claire Michael: None; Behtash Nezami: None

Background: According to the Papanicolaou Society of Cytopathology, Bile Duct Brushings (BDBs) are the preferred evaluation method for sampling from biliary structures due to their low complication rate and their ability to create distinguishing color contrasts between the nuclei and cytoplasm. However, the interpretation of BDBs remains a challenge as there is often presence of inflammatory reactive backgrounds due to strictures and atypical reactive changes. The main goal of this work was to evaluate the ability of computer extracted features of nuclear shape and texture to distinguish malignant from benign cell clusters on BDBs.

Design: BDBs were stained with Thinprep Papanicolaou stain and digitized at 40X magnification. Cell clusters, both malignant and benign, were annotated by an expert cytopathologist on digitized whole slide images (WSI) corresponding to 32 patients, which include 93 malignant clusters and 124 benign clusters. A set of 25 nuclear morphology and image gradient features were extracted from the individual nuclei and corresponding membranes, individual nuclei were segmented using a Laplacian-of-Gaussian watershed algorithm. Wilcoxon rank sum, 2-sample t-test, and minimum redundancy maximum relevance (mrmr) feature selection schemes were used to identify the top 3 features that best separated the malignant and benign clusters on and then used to train a quadratic discriminant classifier to assign a diagnosis to each cluster under 3-fold cross validation.

Results: We obtained a mean area under the Receiver Operating Characteristic curve (AUC) of 0.94. The top 3 features predicting malignancy were nuclear circularity, nuclear perimeter, and nuclear boundary intensity.

Figure 1 - 1771

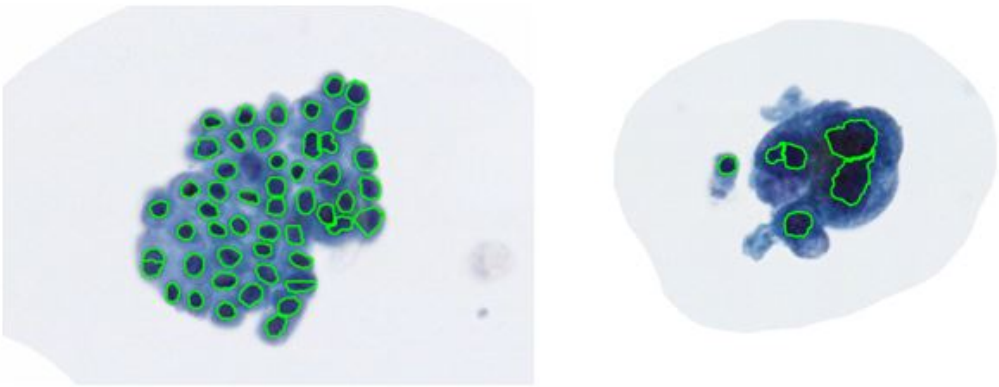

Figure 1 - Nuclear segmentation performed on Papanicolaou stained benign (left) and malignant cluster (right) under 40X magnification. The benign cluster exhibits a 'honeycomb' nuclear architecture and similar nuclear area, while the malignant cluster appears to have a 'drunken honeycomb' nuclear architecture with nuclear molding present. On average, benign nuclei exhibit smaller perimeters, are more circular than malignant nuclei, and have higher boundary intensity values due to nuclear crowding and overlapping.

Figure 2 - 1771

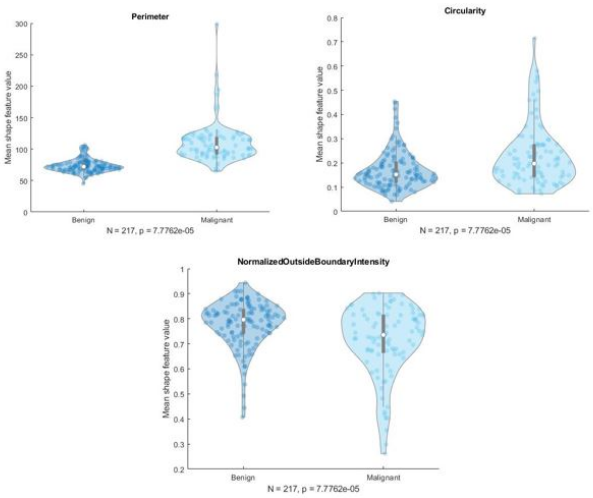

Figure 2- Feature distributions between benign and malignant classes for the top 3 predictive features. A substantial separation between the two classes indicates that the feature can effectively discriminate between malignant and benign cell clusters.

Conclusions: In this study, we demonstrate that nuclear morphological features can quantitatively distinguish benign clusters from adenocarcinomas on digitized BDB images. The benefit to current clinical practice is a high-throughput method of diagnosing new patients, which saves the pathologist time from individually analyzing a new patient's samples. Additional independent validation of these preliminary findings is warranted.

1772 Predicting Morphological Classification of Pancreatic Ductal Adenocarcinoma using Deep Learning

Sangeetha N Kalimuthu[1], Kevin Faust[2], Gavin Wilson[3], Runjan Chetty[1], Phedias Diamandis[1]
[1]University Health Network, Toronto, ON, [2]The University of Toronto, Toronto, ON, [3]Princess Margaret Cancer Centre, Toronto, ON

Disclosures: Sangeetha N Kalimuthu: None; Kevin Faust: None; Gavin Wilson: None; Runjan Chetty: None; Phedias Diamandis: None

Background: Recently, we proposed a revised, pattern based morphological classification system for pancreatic ductal adenocarcinoma (PDAC)[1], where semi-quantitative histopathological scoring for the presence of gland forming (conventional/tubulopapillary) and non-gland forming (composite/squamous) patterns, resulted in 2 groups (A/B) that were strongly associated with the Moffitt transcriptional subtypes (basal/classical)[2] and overall survival. Our work demonstrated that the majority of tumours had patterns from both subtypes, which highlighted the importance of intratumoural heterogeneity and is a rapid and cost-effective approach in predicting prognosis. Herein, we leverage deep learning to automate the grading system to enhance reproducibility and making it more accessible to pathologists for patient care.

Design: 364 haematoxylin and eosin (H&E) stained slides from 58 patients (range 3-11 slides/patient) with treatment naïve PDAC were digitized and used to generate a total of 1.6 x 10^5 image 504 um^2 patches tiles. These images were used to further refine a pathology-optimized convolutional neural network (CNN) developed in our institution using transfer learning[3]. A five-fold cross validation approach was used to assess the performance of our classifier in predicting the A and B morphologic subtypes of our entire cohort.

Results: Of the 58 patients, 30 were classified as Group A and 28 were classified as group B. Group B patients had a poorer OS compared to Group A (p=0.01; unadjusted hazard ratio 95% CI). The CNN analyses yielded a test accuracy of 78% (tile level) and an area under the receiver operator characteristic (ROC) curve (AUC) of 0.75, (Figure 1).

Figure 1 - 1772

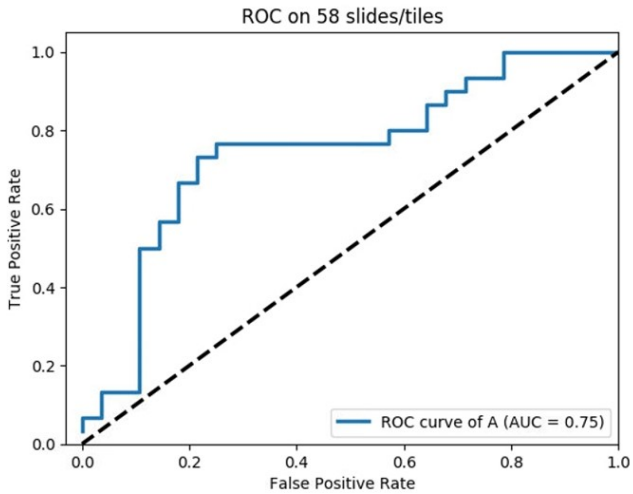

Conclusions: We have demonstrated a proof of concept that deep learning, when applied to PDAC can objectively classify the morphological subtypes we have previously described using H&E slides. The current limitation of our deep learning method is that the classifications are binary and do not provide quantitative information about the proportions of each morphological features. Similarly, the intra and intertumoural heterogeneity of the stromal component may have compromised the analyses. Our future steps will be the segregation of the stromal and epithelial components to improve the accuracy of our deep learning tool and pilot the application at multiple international centers using a cloud-based interface.

1. N Kalimuthu S *et al* Gut BMJ June 2019

2. Moffitt RA *et al* Nat Genet Oct 2015

3. Faust K *et al* Nat. Mach. Intell. July 2019

1773 Association of Inflammatory Cell Infiltrates with Signatures of Immunogenicity in Pancreatic Adenocarcinoma

Julia Naso[1], James Topham[2], Michael Lee[3], Steve Kalloger[1], Joanna Karasinska[4], Janessa Laskin[5], Marco Marra[6], Daniel Renouf[5], David Schaeffer[7]

[1]University of British Columbia, Vancouver, BC, [2]Pancreas Centre BC, Vancouver, BC, [3]Division of Medical Oncology, BC Cancer, Vancouver, BC, [4]BC Cancer, Vancouver, AB, [5]British Columbia Cancer Agency, Vancouver, BC, [6]Michael Smith Genome Sciences Centre, [7]Vancouver General Hospital, Vancouver, BC

Disclosures: Julia Naso: None; James Topham: None; Michael Lee: None; Joanna Karasinska: None; Daniel Renouf: None; David Schaeffer: None

Background: Antitumor immune responses are stimulated by mutations generating novel immunogenic peptides (i.e. neoantigens) and by the aberrant expression of endogenous retrovirus (ERV) containing transcripts. Downregulation of antitumor immune responses contributes to disease progression. The degree of antitumor immune response may be reflected in the gene expression profile of the tumor microenvironment. Histologic correlates of these *in silico* signatures of immunogenicity have not been well characterised.

Design: Whole genome and transcriptome sequencing data were available for 57 advanced stage pancreatic adenocarcinomas through the PanGen (NCT02869802) and POG (NCT02155621) programs. Neoantigens were identified using a bespoke bioinformatics pipeline incorporating MHC binding affinity predictions and sequence alignment to a database of viral and bacterial epitopes. 'High ERV' tumors had high ERV read count z-scores and showed signatures of antiviral response. Gene expression-based subtyping used the Bailey classifier. The abundance of stromal lymphocytes, stromal neutrophils and luminal neutrophils was scored for 46 patients using either the clinical pathology sample taken closest in time to the sequenced biopsy (26 metastatic sites and 11 primary sites sampled) or frozen section slides prepared from the sequenced biopsy (n=9).

Results: Stromal lymphocytes were associated with higher numbers of neoantigens (P=0.013). Luminal but not stromal neutrophils were associated with low levels of neoantigens (P=0.040) and high ERV levels (P=0.039). Using the Bailey classifier, luminal neutrophils were highest in the immunogenic subtype and lowest in the poor prognosis squamous subtype (P=0.0018). The immunogenic subtype was associated with low levels of stromal lymphocytes (P=0.027) and high ERV/low neoantigen tumors (P=0.0010). The Bailey subtypes were significantly associated with overall survival (p<0.0001), with the immunogenic subtype showing longer survival compared to the squamous and progenitor subtypes.

Conclusions: We identify histologic correlates of neoantigenicity and ERV levels that are associated with prognostically significant gene expression-based subtypes. Our findings implicate luminal neutrophils and stromal lymphocytes in the modulation of antitumor immune responses. These histologic features are potential markers of immunogenicity that may be readily assessed in clinical practice.

1774 ARX Reactivity Predicts Recurrence in Non-Functional Pancreatic Neuroendocrine Tumors (panNET)

Azfar Neyaz[1], Deepa Patil[2], Vikram Deshpande[3]
[1]Massachusetts General Hospital, Malden, MA, [2]Brigham and Women's Hospital, Boston, MA, [3]Massachusetts General Hospital, Boston, MA

Disclosures: Azfar Neyaz: None; Deepa Patil: None; Vikram Deshpande: *Grant or Research Support*, Advanced Cell Diagnostics; *Advisory Board Member*, Viela; *Grant or Research Support*, Agios Pharmaceuticals

Background: The optimal therapeutic approach to incidentally detected pancreatic neuroendocrine tumors (panNET) is uncertain and there is an unmet need for biomarkers that predict the outcome. Transcriptional proteins ARX and PDX1 specify two distinct epigenetic and transcriptomic subtypes of PanNETs, the former resembling α and the latter β cells. The aim of this study is to exploit this categorization of PanNETs to identify patients at high risk of recurrence.

Design: In this retrospective study, we analyzed 76 non-functional panNETs. Demographic data, WHO grading, recurrence and survival were recorded. Immunohistochemistry for ARX and PDX1 were performed on whole tissue sections. Nuclear reactivity for ARX and PDX1 was scored either positive or negative. Assessment of alternative lengthening of telomeres (ALT) was done using Telomere-specific FISH.

Results: ARX and PDX1 were diffusely positive in 62% and 65% of cases, respectively. 40% of tumors were dual positive (ARX+PDX1+); 13% were dual negative (ARX-PDX1-). T stage (p=0.04), WHO grade (p=0.03), ALT phenotype (p=0.02) and ARX (p=0.02) expression predicted disease recurrence. Of 12 cases with tumor recurrence, 11 (92%) cases expressed ARX. ARX negative cases showed a recurrence rate of 4% as compared to 23% for ARX positive cases. There was no correlation between the ALT phenotype and ARX expression (p=0.181).

Parameters	Categorical variables	Recurrence; n (%)		p value
		Present	Absent	
Tumor size	<2 cm ≥2 cm	3 (25%) 9 (14.1%)	9 (75%) 55 (85.9%)	0.340
T stage	1 and 2 3	7 (11.5%) 5 (33.3%)	54 (88.5%) 10 (66.7%)	0.038
WHO Grade	G1 G2 G3	5 (11.1%) 6 (26.1%) 1 (100%)	40 (88.9%) 17 (73.9%) 0	0.027
ALT* phenotype (n=47)	Present Absent	4 (30.8%) 2 (5.9%)	9 (69.2%) 32 (94.1%)	0.022
ARX protein expression	Present Absent	11 (23.4%) 1 (3.4%)	36 (76.6%) 28 (96.6%)	0.020
ALT amplification OR ARX protein expression (n=64)	Present Absent	11 (22%) 0	39 (78%) 14 (100%)	0.054
PDX1 protein expression	Present Absent	8 (16.3%) 4 (14.8%)	41 (83.7%) 23 (85.2%)	0.863
Tumor typing based on ARX/PDX profile	A (ARX+PDX1-) B (PDX1+ARX-) DP (ARX+PDX1+) DN (ARX-PDX1-)	4 (23.5%) 1 (5.3%) 7 (23.3%) 0	13 (76.5%) 18 (94.7%) 23 (76.7%) 10 (100%)	0.138
	Type A and DP Type B and DN	11 (23.4%) 1 (3.4%)	36 (76.6%) 28 (96.6%)	0.020

Conclusions: ARX protein expression predicts recurrence in non-functional panNET and could serve as an additional marker to predict the biology of non-functional tumors.

1775 Can Endoscopic Ultrasound-Guided Fine Needle Aspiration Biopsy Accurately Distinguish between Pancreatic Ductal Adenocarcinoma and Tumefactive Pancreatitis? An Interobserver Study

Kenji Notohara[1], Terumi Kamisawa[2], Shinichi Aishima[3], Yuki Fukumura[4], Noriyoshi Fukushima[5], Toru Furukawa[6], Kenichi Hirabayashi[7], Satomi Kasashima[8], Motohiro Kojima[9], Tomoko Mitsuhashi[10], Yoshiki Naito[11], Nobuyuki Ohike[12], Takuma Tajiri[13], Takeshi Uehara[14], Hiroshi Yamaguchi[15], Shigeyuki Kawa[16], Kazuichi Okazaki[17]

[1]Kurashiki Central Hospital, Kurashiki, Japan, [2]Tokyo Metropolitan Komagome Hospital, Tokyo, Japan, [3]Saga University, Saga, Saga, Japan, [4]Juntendo University, Tokyo, Japan, [5]Jichi Medical University, Shimotsuke, Tochigi ken, Japan, [6]Tohoku University Graduate School of Medicine, Sendai, Japan, [7]Tokai University School of Medicine, Isehara, Kanagawa, Japan, [8]Kanazawa University, Kanazawa, Ishikawa, Japan, [9]National Cancer Center Hospital, Kashiwa, Chiba, Japan, [10]Hokkaido University Hospital, Sapporo, Hokkaido, Japan, [11]Kurume University School of Medicine, Kurume, Fukuoka, Japan, [12]Showa University Fujigaoka Hospital, Yokohama, Japan, [13]Tokai University Hachioji Hospital, Hachioji, Japan, [14]Shinshu University School of Medicine, Matsumoto, Japan, [15]Tokyo Medical University, Tokyo, Japan, [16]Matsumoto Dental University, Shiojiri, Nagano, Japan, [17]Kansai Medical University, Hirakata, Osaka, Japan

Disclosures: Kenji Notohara: None; Terumi Kamisawa: None; Shinichi Aishima: None; Yuki Fukumura: None; Noriyoshi Fukushima: None; Toru Furukawa: None; Kenichi Hirabayashi: None; Satomi Kasashima: None; Motohiro Kojima: None; Tomoko Mitsuhashi: None; Yoshiki Naito: None; Nobuyuki Ohike: None; Takuma Tajiri: None; Takeshi Uehara: None; Hiroshi Yamaguchi: None; Shigeyuki Kawa: None; Kazuichi Okazaki: None

Background: The sensitivity and specificity of pancreatic ductal adenocarcinoma (PDAC) diagnosis with endoscopic ultrasound-guided fine needle aspiration (EUS-FNA) cytology is high (both; >90%), but such data on EUS-FNA biopsy has not been evaluated. Such evaluation is warranted because much larger tissues are now available with newly-developed needles, and future EUS-FNA diagnosis may be based on the histology alone.

Design: Nine pathologists (7 specialized in pancreatic pathology and 2 non-specialized) were enrolled in 2 rounds of interobserver studies using virtual slides. Eighty-six biopsy specimens with PDAC and 89 with tumefactive pancreatitis (TP) obtained by EUS-FNA were collected through a nationwide survey, and, in each round, 41 differing large specimens (21 of PDAC and 20 of TP) were evaluated as either PDAC or non-neoplastic by 9 raters. The great majority of the TP cases was definite type 1 AIP. Five other pathologists participated in preparing guidance for the distinction between PDAC and type 1 autoimmune pancreatitis (AIP). Potential diagnostic issues were discussed through the evaluation of some virtual slides, and the 5 members reached a consensus that confusion of acinar-ductal metaplasia (ADM) in type 1 AIP with PDAC seemed to be a problem. Thus, guidance included histological features of ADM, such as poorly-formed shapes of glands and lumens, small and round nuclei, localization within the pancreatic lobules, and some diagnostic pitfalls. Some clues for recognizing PDAC, such as enlarged, hyperchromatic irregular and pleomorphic nuclei, and abnormal mucus production in the cytoplasm, were also described. Before starting the second round of the interobserver study, each rater studied the guidance. The kappa values of the raters, and sensitivity and specificity of each rater were evaluated.

Results: The kappa values in the first round (0.775 in all raters, and 0.875 in 7 specialized) improved in the second (0.851 and 0.958, respectively). The specificity was <90% in 3 raters in the first round, but none in the second. The sensitivity was significantly lower in non-specialized (67% and 76%) than specialized pathologists (median, 100%) even in the second round.

Conclusions: The diagnosis of PDAC by EUS-FNA biopsy was useful, but ADM seemed to be a diagnostic pitfall. In order to prevent the overcalling of PDAC, the guidance created in this project was effective. Sufficient experience in diagnosing PDAC is necessary to improve the sensitivity.

1776 Pancreatic Cystic Lesions can be Reliably Diagnosed Using the Novel Endoscopic Ultrasound Guided Micro-Forceps Biopsies

Gregory Olsen[1], Ashwini Esnakula[1], Xiuli Liu[1], Michael Feely[1], David Hernandez Gonzalo[2], Ashwin Akki[1]
[1]University of Florida, Gainesville, FL, [2]University of Florida-Shands, Gainesville, FL

Disclosures: Gregory Olsen: None; Ashwini Esnakula: None; Xiuli Liu: None; Michael Feely: None; David Hernandez Gonzalo: None; Ashwin Akki: None

Background: Pancreatic cystic lesions (PCLs) carry a high risk of adenocarcinoma but pose a diagnostic challenge owing to their location and lack of techniques that sample the cyst wall. The novel endoscopic ultrasound guided through-the-needle biopsy micro-forceps (EUS-MF; Moray™ microforceps) has enabled targeted biopsy of PCLs vs. the widely used fine needle aspiration. Data on diagnostic utility of EUS-MF for PCLs is sparse. Herein, we evaluate the utility and inter-observer agreement in interpreting EUS-MF biopsies from PCLs.

Design: We retrospectively reviewed 50 EUS-MF biopsies from 49 patients with PCLs over a 36-month period. Four pancreatic pathologists blinded to the original diagnoses independently reviewed biopsies (mean slides/patient: 5; range 2-14) to assess the cyst lining epithelium, sub-epithelial stroma, epithelial dysplasia and/or adenocarcinoma. Each reviewer's interpretations were correlated with final diagnoses, which was based on synthesis of clinical, imaging, lab (cyst fluid CEA and amylase) data, and diagnoses on surgical resections (n=13) when available. Inter-observer agreement was assessed by Cohen's kappa.

Results: Mean patient age was 63.3 years (range 22-88 years; M-16, F-33). Average cyst size was 33.7 mm (range 15-110 mm). Cysts were located in the head (n=20), tail (n=19) and body (n=10) of pancreas. Eighteen cysts communicated with the main pancreatic duct on imaging. Average biopsy size was 1.3 mm (range: 1-3 mm). EUS-MF yielded mucinous epithelium diagnostic of intraductal papillary mucinous neoplasm (IPMN) or mucinous cystic neoplasm (MCN) in 27/49 (55%), serous epithelium in 2/49 (4%), neuroendocrine tumor in 2/49 (4%), and pseudocyst in 1/49 (2%), but no diagnostic tissue in 17/49 (35%) cases. Cyst fluid CEA levels were elevated (>192 ng/dL) in 15/25 (60%) mucinous neoplasms. EUS-MF biopsies were predictive of the diagnoses made at resection (IPMN or MCN) in 8/13 (62%) cases. Three patients (23%) with inconclusive EUS-MF revealed an IPMN or MCN after surgery. Inter-observer agreement was high (k=0.84) for mucinous cysts and perfect (k=1.0) for serous and cystic neuroendocrine tumor. Mean post-biopsy follow-up was 47.3 weeks (range 1-164 weeks). Surgical resections revealed colloid carcinoma in 1 (8%), IPMN with high-grade dysplasia in 6 (46%), and MCN with low-grade dysplasia in 4 (31%).

Conclusions: Majority of PCLs can be reliably diagnosed by EUS-MF. Future technical advances may augment diagnoses in a third of PCLs that yielded non-diagnostic tissue.

1777 STK11 Plays a Canonical Role in Malignant Progression of a Subset of KRAS-mutant Intraductal Papillary Mucinous Neoplasms

Yuko Omori[1], Yusuke Ono[2], Takanori Morikawa[1], Fuyuhiko Motoi[3], Ryota Higuchi[4], Masakazu Yamamoto[5], Hidenori Karasaki[6], Yusuke Mizukami[7], Michiaki Unno[3], Toru Furukawa[8]
[1]Tohoku University Graduate School of Medicine, Sendai, Miyagi, Japan, [2]Institute of Biomedical Research, Sapporo Higashi Tokushukai Hospital, Sapporo, Hokkaido, Japan, [3]Department of Surgery, Tohoku University Graduate School of Medicine, Sendai, Miyagi, Japan, [4]Tokyo Women's Medical University, Tokyo, Japan, [5]Department of Surgery, Institute of Gastroenterology, Tokyo Women's Medical University, Tokyo, Japan, [6]Institute of Biomedical Research, Sapporo Higashi Tokushukai Hospital, Sapporo, Japan, [7]Asahikawa Medical University, Asahikawa, Hokkaido, Japan, [8]Tohoku University Graduate School of Medicine, Sendai, Japan

Disclosures: Yuko Omori: None; Yusuke Ono: None; Takanori Morikawa: None; Fuyuhiko Motoi: None; Ryota Higuchi: None; Masakazu Yamamoto: None; Hidenori Karasaki: None; Toru Furukawa: None

Background: Serine/Threonine Kinase 11 (STK11) is a tumor suppressor molecule. *STK11* is involved in some intraductal papillary mucinous neoplasms (IPMNs), but pathobiological features of STK11 aberrant IPMNs have not been clarified yet.

Design: Our research aimed to elucidate the characteristics of STK11-aberrant IPMNs. We performed immunohistochemistry of STK11, phospho-AMP-activated protein kinase alpha (pAMPKα), and mucins on 187 IPMNs without Peutz-Jeghers syndrome. Mutation analysis of

STK11, KRAS, and GNAS in 68 IPMNs (29 STK11-aberrant expression, 39 STK11-retained expression) using custom-made panel, covering whole exon region of *STK11* and hotspot of *KRAS* and *GNAS* by targeted amplicon sequencing was performed.

Results: Diffuse loss or reduction of expression of STK11 was observed in 29 (16%, STK11-aberrant) of 187 IPMNs, of which 43% pancreatobiliary (PB), 20% oncocytic, 2% gastric, and 0% intestinal of each subtype (p=4.07e-12), and 34% of IPMNs with an associated invasive cancer, 9% of high-grade IPMNs, and 0% of low-grade IPMNs (p=5.30e-07). Aberration was sequentially observed in gastric-type low-grade dysplasia component concurrent with high-grade dysplastic components or invasive carcinoma. 17 *STK11* mutations (6 frameshift, 6 nonsense, 1 splice site, 4 missense mutation) were detected in 15 STK11-aberrant IPMNs (52%, p=2.1e-06). 83% (24/29) of STK11-aberrant IPMNs were *KRAS* mutant, but only 3% (1/29) *GNAS* mutant. Morphologically, STK11-aberrant IPMNs present homogenous growth pattern of hierarchic arborizing papillae with thin delicate fibrovascular core, so called “fern-like” morphology, and aggregated hyaline globules (p=9.62e-13). STK11 was retained in PB-type IPMNs with marked atypia and irregular growth with reduced MUC5AC expression (p=0.00969). STK11-aberrant IPMNs with oncocytic features were differentiated from typical intraductal oncocytic papillary neoplasms, which were STK11-retained, and could be reclassified as PB-type. Expression of pAMPKα was reduced in STK11-aberrant IPMNs (93%, p=1.98e-12). STK11-aberrant IPMNs showed poorer prognosis (disease-free survival p=0.0214, overall survival p=0.03).

Conclusions: These results suggest that STK11 may play a canonical role in malignant progression of the prototype of PB-type *KRAS*-mutant IPMNs. Aberrant expression of STK11 was related with downregulation of pAMPKα, therefore, mTOR inhibitor and AMPK activator could be new therapeutic targets for a certain group of IPMNs and associated pancreatic cancer.

1778 Epithelial Inclusions in the Gallbladder: Cytoisospora belli Organisms or Degenerative Intracytoplasmic PAS-Positive Hyaline Globules

Burcin Pehlivanoglu[1], Ipek Erbarut Seven[2], Bahar Memis[3], Burcu Saka[4], Pelin Bagci[2], Serdar Balci[5], Jeanette Cheng[6], Olca Basturk[7], Michelle Reid[8], N. Volkan Adsay[9]

[1]Adiyaman University Training and Research Hospital, Adiyaman, Turkey, [2]Marmara University, Istanbul, Turkey, [3]SBU Sisli Hamidiye Etfal Training and Research Hospital, Istanbul, Turkey, [4]Istanbul Medipol University, Istanbul, Turkey, [5]Ankara, Turkey, [6]Piedmont Atlanta Hospital, Atlanta, GA, [7]Memorial Sloan Kettering Cancer Center, New York, NY, [8]Emory University Hospital, Atlanta, GA, [9]Koç University Hospital, Istanbul, Turkey

Disclosures: Burcin Pehlivanoglu: None; Ipek Erbarut Seven: None; Bahar Memis: None; Burcu Saka: None; Pelin Bagci: None; Serdar Balci: None; Jeanette Cheng: None; Olca Basturk: None; Michelle Reid: None; N. Volkan Adsay: None

Background: Lai et al. reported 18 cases of Cystoisospora belli in the gallbladders (GBs), detected incidentally in 0.5% of immunocompetent patients (PMID: 27158759). However, a recent molecular study failed to confirm this observation at molecular level (PMID: 30020094). Although Lai et al. indicated that Cystoisospora in the GB is quiescent in immunocompetent patients, this diagnosis nevertheless has major implications, resulting in extensive patient workup for undetected immunosuppression.

Design: 1336 GBs, all removed for various pathologies, (228 of which were totally submitted for evaluation), were reviewed systematically for epithelial inclusions and structures described by Lai study.

Results: While degenerative cytoplasmic changes resembling parasites were not uncommon, true epithelial inclusions were found in 1.7% of cases. There was one case diffusely showing all the characteristics described in the Lai study for Cystoisospora belli (Figure 1) but this case proved not to be a parasite by electron microscopy (Figure 2). The GB mucosa showed no signs of injury, inflammation nor did it have stones. Otherwise, epithelial inclusions were significantly more common in neoplastic GBs (p<0.0001; Table). While some were more elongated and showed parasite-like morphology, most were round, pale acidophilic bodies, often accompanied by halos. For cases with these inclusions, mean age was 63 (vs 49 in our cholecystectomy cohort; p=0.005) supporting their degenerative nature. They were usually (multi)focal or dispersed, except for 2 cases (1 chronic cholecystitis and 1 oncocytic intracholecystic papillary tubular neoplasm (ICPN), in which they were diffuse.

	Total case #	**# of the cases with epithelial inclusions**
Nonneoplastic	**907**	**4 (0.4%)**
Neoplastic	**429**	**19 (4.4%)**
Dysplasia	73	0
Noninvasive ICPN	54	1 (1.9%)
Invasive ICPN	68	5 (7.4%)
Carcinoma	234	13 (5.6%)
Total	**1336**	**23 (1.7%)**

Figure 1 - 1778

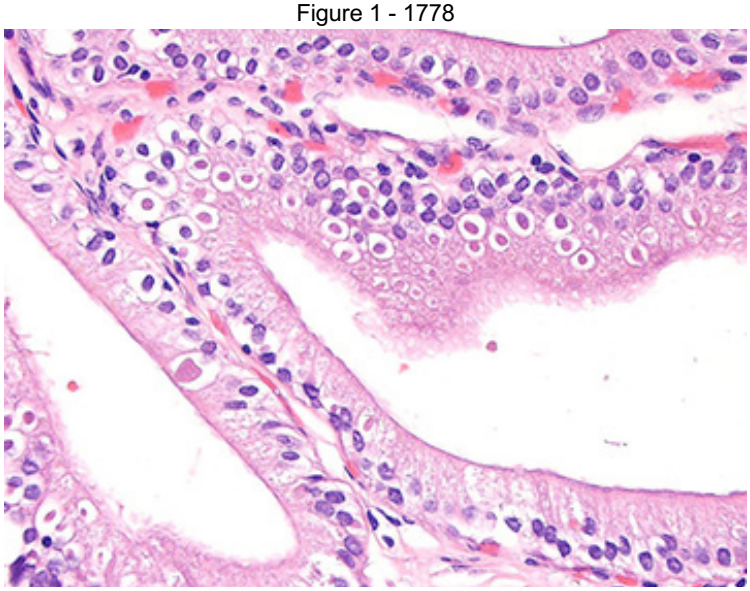

Figure 2 - 1778

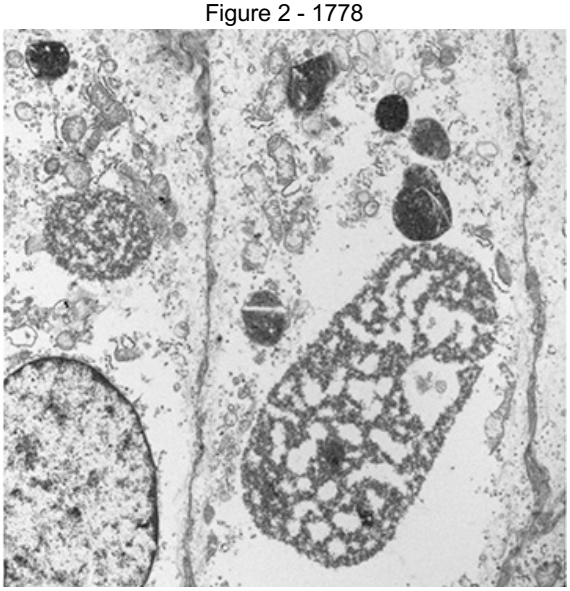

Conclusions: In the GB, there is a spectrum of degenerative epithelial changes that are not uncommon and lead to epithelial inclusions with the differential diagnosis of Cystoisospora belli. More established forms of these inclusions occur in 1.7% of GBs. These include PAS-positive hyaline globules, probably representing a degenerative phenomenon and are seen more commonly in neoplastic lesions and in older patients. Electron microscopy of a GB showing classical histomorphologic features described for Cystoisospora failed to reveal any microorganisms. Further studies are needed to clarify the nature of these inclusions and to determine which of these truly represent quiescent Cystospora infection.

1779 Immune Cell Localization and Spatial Relationships in Pancreatic Acinar Cell Carcinoma

J Peske[1], Dwayne Thomas[2], Laura Wood[3], Elizabeth Jaffee[4], Elizabeth D Thompson[3]
[1]Baltimore, MD, [2]Johns Hopkins, Baltimore, MD, [3]Johns Hopkins Hospital, Baltimore, MD, [4]Johns Hopkins Medical Institutions, Baltimore, MD

Disclosures: J Peske: None; Dwayne Thomas: None; Laura Wood: None; Elizabeth Jaffee: None; Elizabeth D Thompson: None

Background: Pancreatic acinar cell carcinoma (ACC) is an aggressive malignancy with limited treatment options. Immune-based therapies have shown promise in treating tumors with an active tumor immune microenvironment (TME). However, little is known about the TME in ACC. We previously reported PDL1 and IDO expression in a cohort of primary ACC surgical resection specimens. Here, we expand our characterization of the ACC TME.

Design: Whole slides from 23 ACC resection specimens were previously labeled by immunohistochemistry for CD4, CD8, CD20, FoxP3, CD68, MPO, PDL1, PD1 and IDO. Immune infiltration was scored along with PDL1 and IDO expression. Immune cells were quantified within tumor nests, at the invasive tumor-stroma interface, and in adjacent uninvolved pancreatic acini using digital image analysis software (HALO, Indica Labs). Proximity analyses were performed on registered serial sections. Immune parameters were compared to clinical features, including overall survival (OS).

Results: All ACC were infiltrated by lymphocytes and myeloid cells with lymphocytes concentrated at the tumor-stroma interface. Accumulation of CD8+ T cells at this invasive margin was striking, with PDL1+ tumors having the highest CD8+ density (p=0.013). Intratumoral CD8 densities were lower than in adjacent pancreas (p=0.03) or interface regions (p=0.008). CD68+ and MPO+ myeloid cells did not show significant density variations between analyzed regions. The density of PDL1+ and IDO+ cells trended higher both within the tumor and at the invasive margin and PDL1+ cells were more likely to be in close proximity (within 20 μm) to PD1+ cells in intratumoral areas. There was a trend toward decreased OS in patients with PDL1+ tumors.

Conclusions: ACC show an active TME with robust lymphocytic infiltration at the tumor-stroma interface and more diffuse infiltration by myeloid cells. The enrichment of PDL1+ and IDO+ cells and the proximity of PDL1+ to PD1+ cells within tumors, combine with the concentration of lymphocytes at the interface, suggests a pattern of immune exclusion in ACC with active immune responses at the invasive front and an immunosuppressive tumor center. Our prior findings of both adaptive and innate patterns of PDL1 expression combined with the trend for decreased OS in PDL1+ tumors point to a complicated TME in ACC and support further evaluation of mechanisms of immune activation and suppression in these tumors as well as potential benefits of immunomodulatory therapies.

1780 Clinical Utility of Semiquantitative Evaluation of Estrogen and Progesterone Receptor Immunohistochemistry and mRNA Analysis in Neuroendocrine Tumors of the Pancreas and Midgut

Sonya Purushothaman[1], Igor Katsyv[2], Simona De Michele[3], Helen Remotti[4]
[1]New York, NY, [2]Columbia University/New York Presbyterian Hospital, New York, NY, [3]Columbia University Medical Center/New York Presbyterian Hospital, New York, NY, [4]Columbia University Medical Center, New York, NY

Disclosures: Sonya Purushothaman: None; Igor Katsyv: None; Simona De Michele: None; Helen Remotti: None

Background: Tamoxifen has long been used in adjuvant endocrine therapy of steroid hormone receptor– positive breast cancer. Currently, clinical trials are assessing its use in pancreatic neuroendocrine tumors. In this study, we assessed ER and PR immunohistochemical expression in a cohort of neuroendocrine tumors of the pancreas (pNETs) and of the midgut (mNETs) as well and other pancreatic neuroendocrine carcinomas (pNECs). We then performed mRNA expression analysis on an independent cohort of pancreatic and small intestinal NETs. Theoretically tumors with highest ER and PR expression are more likely to respond to adjuvant tamoxifen.

Design: Immunohistochemical staining for ER and PR was performed on tissue microarrays of 54 pNETs, 8 pNECs, and 30 mNETs. A minimum of 4 separate 2mm tumor cores were sampled on each case. RNA-sequencing data (GSE98894) was downloaded from the NCBI Gene Expression OmniBus. Expression data was normalized for library size, lowly-expressed transcripts were removed, and the data was transformed to log2 counts per million (log2CPM). Differentially-expressed genes were called using the edgeR (v 3.24.3) and limma (v 3.38.3) R packages.

Results: ER and PR staining were evaluated using a semiquantitative H-score method. Positive ER staining (defined as greater than 1%) was identified in 20% (6 of 30 cases) of mNETs (mean H-score 113), while 0% of mNETs showed positive PR expression. Conversely, positive PR staining (defined as greater than 1%) was identified in 61% (33 of 54 cases) of pNETs (mean H-score 100), while 0% of pNETs showed positive ER staining. No pNECs (0 of 8 cases) showed positive staining for either ER or PR. These results were further validated at the mRNA level. ESR1 is expressed 3.66 fold higher in small intestine NETs compared to pancreatic NETs (FDR < 0.01), and PGR is expressed 3.03 fold higher in pancreatic NETs compared to small intestine NETs (FDR < 0.01).

Figure 1 - 1780

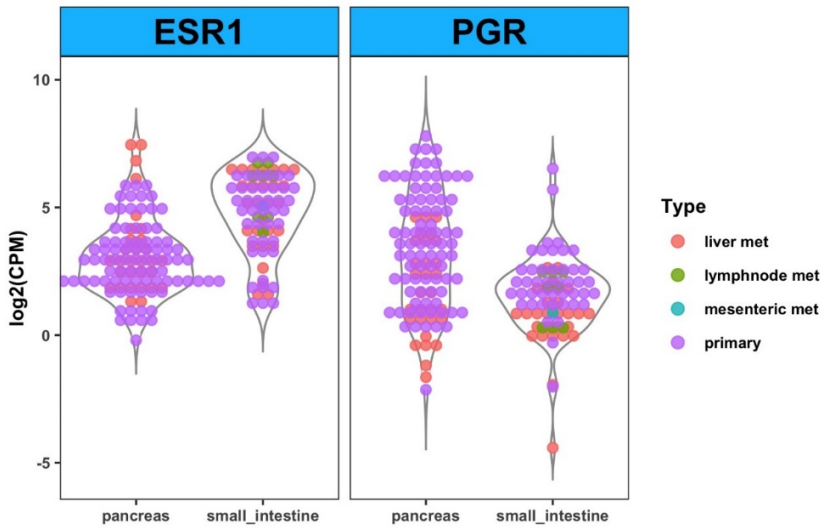

Conclusions: Based on these findings, we suggest analysis of NETs for ER and PR expression should include a quantitative or semiquantitative score for evaluation of hormone receptors, particularly in the evaluation of patients' response to clinical trials with tamoxifen. Further, in view of our RNA seq and immunohistochemical staining results, we propose that patients with mNETs may also benefit from hormone receptor therapy. High grade pNECs showed no PR or ER immunoreactivity and therefore are less likely to derive benefit from adjuvant endocrine therapy.

1781 Characterization of Islet of Langerhans Invasion in Pancreatic Ductal Adenocarcinoma

Shyam Raghavan[1], Chieh-Yu Lin[2], Teri Longacre[1], Gregory Charville[3]
[1]Stanford University, Stanford, CA, [2]Washington University School of Medicine in St. Louis, St. Louis, MO, [3]Stanford University School of Medicine, Stanford, CA

Disclosures: Shyam Raghavan: None; Chieh-Yu Lin: None; Teri Longacre: None; Gregory Charville: None

Background: Despite numerous studies that have defined features of pancreatic ductal adenocarcinoma (PDAC), the distinction between malignant and benign pancreatic ductal epithelium remains challenging. In particular, benign mimics such as chronic pancreatitis can demonstrate similar histologic features of PDAC, including irregular gland formation, fibromyxoid stroma, and cytologic atypia. To distinguish between these two entities, we often use particular histologic clues, such as perineural or lymphovascular invasion, to make a definitive diagnosis. We sought to characterize another potential histologic feature of PDAC—invasion of islets of Langerhans—which has been documented in the literature, but not extensively studied.

Design: Sixty-one resections were reviewed for the presence of islet of Langerhans invasion (ILI). In ambiguous cases, immunohistochemistry for cytokeratin 7 and synaptophysin was performed to better characterize the architecture. The presence of ILI was compared to several other clinicopathologic features. Additionally, twenty-five consecutive surgical resections with chronic pancreatitis in the absence of malignancy were reviewed for the presence of benign ductal epithelial inclusions mimicking islet invasion on H&E-stained histologic sections.

Results: ILI was present in 75.4% of PDAC cases. In addition to correlating with the presence of perineural invasion, ILI was associated with higher pathologic T-stage, increased number of involved lymph nodes, and increased risk of at least one positive or close (<0.1 cm) margin (Table 1). We saw no evidence of ILI in 20 cases of IPMN or in 25 cases of chronic pancreatitis. Benign ductal inclusions were identified in at least one islet in 15 chronic pancreatitis cases (60%), although only two cases (8%) showed benign inclusions in more than two islets. Altogether, benign inclusions were seen in 1.6% (33/2091) of evaluated islets.

Feature	Islet Invasion	No Islet Invasion	p-value
Patient age (y)	69.0 ± 11.0	70.0 ± 7.9	*0.75*
Patient gender (m:f)	25:21	8:7	*1.0*
Tumor size (cm)	3.4 ± 1.2	3.7 ± 3.2	*0.58*
Pathologic T-stage (T3:T2:T1)	13:32:1	3:8:4	***0.011****
Peripancreatic soft tissue invasion (present:absent)	46:0	12:3	***0.013***
Perineural invasion (%)	97.8%	73.3%	***0.011***
Lymphovascular invasion (%)	60.9%	40.0%	*0.23*
Pathologic N-stage (% pN1)	82.6%	86.6%	*1.0*
Number of involved nodes	5.3 ± 4.3	2.5 ± 1.9	***0.028***
Positive or close (<0.1 cm) margin (%)	34.8%	0%	***0.0028***

Conclusions: ILI is a diagnostic feature of PDAC, which correlates with the presence of peri-neural invasion, higher pathologic T-stage, and increased lymph node metastasis. It may be a useful histologic marker of malignancy in ambiguous cases, although benign ductal inclusions represent a potential diagnostic pitfall.

1782 Increased Expression of Transferrin Receptor CD71 in Pancreatic Neoplasia

Deepti Ravi[1], Corwyn Rowsell[2], Shawn Winer[3], Norman Marcon[3], Catherine Streutker[4]
[1]Saskatchewan Health Authority, Saskatoon, SK, [2]St. Michael's Hospital, Toronto, ON, [3]St Michael's Hospital, Toronto, ON, [4]Unity Health Toronto, Toronto, ON

Disclosures: Deepti Ravi: None; Corwyn Rowsell: None; Shawn Winer: None; Norman Marcon: None; Catherine Streutker: None

Background: Pancreatic adenocarcinoma can arise as a result of progression from precursor lesions such as intraductal papillary mucinous neoplasms (IPMN), high grade intraepithelial neoplasia and has a particularly poor prognosis. The distinction between pancreatic adenocarcinoma and reactive ducts, especially in a background of pancreatitis, can be challenging, particularly in tiny biopsy specimens or fine needle aspiration cytology specimens. Several pathways have been implicated in the development of pancreatic adenocarcinoma, however clinically useful markers to distinguish neoplasia from reactive changes are not readily available. One emerging cancer mechanism which fuels the metabolism of neoplastic cells is iron metabolism. Iron enters squamous and glandular epithelial cells through the transmembrane glycoprotein Transferrin receptor (CD71). We surmised that neoplastic cells with increased metabolic drive may show aberrant CD71 expression in pancreatic lesions.

Design: A total of 53 pancreatic fine needle core biopsy samples from 53 cases encompassing pancreatic adenocarcinoma (n = 22), IPMN (n = 10), IPMN with adenocarcinoma (n = 4), and normal / benign (n = 17) were assessed. All biopsies were formalin fixed.

Immunohistochemistry for CD71(Ventana/Cell Marque MRQ-48) was performed as per the protocol. The intensity of CD71 immunohistochemical expression was scored by two independent and blinded observers using a three point scoring system from 0 (no expression) to 3 (high expression). Statistical significance was set at $p<0.05$

Results: Moderate to strong membranous and cytoplasmic CD71 staining was seen in 63% of the adenocarcinoma cases and 60% of IPMN (Figure 1a). The normal / benign pancreatic glandular epithelium showed no staining in nearly all (95%) of the cases, with only a single case with faint minimal staining (Figure 1b). Four cases with adenocarcinoma arising from IPMN showed moderate CD71 staining. The sensitivity of moderate to strong CD71 expression for the detection of adenocarcinoma of the pancreas was 64% (95% CI 0.4 to 0.8), while the specificity was 99.9% (95% CI 0.8 to 1).

Figure 1 - 1782

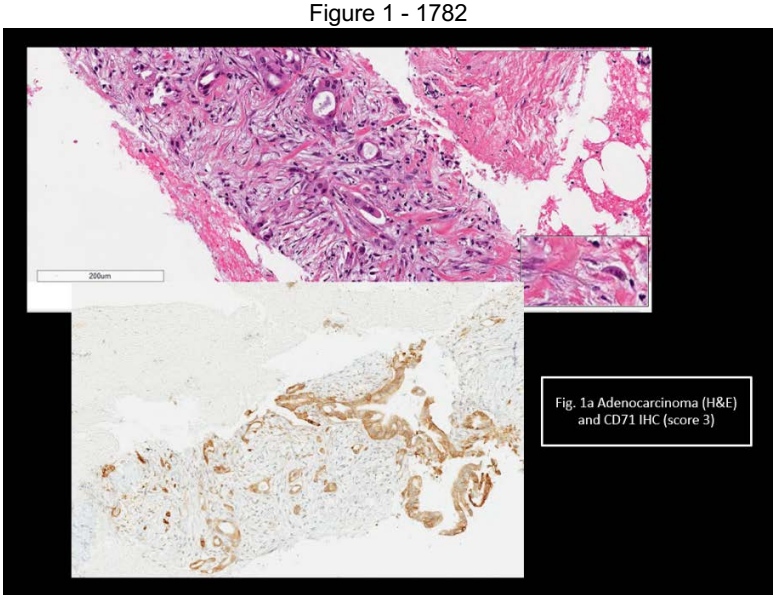

Figure 2 - 1782

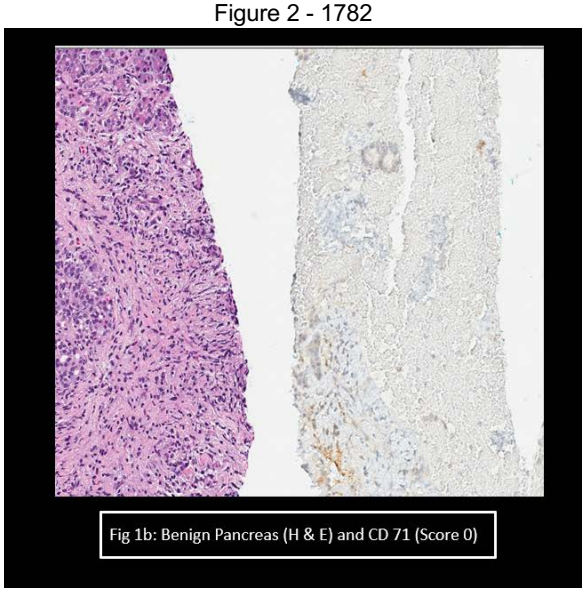

Conclusions: CD71 is moderately up regulated in IPMN and adenocarcinoma of the pancreas compared to benign tissues. Immunohistochemical staining of CD71 can help differentiate between adenocarcinoma and benign reactive pancreatic ducts in chronic pancreatitis . CD71 may represent an important target for future targeted therapies in the pancreas as well.

1783 Is It Justifiable to Move the Grade-1 Ki67 Index Cut-Off from 3% to 5% for Pancreatic Neuroendocrine Tumors as Has Been Proposed? The Cases That Fall to 3-5% Category Have Clinicopathologic Characteristics Closer to Those > 5%

Michelle Reid[1], Serdar Balci[2], Pelin Bagci[3], Burcu Saka[4], Burcin Pehlivanoglu[5], Ipek Erbarut Seven[3], Olca Basturk[6], N. Volkan Adsay[7]
[1]Emory University Hospital, Atlanta, GA, [2]Ankara, Turkey, [3]Marmara University, Istanbul, Turkey, [4]Istanbul Medipol University, Istanbul, Turkey, [5]Adiyaman University Training and Research Hospital, Adiyaman, Turkey, [6]Memorial Sloan Kettering Cancer Center, New York, NY, [7]Koç University Hospital, Istanbul, Turkey

Disclosures: Michelle Reid: None; Serdar Balci: None; Pelin Bagci: None; Burcu Saka: None; Burcin Pehlivanoglu: None; Ipek Erbarut Seven: None; Olca Basturk: None; N. Volkan Adsay: None

Background: Grading of linear parameters into meaningful (clinically relevant) clusters is a well-known challenge. Recently several groups have proposed to change the Ki67 index cut-off for grade 1 (G1) category for PanNETs from < 3% to < 5%. This proposal presupposes that the cases with Ki67 index of 3-5% are NOT clinically different than the 0-3% group and thus can be lumped together with the current G1 (0-3% cases), instead of their current home in the G2 category (≥ 3%).

Design: Ki67 index of 91 resected PanNETs was carefully calculated by manual counting from the print of image-capture of the hot-spot method (Reid et al, PMID: 25412850). Clinicopathologic characteristics of cases with Ki67 index of 3-5% were contrasted with those with index <3% and 5-20% in an attempt to establish the identity of this group whether it is closer to one or the other.

Results: 17 % of PanNETs fell into the 3.0 – 5.0% rate by Ki67. This group was substantially different in its profile of signs of aggressive behavior from the 0-3% group, and in various aspects appeared to be closer to the 5-20% group (Table).

	G1, <3	G2, 3-5	G2, 5-20	G3 >20	Total	p
N (%)	48 (53)	15 (16)	23 (25)	5 (5)		
Mean age, yr (SD)	59 (14)	54 (17)	53 (13)	50 (19)	57 (14)	0.205
F:M	1,3	0,8	1,9	1,5	1,3	0.615
Mean Ki67 (SD)	1.5 (0.7)	3.6 (0.5)	7.6 (2.9)	44.0 (33.6)	5.7 (12.0)	<0.001
Mean size, cm (SD)	2.8 (2.2)	3.7 (2.0)	4.0 (2.8)	5.5 (1.8)	3.4 (2.3)	0.006
T1+T2:T3+T4	3,6	1	1,5	0	1,9	0.003
T1:T2+T3+T4	1,1	0,2	0,3	0	0,6	0.013
PNI, %	11	43	30	60	24	0.009
LVI, %	19	50	65	100	40	<0.001
LN metastasis, %	19	31	45	25	29	0.246
Liver metastasis, %	10	25	33	75	22	0.011

Conclusions: 17% of PanNETs have a Ki67 index of 3-5%, indicating that this is not a trivial group and a change in the grading system will effect 1 out of 6 PanNET patients. This group shows substantial differences from the 0-3% Ki67 index group (current G1 cases) in their pathologic signs of aggressiveness, and appears to be closer to the ≥ 5% group in many respects. Therefore there does not seem to be enough justification at this time to move this subset into G1 category as has been proposed in several recent studies. More studies are needed to justify such a shift. For the time being, it is advisable to also report the exact Ki67 index in a given case, in addition to the final grade recording as G1, G2 or G3.

1784 Keratin 17 Is a Negative Prognostic Biomarker in Pancreatic Cancer Needle Aspiration Biopsies

Lucia Roa-Peña[1], Babu Sruthi[1], Maoxin Wu[2], Sofia Taboada[3], Luisa Escobar-Hoyos[4], Kenneth Shroyer[1]
[1]Stony Brook Medicine, Stony Brook, NY, [2]Stony Brook University Hospital, Stony Brook, NY, [3]ProHealth, New York, NY, [4]Renaissance School of Medicine at Stony Brook University, Stony Brook, NY

Disclosures: Lucia Roa-Peña: None; Babu Sruthi: None; Maoxin Wu: None; Sofia Taboada: None; Luisa Escobar-Hoyos: None; Kenneth Shroyer: None

Background: Pancreatic ductal adenocarcinoma (PDAC) was recently reported to be composed of two molecular subtypes based on mRNA expression that correlate with overall survival. We recently demonstrated that Keratin 17 (K17) expression, measured by mRNA or protein levels, is as accurate as molecular subtyping and can serve as an independent, negative prognostic and predictive biomarker that stratifies patient outcome in stage-matched cases. All prior conclusions were based on assays performed on surgical resection specimens. Since the vast majority (80%) of cases, however, are not candidates for resection, there is an urgent need to develop prognostic methods using needle aspiration (NA) biopsies of unresectable or metastatic disease.

Design: To test the hypothesis that K17 is a negative prognostic biomarker in PDAC NA biopsies, we performed K17 immunohistochemistry (IHC) test in 193 cases of formalin-fixed paraffin-embedded NA cell block samples collected from 2012-17 and

correlated levels of K17 with patient outcome. To measure K17 protein expression, we used a corroborated pathology-based scoring system, employed by two pathologists. Kaplan-Meier and Cox proportional-hazard regression models were analyzed to determine survival differences in cases with different levels of K7-IHC expression. Univariate and multivariate analyses were used to account for other clinical-pathological risk factors.

Results: NA samples were classified as high for K17 based on the proportion of cells that showed strong (2+) staining in > 80% of tumor cells and the Akaike Information Criterion. High-K17 cases had shorter survival (median= 8m) compared to low-K17 cases (median= 14m). These findings are consistent with our previous report. The overall survival analysis showed K17 as a powerful independent prognostic biomarker in NA samples (HR=1.5, p=0.01), even in stage-matched cases (HR=2.5, p=0.001), providing additional prognostic value beyond tumor staging.

Conclusions: K17 was identified as a robust and independent, clinically relevant, prognostic biomarker that stratifies clinical outcome in cases that are diagnosed by NA biopsies in stage-matched cases. These results suggest that K17 IHC testing enables prognostic stratification of PDACs patients that are not candidates for surgical resection. Thus, K17 IHC testing in NA should be further validated and tested in clinical trials, to determine if it also has predictive value that could impact clinical opportunities for chemotherapeutic intervention.

1785 CPA1 and REG1a as New Markers for Pancreatic Acinar Cell Carcinoma

Samar Said[1], Paul Kurtin[1], Samih Nasr[1], Rondell Graham[1], Surendra Dasari[1], Julie Vrana[1], Saba Yasir[1], Michael Torbenson[2], Lizhi Zhang[1], Taofic Mounajjed[1], Zongming Eric Chen[1], Hee Eun Lee[2], Tsung-Teh Wu[1]
[1]Mayo Clinic, Rochester, MN, [2]Mayo Clinic Rochester, Rochester, MN

Disclosures: Samar Said: None; Paul Kurtin: None; Samih Nasr: None; Rondell Graham: None; Surendra Dasari: None; Julie Vrana: None; Saba Yasir: None; Michael Torbenson: None; Lizhi Zhang: None; Taofic Mounajjed: None; Zongming Eric Chen: None; Hee Eun Lee: None; Tsung-Teh Wu: None

Background: Carboxypeptidase A1 (CPA1) and regenerating islet-derived 1a (REG1a) are proteins that originate almost exclusively from the pancreatic acinar cells. Acinar cell carcinoma (ACC) is a rare tumor that derives from acinar cells and shows evidence of pancreatic enzyme production. Mixed acinar-neuroendocrine carcinoma (MANC) is defined as having more than 30% proportion of both acinar and neuroendocrine cell types. Trypsin and lipase are the most commonly used ACC immunohistochemical markers. However, the expression of CPA1 and REG1a in pancreatic tumors has not been studied in details. The goal of this study is to determine whether immunohistochemical staining for CPA1 and REG1a is useful in the histologic diagnosis of pancreatic ACC.

Design: CPA1 and REG1a immunostains were performed on a variety of pancreatic tumors including 14 ACC (7 biopsies/FNA, 7 resection), 5 MANC (2 FNA, 3 resection) and 80 non-acinar cell pancreatic tumors (all resection). The latter included 20 ductal adenocarcinoma (DA), 20 well differentiated neuroendocrine tumor (WNET), 20 mucinous cystic neoplasm (MCN) and 20 solid pseudopapillary tumor (SPT). The staining was reported as negative, focal (< 25% of tumor with cytoplasmic positivity), patchy (25-50%) or diffuse (>50%).

Results: The results are shown in Table 1. Normal acinar cells in the background showed diffuse strong staining. All 19 ACC/MANC cases were positive for CPA1 (all diffuse) and REG1a (12 diffuse, 4 patchy, 3 focal). CPA1 was also positive in 10% of DA cases (2 focal), 50% of WNET (2 patchy, 8 focal), 10% of MCN (1 diffuse, 1 focal) and 5% of SPT (1 patchy). REG1a was positive in 65% of DA cases (1 patchy, 12 focal), 5% of WNET (1 focal), 45% (5 diffuse, 4 focal) of MCN and 0% of SPT. The diffuse or patchy staining was significantly more common in ACC/MANC (100% diffuse/patchy for CPA1 and 84% for REG1a) as compared to other pancreatic tumors (5% diffuse/patchy for CPA1 and 7.5% for REG1a) with a P value of 0.0001 for both CPA1 and REG1a. The sensitivity and specificity of diffuse/patchy staining for CPA1 and REG1a in diagnosing pancreatic ACC were 100% and 95% for CPA1 and 84% and 93% for REG1a.

Tumor type	Cases	Number of REG1a positive cases (%) (diffuse, patchy, focal)	Number of CPA1 positive cases (%) (diffuse, patchy, focal)
Acinar cell carcinoma	19	19 (100%)(12,4,3)	19 (100%)(19,0,0)
Non-acinar cell carcinoma:	80	23 (29%)(5,1,17)	15 (19%)(1,3,11)
Ductal adenocarcinoma	20	13 (65%)(0,1,12)	2 (10%) (0,0,2)
Neuroendocrine tumor	20	1 (5%)(0,0,1)	10 (50%)(0,2,8)
Solid pseudopapillary tumor	20	0	1 (5%)(0,1,0)
Mucinous cystic neoplasm	20	9 (45%)(5,0,4)	2 (10%)(1,0,1)

Conclusions: CPA1 and REG1 are novel immunohistochemical markers for ACC that can be used as additional acinar cell differentiation markers to confirm the diagnosis of pancreatic ACC.

1786 Histologic Assessment of Endoscopic Ultrasound–Fine-Needle Biopsies of Pancreatic Solid Neoplasms Improves Diagnostic Yield and Adequacy for Ancillary Testing

David Saulino[1], Ashwin Akki[2], David Hernandez Gonzalo[3], Joanna Chaffin[2], Michael Feely[2], Jesse Kresak[2], Marino Leon[2], Dennis Yang[2], Peter Draganov[2], Xiuli Liu[2], Ashwini Esnakula[2]
[1]Immunology and Lab Medicine, University of Florida, Gainesville, FL, [2]University of Florida, Gainesville, FL, [3]University of Florida-Shands, Gainesville, FL

Disclosures: David Saulino: None; Ashwin Akki: None; David Hernandez Gonzalo: None; Joanna Chaffin: None; Michael Feely: None; Jesse Kresak: None; Marino Leon: None; Dennis Yang: None; Peter Draganov: None; Xiuli Liu: None; Ashwini Esnakula: None

Background: Endoscopic ultrasound with fine needle aspiration (EUS-FNA) is frequently used for the diagnosis of pancreatic solid neoplasm (PSN). However, in the era of personalized medicine, there is an additional demand of tissue for ancillary testing. Recently, fine needle devices have been refined to procure fine needle core biopsies (FNB) and the processing of such specimen is still unclear. Herein, we compared the diagnostic yield of EUS guided FNB processed by histology and cytology in patients with PSNs and reviewed the adequacy for clinically needed ancillary testing.

Design: We identified 40 patients who underwent EUS with tissue acquisition using EchoTip ProCore 20-gauge needle (Cook Medical LLC, Bloomington, IN, USA) for PSNs from January 2018 to August 2019. Routine practice by our endoscopists is to submit tissue from at least two passes for cytology and two passes for histology. Cytology processing included routine slide smears and cell block preparations. The Fisher exact test was performed for categorical variables.

Results: Demographics, clinical features and diagnostic categories of the study population were summarized in Table 1. In 35 patients with mass lesion on EUS, a definitive diagnosis of malignancy was rendered in 30 patients (85.7%) on histology vs.14 patients (40%; p=0.0001) on cytology. Diagnoses on histology included ductal adenocarcinoma (23), suspicious for ductal adenocarcinoma (4), grade 1 pancreatic neuroendocrine tumor (1), diffuse large B cell lymphoma (2), and metastatic tumor [lung (2), melanoma (1) and gastric primary (1)]. In 11 patients a diagnosis of malignancy (7) or suspicious for malignancy (4) was rendered only on histology. FNB histology diagnoses were 89% concordant with resected or metastatic biopsy specimens (8 of 9). In 1 patient with discordant diagnosis, histology was non diagnostic, but cytology was suspicious for adenocarcinoma. In patients with advanced disease, 15 of 17 (88.2%) histology cases had adequate tissue for ancillary testing for predictive and prognostic biomarkers by next generation sequencing and immunohistochemistry.

Table 1: Patient demographics, clinical features and diagnosis

Age: range; mean, y	14 - 84; 64.5	
Sex, n (%)		
Male	19 (47.5)	
Female	21 (52.5)	
EUS, n (%)		
Mass lesion	35 (87.5)	
No mass lesion	5 (12.5)	
EUS mass size, range; median cm	1.5 – 9.0; 2.5	
Mass location, n (%)		
Head	25 (71.4)	
Neck/Body	9 (25.8)	
Tail	1 (2.8)	
Diagnostic categories, n (%) (N=40)	**Histology**	**Cytology**

Non-Diagnostic/Unsatisfactory	1 (2.5)	3 (7.5)
Benign pancreatic tissue	5 (12.5)	4 (10)
Atypical	0 (0)	9 (22.5)
Suspicious for malignancy	4 (10)	10 (25)
Malignancy/Neoplasm (35) p=0.0001 (primary or metastatic)	30 (75)	14

Conclusions: Histologic assessment of FNB has better diagnostic yield in PSNs when compared to cytologic analysis and provides adequate tissue for essential ancillary testing in the majority of cases. Better preservation of the cores by histology processing potentially maintains the relationship of tumor to background tissue may have helped improve the diagnostic accuracy.

1787 The Identification of Non-V600E BRAF Mutations in GNAS-Mutant Intraductal Papillary Mucinous Neoplasms

Aatur Singhi[1], Abigail Wald[2], N. Paul Ohori[3], Sara Monaco[2], Marina Nikiforova[2]
[1]University of Pittsburgh Medical Center, Sewickley, PA, [2]University of Pittsburgh Medical Center, Pittsburgh, PA, [3]UPMC-Presbyterian Hospital, Pittsburgh, PA

Disclosures: Aatur Singhi: None; Abigail Wald: None; N. Paul Ohori: None; Sara Monaco: None; Marina Nikiforova: None

Background: Intraductal papillary mucinous neoplasms (IPMNs) are precursor neoplasms to pancreatic ductal adenocarcinoma (PDAC) and frequently harbor mutations in *KRAS* and/or *GNAS*. In fact, the detection of *GNAS* mutations in preoperative pancreatic cyst fluid (PCF) is specific for IPMNs. However, these oncogenes are not mutually exclusive and are involved in distinctly, different signaling mechanisms. *KRAS* is associated with the mitogen-activated protein kinase (MAPK) pathway and *GNAS* with the protein kinase A (PKA) pathway. Considering MAPK activation is present in >90% of PDACs and *KRAS* mutations are reported in up to 76% of IPMNs, we hypothesized that other molecular alterations may drive the MAPK pathway in *KRAS* wild-type IPMNs, especially those with a *GNAS* mutation.

Design: Within a 16-month period, a multi-institutional cohort of 854 endoscopic ultrasound-fine needle aspiration (EUS-FNA) obtained PCF specimens were prospectively evaluated by next-generation sequencing (NGS) that includes 22 genes implicated in pancreatic cysts and PDAC, such as *KRAS*, *GNAS*, *BRAF*, *NRAS*, *HRAS* and *PIK3CA*. The average depth of coverage was >1000X (Ion Torrent Proton). Molecular results were correlated with pre- and post-operative clinicopathologic findings.

Results: *KRAS*, *GNAS*, *BRAF* and *NRAS* mutations were detected in 423 (50%), 272 (32%), 49 (6%) and 4 (1%) PCF specimens. No mutations in *HRAS* were identified. Interestingly, the majority of *BRAF* mutations were non-V600E (n=47, 96%) and included class 2 (n=14, 29%) and class 3 (n=32, 65%) alterations. Among the 272 *GNAS*-mutant pancreatic cysts, 221 (81%) cases had *KRAS* mutations and 41 (15%) cases had *BRAF* mutations. In total, mutations in *KRAS* and *BRAF* were detected in 253 (93%) *GNAS*-mutant cysts. Diagnostic pathology was available for 102 (12%) PCF specimens: 53 IPMNs, 3 mucinous cystic neoplasms (MCNs) and 46 non-mucinous cysts. All 53 IPMNs harbored *KRAS* (n=47) and/or *GNAS* mutations (n=31). Among 31 *GNAS*-mutant IPMNs, 25 (81%) had *KRAS* mutations and 4 (13%) had *BRAF* mutations, which were mutually exclusive. Only 2 (6%) *GNAS*-mutant IPMNs lacked mutations in *KRAS* and *BRAF*; however, both cases harbored *PIK3CA* mutations. No mutations in *GNAS* and *BRAF* were present in MCNs and non-mucinous cysts.

Conclusions: Non-V600E *BRAF* mutations were identified among *GNAS*-mutant/*KRAS* wild-type IPMNs and, similar to *GNAS*, may be a specific marker of IPMNs. Moreover, our findings suggest that activation of the MAPK pathway may be a critical driver in the pathogenesis of IPMNs.

1788 An Immunohistochemical Evaluation of ARX and PDX1 in Pancreatic/Non-Pancreatic Neuroendocrine Tumors and Pancreatic Neuroendocrine Carcinomas

Aatur Singhi[1], Michael Nalesnik[2], Roderick O'Sullivan[3], Amer Zureikat[3]
[1]University of Pittsburgh Medical Center, Sewickley, PA, [2]UPMC-Montefiore, Pittsburgh, PA, [3]University of Pittsburgh Medical Center, Pittsburgh, PA

Disclosures: Aatur Singhi: None; Michael Nalesnik: None; Roderick O'Sullivan: None; Amer Zureikat: None

Background: Whole transcriptome and epigenome studies of pancreatic neuroendocrine tumors (PanNETs) have identified two distinct subtypes, α-cell and β-cell lineage, based on the differential expression of the transcription factors ARX and PDX1. α-cells are defined by ARX expression and absence of PDX1, and β-cells by PDX1 expression regardless of ARX status. Prior reports have found patients with PanNETs of α-cell lineage are associated with a poor prognosis that is statistically independent from other prognostic markers, such as alternative lengthening of telomeres (ALT). However, expression of ARX and PDX1 has not been systematically validated on a large patient cohort. Moreover, the status of these transcription factors in other neuroendocrine tumors (NETs) and pancreatic neuroendocrine carcinomas (PanNECs) remains unknown.

Design: Immunohistochemistry for ARX and PDX1 was performed on whole sections of 322 PanNETs and 10 PanNECs. Additionally, tissue microarrays were created for 18 gastric, 22 ampullary/duodenal, 123 jejunal/ileal, 9 colonic, 13 rectal, 20 appendiceal, 2 gallbladder, and 46 pulmonary NETs/carcinoids. Positive immunoreactivity for ARX and PDX1 was defined as >5% staining of neoplastic nuclei. Telomere fluorescence in situ hybridization was also performed to assess for ALT.

Results: ARX and PDX1 immunohistochemistry categorized 196 (61%) PanNETs as α-cell lineage and 126 (39%) PanNETs as β-cell lineage. In comparison to β-cell cases, PanNETs of α-cell lineage were associated with larger mean tumor size, higher WHO grade, lymphovascular invasion, distant metastases and ALT-positivity ($p<0.03$). Patients with a-cell PanNETs had shorter disease-free survival. However, by multivariate analysis with ALT, the a-cell lineage did not retain its prognostic significance. In addition to PanNETs, ARX and PDX1 were expressed in 78% and 17% of gastric NETs, 41% and 77% of ampullary/duodenal NETs, 36% and 14% of appendiceal NETs, and 100% and 15% of rectal NETs, respectively. Of note, all ARX-positive gastric NETs arose in autoimmune metaplastic atrophic gastritis. PDX1 was also expressed in 60% of PanNECs, but ARX was absent in all cases. In comparison, ARX was expressed in 6 of 6 grade 3 PanNETs, which were negative for PDX1.

Conclusions: The identification of an α-cell PanNET portends a poor prognosis, but is no longer significant in the setting of ALT. Further, ARX and PDX1 can be expressed in other NETs. However, ARX may be useful in discriminating between grade 3 PanNETs and PanNECs.

1789 Accuracy of Frozen Section Diagnoses of Gastrointestinal Specimens: Identification of Most Frequent Error Types

Lena Stuart[1], Azfar Neyaz[2], Vania Nose'[3], Lawrence Zukerberg[4], Vikram Deshpande[1]
[1]Massachusetts General Hospital, Boston, MA, [2]Massachusetts General Hospital, Malden, MA, [3]Massachusetts General Hospital, Harvard Medical School, Boston, MA, [4]Auburndale, MA

Disclosures: Lena Stuart: None; Azfar Neyaz: None; Vania Nose': None; Lawrence Zukerberg: None; Vikram Deshpande: *Grant or Research Support*, Advanced Cell Diagnostics; *Advisory Board Member*, viela; *Grant or Research Support*, Agios pharmaceuticals

Background: The use of frozen section diagnosis plays a critical role in assisting gastrointestinal (GI) surgeons with intraoperative decisions. However, there are several GI entities (primarily hepatobiliary specimens) that are notoriously challenging, and often result in higher rates of discordance between frozen section and final diagnosis. In the current study, we aimed to evaluate the accuracy of gastrointestinal frozen section diagnoses with the goal of identifying the root cause of these discrepancies.

Design: All gastrointestinal (GI) frozen section diagnoses rendered at our institution during the 2018-2019 academic year were evaluated for accuracy. Discordant cases were classified by the type of analytic error (gross sampling, block sampling or interpretation) and analytic error subclass (change in category, change within category, change in the threshold, change in lymph node status and change in margin status). The discrepancies were also categorized as major (altered surgical approach) and minor (all others). Cases were also flagged as being reviewed either by a GI or a non-GI pathologist.

Results: A total of 1135 GI frozen section diagnoses were rendered by 25 pathologists on 462 cases. A total of 62 (5%) diagnoses were found to be discordant with the final diagnosis: 40% (n=25/62) were characterized as major discrepancies. Tissue sampling accounted for 66% of errors while 34% were related to interpretation. Pancreatic and hepatic specimens accounted for 69% of errors. The most common error subclass was a change in category from benign to malignant (45% of all discordant calls), with the next most common error subclass being a change in margin status from negative to positive (21%). 38% of cases were interpreted by GI pathologist, with 62% by non-GI staff. For the GI-pathologists, the greatest error type was interpretation (N=13, 45% of GI-specialist discordant calls), which was greater than for the non-GI staff (N=8, 24% of non-GI specialist calls), $p=0.025$. Tissue sampling error rates were similar between the GI and non-GI subspecialists.

Conclusions: The frozen section error rate is highest in hepatic and pancreatic specimens and subspecialized frozen section sign-out may not improve diagnostic accuracy. Most these errors are related to inadequate sampling of tissue for intraoperative analysis and can be addressed by: a) taking additional sections at the time of frozen section, and, b) mandatory deeper levels performed on all hepatobiliary frozen sections.

1790 Correlation Between the Tumor Budding and Tumor Microenvironment in Pancreatic Ductal Adenocarcinoma

Lei Sun[1], Joshua Nguyen[2], Feng Yin[1]
[1]*University of Missouri, Columbia, MO,* [2]*University of Missouri, Northridge, CA*

Disclosures: Lei Sun: None; Joshua Nguyen: None; Feng Yin: None

Background: Tumor budding (TB, defined as single tumor cell or clusters of up to four tumor cells per ITBCC 2016 recommendation) has been suggested as an additive prognostic factor in pancreatic ductal adenocarcinoma. However, the relationship between tumor budding and tumor microenvironment has not been well studied. This study explores the relationship between TB and tumor microenvironment, specifically tumor-infiltrating lymphocytes (TILs, defined as lymphocytes in the stromal tissue within the tumor) and tumor-infiltrating neutrophils (TIN, defined as prominent neutrophil infiltration in the stromal tissue within the tumor), in pancreatic ductal adenocarcinoma.

Design: TB, TILs, and TIN were assessed in fifty-eight pancreatic ductal adenocarcinoma cases between 2007 and 2019. TB was scored as follows: low TB (0-4) and high TB (>4) in a 20× objective field. TILs were scored as follows: low TILs (0-50%) and high TILs (>50%) (calculated as area occupied by lymphocytes over intratumoral stromal area). The presence or absence of TIN was also recorded for each case. Statistical analysis was performed using Fisher's exact test.

Results: The study group consists of 33 men and 25 women. The mean age was 64.8 years, with age ranging from 38 to 85. Through histopathological evaluation, 18 cases had low TB, and 40 cases had high TB. In the low TB group, 33.3% of cases showed a large number of lymphocytes within the tumor stroma (high TILs), and only 5.0% of the high TB group cases showed high TILs (P=0.008). In contrast, in the low TB group, 33.3% of cases showed prominent neutrophil infiltration within the tumor stroma (positive TIN), and 72.5% of the high TB group cases were positive for TIN (P=0.008). High TB was not significantly associated with the tumor size nor the pT stage, instead it showed a trend of having higher risk of nodal metastasis (77.5%, vs. 55.6% in low TB group, P=0.122).

Conclusions: TB has a negative correlation with TILs, and a positive correlation with TIN in pancreatic ductal adenocarcinoma. High TB tends to have a higher risk of nodal metastasis. The comprehensive analysis of TB and tumor microenvironment may provide insight into a better prediction of tumor prognosis and treatment response.

1791 Clinical, Pathological and Radionuclide Receptor Expression Correlates of the Novel Enhancer Signature Classification of Pancreatic Neuroendocrine Tumors

Vincent Quoc-Huy Trinh[1], Marcus Tan[1], Satya Das[1], Chanjuan Shi[1]
[1]*Vanderbilt University Medical Center, Nashville, TN*

Disclosures: Vincent Quoc-Huy Trinh: None; Satya Das: *Consultant*, Targeted Oncology; *Consultant*, Clarivate Analytics; Chanjuan Shi: None

Background: The enhancer signature classification (ESC) of pancreatic neuroendocrine tumors (PNETs) has proposed that PNETs fall into two major subtypes, with epigenomes and transcriptomes that partially resemble islet α- (expressing ARX) and β-cells (expressing PDX-1). Metastases were shown to occur almost exclusively in ARX+/PDX1- tumors. In the context of novel radionuclide therapy in use and unders study, SSTR2A is commonly expressed by PNETs, whereas CXCR4 expression is mostly observed in highly proliferative and advanced tumors. Our primary goal was to analyze the degree of positivity of SSTR2A and CXCR4 in PNETs, stratified according to the novel ESC. Our secondary goal was to determine the clinical and pathological features of the novel ESC groups.

Design: We used tissue microarrays generated from resected PNETs from 2002-2012. Clinical, radiographic and pathological outcomes were extracted from medical records. Immunohistochemistry was performed with PDX1, ARX, SSTR2A and CXCR4. Patients were grouped as ARX+/PDX1+, ARX+/PDX1-, and ARX-(PDX1+/-). Time-dependent ROC analysis was performed in R (v3.6.1; suvivalROC v1.0.3) to determine positive threshold for ARX and PDX1. Strong staining was required for positive SSTR2A and CXCR4. Comparative analyses were performed in SPSS v23.0 (Kruskal-Wallis, Freeman-Halton exact). The study was approved by our institutional review board.

Results: Of 71 PNETs, 49, 12 and 10 were ARX+/PDX1+, ARX+/PDX1-, ARX-(PDX1+/-), respectively. Metastases almost exclusively occurred in ARX+ cases (including ARX+/PDX1+ and ARX+/PDX1- groups) (Table 1). Patients with ARX+ tumors tended to be younger and with larger primary tumors. ARX- negative tumors were more common in women, and none of them were associated with a genetic syndrome. There were no differences in other pathological features between ARX+ and ARX- groups. In addition, no differences were observed in SSTR2A expression between 2 groups. However, CXCR4 was only positive in ARX+ tumors.

Factor	ARX+ / PDX1+ (n=49)	ARX+ / PDX1- (n=12)	ARX- (n=10)	P
Metastasis during follow-up	17 (34.7%)	5 (41.7%)	1 (10.0%)	0.186
Median Follow-Up (IQR)	83 (44.3-100.8)	58 (19-133)	91 (26-146)	0.654
Immunohistochemistry SSTR2A CXCR4	27 (55.1%) 16 (34.0%)	6 (50.0%) 4 (33.3%)	3 (37.5%) 0 (0.0%)	0.341 0.102
Median Age (IQR)	55 (41.3-64)	45 (35.5-57.8)	65.5 (58.5-70)	0.009
Gender Male Female	25 (51.0%) 24 (49.0%)	5 (41.7%) 7 (58.3%)	1 (10.0%) 9 (90.0%)	0.037
Median Size (IQR)	2.5 (1.7-4.1)	3.25 (2.1-4.5)	1.2 (1.0-3.9)	0.075
Syndrome MEN1 VHL	5 (10.2%) 4 (8.2%)	3 (25.0%) 1 (8.3%)	0 (0.0%) 0 (0.0%)	0.345
Lymphovascular invasion	17 (34.7%)	6 (50.0%)	2 (20.0%)	0.352
Perineural invasion	7 (14.3%)	1 (8.3%)	1 (10.0%)	1.000
Necrosis	6 (12.2%)	1 (8.3%)	2 (20.0%)	0.848
Infiltrative borders	14 (29.2%)	3 (25.0%)	3 (33.3%)	1.000
Significant fibrosis	23 (46.9%)	4 (36.4%)	4 (40.0%)	0.712
T stage at diagnosis T1-T2 T3-T4	34 (69.4%) 15 (30.6%)	6 (50.0%) 6 (50.0%)	7 (70.0%) 3 (30.0%)	0.438
N stage at diagnosis N0 N1	34 (69.4%) 15 (30.6%)	6 (50.0%) 6 (50.0%)	9 (90%) 1 (10.0%)	0.226
M stage at diagnosis M0 M1	41 (83.7%) 8 (16.3%)	12 (100%) 0 (0.0%)	10 (100.0%) 0 (0.0%)	0.200
WHO Grade G1 G2 G3	28 (57.1%) 14 (28.6%) 7 (14.3%)	5 (45.5%) 3 (27.3%) 3 (27.3%)	7 (70.0%) 2 (20.0%) 1 (10.0%)	0.791

Conclusions: Our study confirms that ARX+ PNETs have different clinical features from ARX- PNETs. In addition, CXCR4, a potential prognosticator and therapeutic target, is expressed differently by ARX+ and ARX- tumors.

1792 Molecular Profiling of Grade 3 Pancreatic Neuroendocrine Neoplasms (NEN) Reveals Frequent TP53 and CDKN2A Alterations in both NET and NEC

Sarah Umetsu[1], Sanjay Kakar[1], Kirk Jones[1], Emily Bergsland[1], Grace Kim[1], Nancy Joseph[1]
[1]*University of California San Francisco, San Francisco, CA*

Disclosures: Sarah Umetsu: None; Sanjay Kakar: None; Kirk Jones: None; Emily Bergsland: None; Grace Kim: None; Nancy Joseph: None

Background: Grade 3 neuroendocrine tumor (G3 NET) and neuroendocrine carcinoma (NEC) are both defined by Ki67 >20% and/or mitoses >20 per 2mm^2; however the clinical behavior and therapies differ. Pancreatic NET have been shown to harbor mutations in *MEN1*, *DAXX*, *ATRX,* and mTOR genes (*TSC2*, *PTEN*). NEC rarely evolves from NET and shows frequent co-alteration of *TP53* and *RB1* and mutations in pancreatic adenocarcinoma (PDAC) genes (*CDKN2A, SMAD4,* RAS/RAF genes). Distinguishing G3 NET from NEC based on morphology alone is often challenging and immunostains (p53/Rb/DAXX/ATRX) are useful in this distinction. We have observed co-alteration of *MEN1* and *TP53* in cases with history of G1/G2 NET, despite the literature suggesting this is rare. This study examines a series of pancreatic G3 NEN to determine the extent of molecular overlap between G3 NET and NEC.

Design: 20 pancreatic G3 NEN were reviewed by 5 pathologists, using only H&E and Ki67, and classified as G3 NET (n=5), NEC (n=5), or ambiguous (n=10) if there was no consensus or morphologic features were indeterminate. Capture-based NGS of 479 cancer genes was performed on all 20 cases. Mutations, copy number alterations, and rearrangements were evaluated.

Results: 60% (3/5) of G3 NET had alterations in both *MEN1* and *DAXX,* 20% (1/5) had *TP53* mutation, and 40% (2/5) had deep deletion of *CDKN2A*. Of the 10 ambiguous cases, 7/10 had *MEN1* alterations, 6 of which had prior history of G1/G2 NET, and 5 of which also had mutations in *ATRX, DAXX*, *TSC2*, or *PTEN*, strongly favoring a diagnosis of G3 NET. 2 additional ambiguous cases demonstrated mutations in *DAXX*, *TSC2*, and *CDKN1A*, also favoring G3 NET. Of these 9 cases, 44% (4/9) harbored mutation in *TP53* and 33% had deletions in *CDKN2A*. Of the 5 NEC, 80% (4/5) had *TP53* mutations, which were all accompanied by alterations in *RB1* or PDAC genes; none had alterations in *MEN1, DAXX,* or *ATRX.*

Figure 1 - 1792

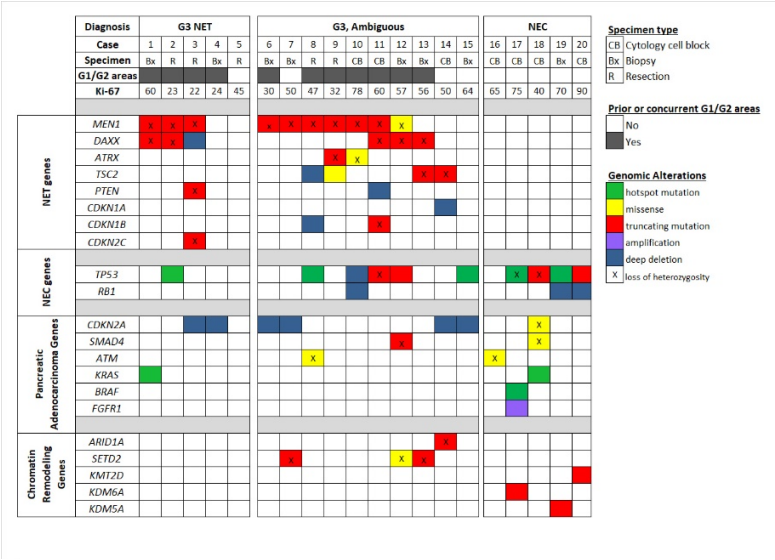

Conclusions: Molecular alterations typical of NET (*MEN1, DAXX, ATRX*) were demonstrated in 90% of cases classified as ambiguous; 77% of these also had history of G1/G2 NET, strongly favoring a final diagnosis of G3 NET. In contrast to published data, our study demonstrates that alterations in *TP53* and *CDKN2A* are frequent in G3 NET; 72% (10/14) had either *TP53* (5/14) or *CDKN2A* (5/14) alterations. Our data argue against the routine use of p53 immunostaining in the distinction of G3 NET versus NEC. Further studies examining the clinical behavior and response to treatment of G3 NET harboring *TP53* or *CDKN2A* alterations are needed.

1793 Characterization of SND1 Cytogenetic Aberrations in Pancreatic Neoplasms

Benjamin Van Treeck[1], Dora Lam-Himlin[2], Erik Jessen[1], Jaime Davila[1], Patricia Greipp[1], Lizhi Zhang[1]
[1]Mayo Clinic, Rochester, MN, [2]Mayo Clinic, Scottsdale, AZ

Disclosures: Benjamin Van Treeck: None; Dora Lam-Himlin: None; Jaime Davila: None; Lizhi Zhang: None

Background: Elucidation of therapeutic targets and further understanding of the molecular biology of pancreatic neoplasms is important for proper treatment and management. *SND1*, originally described as a transcriptional coactivator, has recently been shown to act as an oncogene, involved in RNA splicing, interference, and editing and also in other signaling pathways including TGFβ1 pathway. Rearrangements of *SND1* involving fusion with various genes in pancreatic acinar cell carcinoma have been found in 23% of cases in prior studies. The most frequent *SND1* fusion partner identified was *SND1-BRAF* leading to activation of the MAPK pathway. Such a rearrangement may be a potential future therapeutic target. Therefore, we aimed to characterize *SND1* cytogenetic aberrations in pancreatic tumors by fluorescent *in situ* hybridization (FISH).

Design: The following pancreatic tumor cases were procured retrospectively and met the WHO 2019 diagnostic criteria for each entity: pancreatoblastoma (n=4), acinar cell carcinoma (n=12), pancreatic undifferentiated carcinoma (n=15), and well differentiated pancreatic neuroendocrine tumor grade 3 (n=8). All 39 cases of pancreatic neoplasms were initially screened by an *SND1* break-apart FISH probe set followed by a dual-fusion probe set for *SND1-BRAF* and *APC-SND1* in *SND1* rearranged cases. All intact copy number variations of *SND1* were also recorded.

Results: An *APC-SND1* translocation was found in a single pancreatoblastoma (1/4), a *SND1-BRAF* fusion was identified in one acinar cell carcinoma (1/12), and *SND1* was rearranged with an unknown gene partner in one undifferentiated carcinoma (1/15). Intact copy number variation of the *SND1* gene (no structural rearrangement) was identified in pancreatoblastoma (0/4 gain; 1/4 loss), acinar cell carcinoma (3/12 gain; 4/12 loss), undifferentiated carcinoma (11/15 gain; 0/15 loss), and neuroendocrine tumor (7/8 gain; 0/8 loss) (Table 1). The pancreatoblastoma with *APC-SND1* translocation was further evaluated with RNAseq confirming the translocation and demonstrating upregulation of TGFβ1 (z-score=4.304, p=1.08x10^-46) and WNT/β-catenin (z-score=0.289, p=3.68x10^{-7}) pathways as a result of the translocation.

Figure 1 - 1793

Table 1. Summary of *SND1* Cytogenetic Aberrations in Pancreatic Neoplasms

	PB (n=4)	ACC (n=12)[3]	UC (n=15)[4]	WDPNETG3 (n=8)
Clinicopathologic Characteristics:				
Age (in years), median (range)	45 (24-58)	55 (33-78)	61 (42-83)	59 (45-73)
Male:Female	4:0	8:3	8:7	4:4
Tumor Size (in cm), median (range)	unknown[2]	6 (3.1-16)	6 (2.9-16)	5.75 (3.2-18)
pTis/pT1/pT2/pT3/pT4[1]	unknown[2]	0/0/4/7/0	0/0/4/9/0	NA/0/2/6/0
pN0/pN1/pN2[1]	unknown[2]	8/3/0	7/5/1	4/4/NA
pM0/pM1[1]	unknown[2]	9/2	13/2	4/4
Specimen type (biopsy/resection)	4/0	1/11	2/13	0/8
Intact SND1 Copy Number Variation:				
Cases with CN gain	0/4	3/12	11/15	7/8
Cases with CN loss	1/4	4/12	0/15	0/8
Median *SND1* CN per cell with gain (range)	NA	3.59 (2.81-3.92)	3.01 (2.08-6.12)	3.06 (2.60-3.78)
Percent of Nuclei per Case with CN Variation:				
CN gain, median (range)	NA	83% (74-89)	69% (27-99)	73% (50-93)
CN loss, median (range)	81% (NA)	71.5% (59-82)	NA	NA
***SND1* Translocations:**				
APC-SND1	1/4	0/12	0/15	0/8
SND1-BRAF	0/4	1/12	0/15	0/8
SND1-unknown partner	0/4	0/12	1/15	0/8

1. pTNM staging classification is based on AJCC 8th Edition.
2. All 4 PB cases are biopsies and synoptic reports are unable.
3. Clinicopathologic characteristics of one ACC case is unable to be procured and therefore not included in the table.
4. Two UC cases are biopsies of metastases. Thus, primary tumor size, pT, and pN information is excluded from the table.

Abbreviations: PB: Pancreatoblastoma; ACC: Acinar Cell Carcinoma; UC: Undifferentiated Carcinoma; WDPNETG3: Well Differentiated Pancreatic Neuroendocrine Tumor, Grade 3; CN: Copy Number; NA: Not Applicable

Conclusions: In conclusion, we discovered a novel *APC-SND1* translocation in a pancreatoblastoma and identified intact copy number gains of the *SND1* gene in acinar cell carcinoma, undifferentiated carcinoma, and pancreatic neuroendocrine tumor which may contribute to carcinogenesis and may be a future therapeutic target.

1794 Prognostic Significance and Genomic Correlates of Myeloid Cell Populations in the Pancreatic Cancer Microenvironment

Sara Väyrynen[1], Chen Yuan[1], Juha Väyrynen[1], Andressa Dias Costa[1], Hannah Williams[1], Vicente Morales-Oyarvide[1], Mai Chan Lau[2], Douglas Rubinson[1], Richard Dunne[3], Margaret Kozak[4], Wenjia Wang[5], Diana Agostini-Vulaj[5], Daniel Chang[6], Shuji Ogino[2], Brian Wolpin[1], Jonathan Nowak[2]

[1]Dana-Farber Cancer Institute, Boston, MA, [2]Brigham and Women's Hospital, Boston, MA, [3]University of Rochester, Rochester, NY, [4]Stanford Cancer Institute, Palo Alto, CA, [5]University of Rochester Medical Center, Rochester, NY, [6]Stanford Cancer Institute, Stanford, CA

Disclosures: Sara Väyrynen: None; Chen Yuan: None; Juha Väyrynen: None; Andressa Dias Costa: None; Hannah Williams: None; Vicente Morales-Oyarvide: None; Mai Chan Lau: None; Douglas Rubinson: None; Richard Dunne: None; Margaret Kozak: None; Wenjia Wang: None; Diana Agostini-Vulaj: None; Daniel Chang: None; Shuji Ogino: None; Brian Wolpin: *Consultant*, Grail; *Consultant*, Celgene, Inc; *Consultant*, BioLineRx; Jonathan Nowak: None

Background: Immunotherapy has advanced the treatment of many solid cancers but has not yet demonstrated efficacy in pancreatic ductal adenocarcinoma (PDAC). While abundant myeloid cell populations in the PDAC microenvironment have been postulated to suppress the anti-tumor immune response, the significance of these populations and the factors that regulate their composition are incompletely understood.

Design: We developed a quantitative, multiplex immunofluorescence assay to interrogate myeloid cell populations and suppressive status (CD33, CD15, CD14, HLADR, ARG1) which was applied to a multi-institutional cohort of 305 primary pancreatic cancer resection specimens with extensive clinicopathologic annotation and genomic characterization. We used Cox proportional hazards models to compute hazard ratios (HRs) and confidence intervals (CIs) of overall survival (OS) and disease-free survival (DFS) according to ordinal quartiles (Q1-Q4) of spatially-resolved immune cell densities, controlling for potential confounders, including age, gender, tumor characteristics, perioperative treatment, and institution.

Results: Expression of suppressive marker ARG1 was common in $CD15^+$ granulocytic cells but relatively rare in $CD14^+$ monocytic lineage cells. High stromal $CD15^+ARG1^+$ cell density was associated with shorter DFS in multivariable Cox regression models (Q4 vs. Q1: HR 1.93, CI 1.25-2.97, P_{trend}=0.0021). Most $CD14^+$ cells had a $CD33^-HLADR^{low/high}$ phenotype, consistent with macrophages. High $CD14^+CD33^-HLADR^{high}$ cell densities, representing a predominantly M1 macrophage phenotype, showed a multivariable-adjusted association with longer OS (Q4 vs. Q1: HR 0.77, CI 0.52-1.15, P_{trend}=0.02). Myeloid cells showed divergent associations with tumor molecular features; *TP53*-mutant tumors exhibited higher overall densities of $CD15^+$ cells (P=0.04), while *SMAD4*-mutant tumors exhibited lower overall densities of $CD14^+$ cells (P=0.04). The association between high stromal $CD15^+ARG1^+$ cell density and shorter DFS remained significant after controlling for *TP53* status (P_{trend}=0.001).

Conclusions: Suppressive $CD15^{+}ARG1^{+}$ granulocytic cells are abundant in the PDAC microenvironment and are associated with worse DFS, while higher $CD14^{+}CD33^{-}HLADR^{high}$ macrophage densities are associated with better OS. Myeloid cell densities are associated with the status of driver genes *TP53* and *SMAD4.* Our results highlight the value of using multimarker approaches to interrogate myeloid cell phenotypes and significance in the PDAC microenvironment.

1795 Morphologic Changes Associated with Neoadjuvant-Treated Pancreatic Ductal Adenocarcinoma and Comparison of Two Tumor Regression Grading Systems

Jennifer Vazzano[1], Wendy Frankel[1], Adam Wolfe[1], Terence Williams[1], Wei Chen[1]
[1]*The Ohio State University Wexner Medical Center, Columbus, OH*

Disclosures: Jennifer Vazzano: None; Wendy Frankel: None; Adam Wolfe: None; Terence Williams: None; Wei Chen: None

Background: Pancreatic ductal adenocarcinoma is an aggressive cancer with an overall five-year survival rate of 9%. Only 15%-20% of patients are candidates for pancreatectomy at presentation. The role of neoadjuvant therapy (NAT) is evolving, especially for high-risk potentially resectable tumors. Due to the increasing number of NAT resection specimens, we aim to characterize the histologic changes associated with NAT to better identify residual tumor, and to compare two tumor regression grading schemes.

Design: 118 resections for pancreatic ductal adenocarcinoma were identified at our institution from 2011-2018, 59 not treated and 59 treated with NAT. Patient age, sex, and outcome data were noted. H&E stained slides were reviewed for histologic changes and graded using the four-tier modified Ryan score (recommended by College of American Pathologists) and the three-tier HTRG score (by *Lee etc*, Am J Surg Pathol 2016; 40:1653-1660). The histologic changes evaluated included blue/grey fibrosis, islet cell hyperplasia, calcification, amyloid deposition (Congo red stain), cholesterol clefts, nerve hypertrophy, elastotic stromal/vascular change, abscess formation, and cytoplasmic changes. Statistical analyses were performed using Fisher's exact test and Kaplan-Meier analysis.

Results: Patient's average age is 63.7 years. Female:male ratio is 1.6:1. Average time to follow-up is 21.25 months for treatment-naïve group and 29.01 months for NAT group. There were statistically significant differences for dystrophic calcification, cytoplasmic changes, elastotic stromal/vascular change, islet cell hyperplasia, and nerve hypertrophy between the two groups. There was no significant difference for abscess formation, blue/grey fibrosis, amyloid deposition, and cholesterol clefts. Blue/grey fibrosis was present in all cases with tumor regardless of NAT, except 1 treated case with intraneural invasion only. By Kaplan-Meier analysis, the HTRG score correlates better with time to primary tumor recurrence (p=0.002) and time to distant recurrence (p=0.04) than modified Ryan. Neither grading schemes correlate with overall survival or time to progression.

Table 1. Histologic features of pancreatic adenocarcinoma in treatment-naïve and NAT resection specimens.

Histomorphologic features	Treatment-naïve group # (%) of positive case	Neoadjuvant-treated group # (%) of positive case	p-value for group difference
Calcification	4 (7%)	19 (32%)	p=0.0008
Cytoplasmic changes	0	52 (88%)	p<0.0001
Elastotic stromal/vascular change	0	55 (93%)	p<0.0001
Islet cell hyperplasia	38 (64%)	58 (98%)	p<0.0001
Nerve hypertrophy	46 (78%)	57 (97%)	p=0.0158
Abscess formation	5 (12%)	4 (7%)	p=1.000
Blue/grey fibrosis	59 (100%)	54 (92%)	p=0.0572
Amyloid deposition	0	3 (5%)	p=0.2436
Cholesterol clefts	0	2 (3%)	p=0.4957

Conclusions: Elastotic stromal/vascular change, dystrophic calcification, cytoplasmic changes, islet cell hyperplasia, and nerve hypertrophy are more frequently seen in post-NAT cases. Blue/grey stromal fibrosis is a helpful clue to suggest foci of residual tumor. On outcome analysis, HTRG score correlates better with time to recurrence than modified Ryan scheme.

1796 Clinicopathological Correlation of Radiologic Measurement of the Post-Therapy Tumor Size for Pancreatic Ductal Adenocarcinoma

Dongguang Wei[1], Mohamed Zaid[1], Eugene Koay[1], MH Katz[2], Michael Kim[1], Jeffrey Lee[2], Gauri Varadhachary[2], Robert A. Wolff[2], Priya Bhosale[1], Anirban Maitra[1], Asif Rashid[1], Huamin Wang[1]
[1]*The University of Texas MD Anderson Cancer Center, Houston, TX,* [2]*The University of Texas MD Anderson Cancer Center*

Disclosures: Dongguang Wei: None

Background: The current AJCC staging system for pancreatic ductal adenocarcinoma (PDAC) uses only tumor size in maximum dimension for pT1 to pT3. However accurate tumor size measurement in post-therapy pancreatectomies is extremely difficult due to the treatment induced fibrosis in both tumor and adjacent pancreatic tissue. In this study, we sought to correlate the tumor size measured on posttherapy scans with clinicopathological parameters and survival in PDAC patients who received neoadjuvant therapy and pancreatectomy.

Design: A total of 312 PDAC patients who received neoadjuvant therapy and pancreatectomy at our institution between 1999 and 2012 were included in this study. The largest tumor size (RadL) was measured on post-therapy CT or MRI by a radiologist. The results were correlated with the tumor size measured by pathology (ypT), CAP tumor regression grading, ypN stage, margin status and survivals. Statistical analyses were performed using the IBM SPSS Statistics (version 24).

Results: Post-therapy RadL showed a positive linear correlation with the pathologic tumor size (Pearson correlation: 0.73, P < 0.001) and correlated with the ypT stage. The mean RadL was 1.76 +/- 0.52 for ypT1 patients (n=110), 2.64 +/- 0.70 for ypT2 patients (n=175); and 3.56 +/- 0.96 for ypT3 patients (n=27), respectively (P < 0.001). The mean RadL was 2.16 +/- 0.91 for patients with CAP regression grade 1 (n=32), 2.34 +/- 0.89 for patients with CAP regression grade 2 (n=185); and 2.62 +/- 0.74 for patients with CAP regression grade 3 (n=95), respectively (P=0.007). However no significant correlations were found between post-therapy RadL and ypN stage, margin status, disease-free or overall survivals (P > 0.05).

Conclusions: Post-therapy RadL shows significant correlations with pathologic tumor size measurement, ypT stage and CAP tumor regression grading. Radiologic measurement of post-therapy tumor size may be used as a marker for the pathologic tumor staging and tumor response to neoadjuvant therapy.

1797 Morphological Features of Colonization of Ampullary and Duodenal Mucosa by Invasive Carcinoma: An Interobserver Variability Study

Yue Xue[1], Rebecca Obeng[2], Rondell Graham[3], Hongmei Jiang[4], Guang-Yu Yang[5], Michelle Reid[6]
[1]Northwestern University Feinberg School of Medicine, Chicago, IL, [2]Emory University, Atlanta, GA, [3]Mayo Clinic, Rochester, MN, [4]Northwestern University, Evanston, IL, [5]Northwestern University, Chicago, IL, [6]Emory University Hospital, Atlanta, GA

Disclosures: Yue Xue: None; Rebecca Obeng: None; Rondell Graham: None; Hongmei Jiang: None; Guang-Yu Yang: None; Michelle Reid: None

Background: Colonization of duodenal and ampullary mucosa by invasive ampullary carcinoma cells can mimic high-grade precursor lesions of this region, causing a diagnostic challenge especially in limited biopsy specimens. It is unclear if colonization can be diagnosed reproducibly. We evaluated interobserver agreement in the diagnosis of colonization of mucosa by underlying invasive carcinoma and determined the morphologic features that were most helpful in accurate diagnosis.

Design: 125 invasive ampullary carcinoma resections were reviewed for histologic features of mucosal colonization including adjacent histologically similar invasive ampullary carcinoma and an abrupt transition between markedly atypical and normal epithelium (PMID:30212393). Selected cases with foci of colonization, adenoma with low (LGD) or high-grade dysplasia (HGD), and reactive atypia were photographed at low and/or high power. Images were blindly and independently reviewed by 5 pathologists (1 GI fellow, 3 GI, and 1 GI/cytopathologist). Reviewers diagnosed each case using 6 categories (reactive atypia, atypia, LGD, HGD, at least HGD, and colonization) and also selected morphologic features that were helpful for a diagnosis. Interobserver variability was assessed using Fleiss' Kappa statistics. Classification tree was used to predict reviewers' diagnosis based on morphologic features.

Results: 41.8% of true colonization cases were misclassified. Reactive atypia (κ=0.73), LGD (κ=0.63) and colonization (κ=0.55) showed the highest concordance between the senior and junior pathologist with a fair-good overall agreement (κ=0.51) between them. Pathologists showed overall poor agreement (diagnostic concordance, κ=0.326) for all diagnostic categories. Reactive atypia and LGD showed the best interobserver agreement (both κ=0.46) while colonization had poor agreement (κ=0.37). Atypia (κ=0.003), HGD (κ=0.07), and at least HGD (κ=0.08) had the worst overall agreement. Two-cell population, abrupt transition, and irregular glands were the most helpful morphologic features in the accurate diagnosis of colonization.

Table 1. Summary of Reviewed Cases and Degree of Agreement Among Pathologists

	Reactive atypia	Atypia	LGD	HGD	At least HGD	Colonization	Overall agreement
# cases (50)	12	0	4	2	0	32	
All Reviewers							
Kappa	0.461	0.003	0.459	0.065	0.078	0.365	**0.326**
Agreement Between Senior and Junior Pathologist							
Kappa	0.729	-0.075	0.625	-0.02	0.333	0.551	**0.505**

The number of cases from each category that was present to the pathologists for review is shown. Kappa and p values for all pathologists and between the senior and junior pathologist are indicated for each category and for the overall degree of agreement.

Figure 1 - 1797

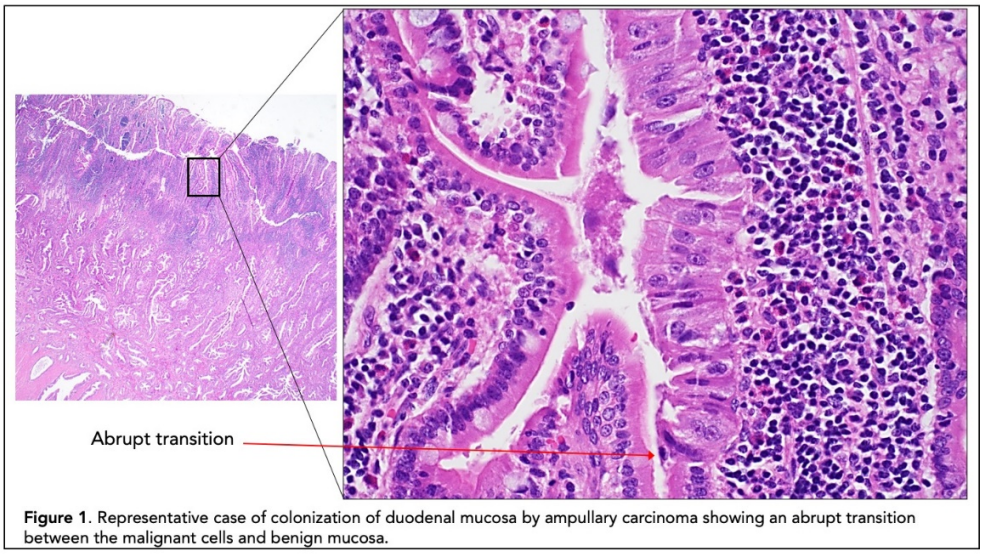

Figure 1. Representative case of colonization of duodenal mucosa by ampullary carcinoma showing an abrupt transition between the malignant cells and benign mucosa.

Conclusions: The use of morphologic features to distinguish colonization from reactive atypia and LGD/HGD has low diagnostic concordance among GI pathologists. Two-cell population, abrupt transition, and irregular glands are the most reproducible morphologic features in establishing the diagnosis of colonization. Recognition of these features may aid pathologists in identifying colonization of mucosa by carcinoma.

1798 Solitary Fibrous Tumor of the Pancreas

Aslihan Yavas[1], Jianyou Tan[2], Funda Yilmaz[3], Michelle Reid[4], Pelin Bagci[5], Jiaqi Shi[6], Marcela Santos Cavalcanti[7], Jinru Shia[1], David Klimstra[1], Olca Basturk[1]

[1]Memorial Sloan Kettering Cancer Center, New York, NY, [2]NewPath Diagnostics, Flushing, NY, [3]University of Ege, Izmir, Turkey, [4]Emory University Hospital, Atlanta, GA, [5]Marmara University, Istanbul, Turkey, [6]University of Michigan, Ann Arbor, MI, [7]Neopath Dx, Curitiba, PR, Brazil

Disclosures: Aslihan Yavas: None; Jianyou Tan: None; Funda Yilmaz: None; Michelle Reid: None; Pelin Bagci: None; Jiaqi Shi: None; Marcela Santos Cavalcanti: None; Jinru Shia: None; David Klimstra: None; Olca Basturk: None

Background: Solitary fibrous tumor (SFT), primarily found in the pleura, has been increasingly reported in other anatomic sites. However, it is still extremely rare in the pancreas. Here, we present the first series of primary pancreatic SFTs, with the aim of further defining their clinicopathologic features.

Design: Nine cases of primary pancreatic SFTs were analyzed.

Results: The mean patient age was 56 years (range, 30-76), and the male:female ratio was 0.8. Five patients presented with abdominal/back pain or discomfort; four tumors were detected incidentally during work-up for other conditions. Seven tumors were located in the head of the pancreas, and two were in the body/tail. On imaging, two were described as cystic lesions, others as solid masses (two were favored to be a neuroendocrine tumor). One case had a biopsy diagnosis of “atypical spindle cell tumor, suspect sarcoma” and two were diagnosed as sarcoma on frozen section. Grossly, the tumors ranged from 0.9 cm to 15 cm (median, 3.7). Microscopically, the tumors were well-circumscribed though not capsulated. The tumor cells were ovoid to spindled, cytologically bland with alternating hypercellular and hypocellular areas, arranged in a so-called patternless fashion and were accompanied by the deposition of hyalinized collagen. Staghorn-like vessels with perivascular hyalinization were present at least focally. Interestingly, there was also considerable amount of entrapped pancreatic parenchyma, not restricted to the periphery of the tumor, intimately admixed between the tumor cells. All tumors had ≤3 mitoses per 10 HPFs, and only one revealed focal necrosis. Immunohistochemically, the tumor cells revealed diffuse/strong STAT6 (nuclear, 100%), Bcl-2 (100%), and CD34 (75%) expression. Electron microscopy (n=2) demonstrated fusiform and spindle shaped tumor cells with a moderately developed rough endoplasmic reticulum embedded in a prominent collagenous stroma, and intimately associated with pancreatic epithelial components. All patients were free of disease at a mean follow-up of 61 months (range, 8-140).

Conclusions: SFT should be considered in the differential diagnoses of mesenchymal neoplasia identified in the pancreas. The alternating cellularity, the intermixing of tumor cells with entrapped pancreatic parenchyma, and characteristic immunophenotype (especially nuclear STAT6 expression) are helpful features. Although SFTs exhibit a broad spectrum of biological behaviors, pancreatic ones seem to have a favorable prognosis in our series.

1799 Three-Dimensional Analysis of Tumor Budding in Extrahepatic Cholangiocarcinoma Using Immunolabeling of Cleared Resected Specimens

Tadashi Yoshizawa[1], Seung-Mo Hong[2], Michael Noe[3], Dong Jun Jung[4], Ralph Hruban[1], Laura Wood[5], Kiyoko Oshima[6]
[1]Johns Hopkins Medical Institutions, Baltimore, MD, [2]Asan Medical Center, Songpa-gu, Seoul, Korea, Republic of South Korea, [3]Johns Hopkins School of Medicine, Baltimore, MD, [4]University of Ulsan College of Medicine, Seoul, Korea, Republic of South Korea, [5]Johns Hopkins Hospital, Baltimore, MD, [6]Johns Hopkins University, Baltimore, MD

Disclosures: Tadashi Yoshizawa: None; Seung-Mo Hong: None; Dong Jun Jung: None; Laura Wood: None

Background: Advances in tissue clearing, and microscopy make it possible to study human pathogenesis in 3-dimensions (3D). Tumor budding (TB) is known to be associated with prognosis in various cancers; however, little is known about the 3D architecture of TB. Using tissue clearing, we analyzed the 3D structure of TB of extrahepatic cholangiocarcinoma (CC). We supplemented this with 3D labeling for e-cadherin, a marker of epithelial to mesenchymal transition.

Design: A total 27 hilar and 4 distal CC thick slabs (up to 20 mm) were harvested from surgical resected tissue. 10 cases were fresh samples, and 21 samples were formalin-fixed, paraffin embedded tissue (FFPE). After clearing, immunolabeling with two antibodies, cytokeratin 19 and e-cadherin were used and tissues were visualized by using lightsheet and confocal laser scanning microscopies. TB was defined on 2D H&E as single cells or clusters composed of fewer than five cells, and classified into low (0-4 buds) and high (≥5) budding cases.

Results: 2D H&E analysis identified13 low budding cases and 18 high budding cases. 3D analysis revealed that: 1) the neoplastic cells in TB are not individual islands of cells, but rather are connected complex branching tubular structures. 2) Low budding tumors branch less and have a solid configuration of tumor (Fig. 1: CK19 is green, e-cadherin is red in rendering image). High budding tumors have more complex branching (Fig. 2: CK19 is green, e-cadherin is red in rendering image). 3) Only undifferentiated carcinoma (carcinoma without tubular formation) were composed of isolated single cells embedded in the stroma. 4) Immunolabeling of e-cadherin is heterogeneous and decreased expression was observed mainly at the tips of 3D protrusions (Fig 1 and 2) .

Figure 1 - 1799

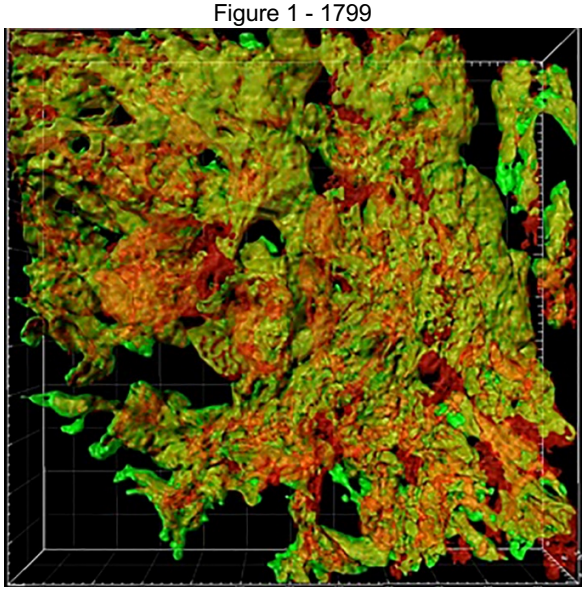

Figure 2 - 1799

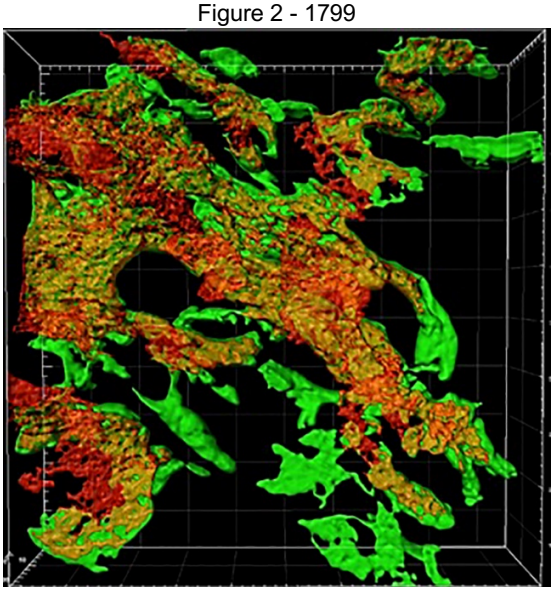

Conclusions: Analysis of 3D structure of tumor budding revealed that tumor budding is the result of complex 3D branching of tubular structures. Undifferentiated carcinoma had a distinctive 3D appearance with individual unconnected cells. The tissue clearing method enables us to obtains the new insights into the drivers of 2D morphology.

1800 Systemic Analysis of C4d Deposition Patterns in Pancreas Allograft Biopsy and Their Correlation with Donor Specific Antibodies and Histopathologic Features: The University of Wisconsin Experience

Qiqi Yu[1], Hui-Hua Li[2], Xiaofei Zhang[3]
[1]University of Wisconsin, Madison Hospital and Clinics, Madison, WI, [2]School of Medicine and Public Health, The University of Wisconsin-Madison, Madison, WI, [3]University of Wisconsin-Madison, Madison, WI

Disclosures: Qiqi Yu: None; Hui-Hua Li: None; Xiaofei Zhang: None

Background: The current Banff scheme uses C4d staining in combination with Donor Specific Antibody (DSA) and histologic features for the diagnosis of AMR. However, the highly heterogenous staining patterns of C4d in pancreas allograft biopsy impairs its sensitivity and specificity. We conducted a systematic and detailed analysis of C4d staining patterns in pancreas allograft biopsy, and their correlation with DSA and clinicopathologic features.

Design: All 25 pancreas allograft biopsies (18 patients, 10 males/8 females, 45.9±2.7 years old) performed at our institution last year (08/2017-08/2018) were included. Clinical information including DSA titers tested within 5 days of biopsy were obtained from electronic record. H&E slides and C4d immunostain slides were reviewed. Continuous variables were expressed as mean ± standard error and compared with the Student *t* test. Categorical variables were compared with Fisher exact test.

Results: Of these 25 biopsies, 16 (64%) are positive for ACR (10 mild and 6 moderate); 8 (32%, from 7 patients) are DSA positive (DSA+); 2 are DSA borderline positive (mean fluorescence intensity<500), and 15 are DSA negative (DSA-). In DSA+ group, 4 (50%) showed features of combined AMR and ACR. 5 of 7 DSA+ patients received AMR treatments and all showed good response. The locations of C4d deposition include: acinar cells (22/25, focal weak to diffuse moderate staining); interacinar endothelial cells (23/25, from 1% to 30% of all interacinar endothelial cells); islet endocrine/endothelial cells (12/25); intercalated ducts (4/25=16%); interlobular duct (2/25=4%); interlobular large vessel endothelial cells (23/25) and septal stromal cells (22/25). The DSA+ group has significantly higher percentage of C4d+ interacinar endothelial cells (9.6±3.4% vs 3.1±1.0% of all endothelial cells, p=0.008) and islet C4d staining (12/25 vs 5/25; p=0.022) than DSA- group, but no significant difference in other locations. While both group show similar degree of mononuclear infiltration, DSA+ group has more neutrophil/eosinophil infiltrates (5/8 vs 4/15, p=0.18) and hemorrhage/necrosis (1/8 vs 0/15, p=0.34).

Conclusions: The C4d footprint is more heterogenous in pancreas allograft. While C4d staining in interacinar endothelial cells and islet cells are relatively specific for AMR, other stain inpatterns can be seen in both AMR and ACR. Combined ACR and AMR are not uncommon, thus routine C4d staining and more careful interpretation are necessary for the diagnosis of AMR in pancreas allograft.

1801 Differential Gene Expression Profiling Identifies a Candidate Inflammatory Signature for Primary Sclerosing Cholangitis

Melissa Zhao[1], Amitabh Srivastava[2], Matthew Hamilton[1], Joshua Korzenik[1], Michael Drage[3]
[1]Brigham and Women's Hospital, Boston, MA, [2]Brigham and Women's Hospital, Harvard Medical School, Boston, MA, [3]University of Rochester Medical Center, Rochester, NY

Disclosures: Melissa Zhao: None; Amitabh Srivastava: None; Matthew Hamilton: None; Michael Drage: None

Background: Primary sclerosing cholangitis (PSC) is a distinctive idiopathic autoinflammatory process characterized by progressive stricturing of the biliary system. We retrospectively identified chronic cholecystitis specimens from patients with PSC and compared the differential gene expression (DGE) profile to chronic cholecystitis from patients without PSC.

Design: Messenger RNA was isolated from FFPE gallbladder/extrahepatic duct tissue from 20 patients, including 7 with PSC-associated chronic cholecystitis (PSC-CC), 9 with PSC-associated extrahepatic ductal inflammation (PSC-DI), 2 with PSC-unrelated chronic cholecystitis (CC), and 2 with histologically normal gallbladders removed during native hepatectomy for non-PSC cirrhosis. Expression levels of 692 genes were quantified via nCounter assay and were subjected to agglomerative hierarchical clustering. DGE was compared between groups based on pathologic diagnosis. Cell-specific gene expression profiles were also used to quantify the relative proportions of immune cell types.

Results: There were no significant gene expression differences between PSC-CC and PSC-DI. The PSC-CC groups showed more heterogenous DGE than the CC group. Compared to histologically normal gallbladders, the PSC-CC group showed increased expression of six genes including TNFRSF17, CXCL13, and CTLA4-TM (FDR P-value < 0.10), and changes in immune cell recruitment involving higher levels of B cells, CD8 T cells, CD45 T cells, and lower level of neutrophils. Compared to the CC group, PSC-CC showed a higher proportion of CD8 T cells and NK cells, and a lower level of neutrophils.

Conclusions: DGE profiling of cholecystectomy specimens suggests differences in inflammatory cell infiltrates, which may be of biologic significance in this disease process. Similar expression profiles within PSC-associated chronic cholecystitis and PSC-associated extrahepatic ductal inflammation suggests a consistent extrahepatic inflammatory pathway with a unique inflammatory signature.